

# **EXPERIMENTAL METHODS TOWARDS CONTROLLING THE GLYCOFORM**

by

Sean Alexander Ponce

A thesis submitted to Johns Hopkins University in conformity with the requirements for  
the degree of Master of Science in Engineering.

Baltimore, Maryland

August, 2017

© 2017 Sean A. Ponce  
All Rights Reserved

## **Abstract**

The glycosylation profiles of biopharmaceuticals have a major impact on the bioactivity, bioavailability, biocompatibility and biosafety of the therapeutic. As modulation of the glycosylation profile can enhance or attenuate therapeutic properties of the drug, methods towards control of glycosylation therefore are of interest to the research, clinical and industrial communities. This work embarks on a multipronged approach towards achieving uniform, consistent and specified protein glycosylation through development of analytical methodologies to monitor attributes of glycosylation (Chapters 2-4), and by construction of a cell-free bioreactor for In-Vitro Glyco-Engineering (Chapter 5).

In objective (1) development of state-of-the-art analytical technologies demonstrated how Chinese Hamster Ovary (CHO) cells, subjected to high-flux substrates and cellular and protein engineering strategies, can be manipulated towards achieving control over the protein glycosylation pathway in mammalian cells. HPLC-based methods were employed to determine: amino acid composition, glycosylation patterns, nucleotide sugar distributions and titer. Modulation of the feed was shown to increase nucleotide sugars, specifically CMP-Neu5Ac, resulting in increased sialylation of proteins. This detailed representation facilitated fundamental insight into the physiology of cellular responses, by synergizing how the glycosylation profile is inextricably coupled to substrate availability, enzyme activities and cellular metabolism, thereby revealing the interplay of the glycosylation processes at the systems level.

In objective (2) implementation of a novel, transformative and scalable biofabrication process applying In-Vitro Glyco-Engineering of glycoproteins to produce

structurally well-defined, homogeneous glycans. This chemo-enzymatic approach utilizes Endoglycosidase-H covalently coupled to a solid phase support of silicon nanowires to deglycosylate proteins. Select model glycoproteins: RNaseB, alpha-amylase and IgG, showed the flexibility of the process towards different classes of biomolecules.

These efforts will lead to higher productivity, increased product homogeneity and greater therapeutic efficacy. Ultimately, to enable the cost effective and routine production of biopharmaceuticals to facilitate increased patient affordability and larger profit margins.

Advisor: Michael Betenbaugh

Reader: Kevin Yarema

*It seems that the human mind has first to construct forms independently, before we can find them in things. Kepler's marvelous achievement is a particularly fine example of the truth that knowledge cannot spring from experience alone, but only from the comparison of the inventions of the intellect with observed fact.*

*-Albert Einstein in the Frankfurter Zeitung, November 9, 1930*

## **Acknowledgements**

“Baltimore has been a good city to me and our family. It’s given me jobs at times when there were none, and the ability to raise a family.” -Richard S. Udoff

The legacy my grandfather began in this city in 1962 continues with his grandson; me. I am thankful for the opportunity to study at Johns Hopkins University, and despite my short two years here, I will always remember the privilege and challenge that defines the Hopkins experience. I am thankful of Baltimore for endless parking tickets, introduction of east coast culture and etiquette, and new scenery to my Southern California based life. I would like to thank my family for their endless support, consolation, encouragement and love. I am proud of myself for being multi-faceted enough to adapt from science to engineering; this was no easy feat.

In these two years, I have had the pleasure to work with many Professors and Professionals without whom this work would not be possible. I am forever indebted to you all for contributing to my development as a scientist, but more importantly for getting me to think differently than I when arrived here. It is not the equations, nor experiments, that make nor define great scientists, but rather the philosophy they embrace and apply to whatever system or application they might choose to study that make them great scientists. My eyes were opened to see the world differently, and from far above. While I had head in the clouds, I always tried my best to keep my feet on the ground. I am firm believer that all boats float on a rising tide, and through surrounding myself with the great people here, they made me better than better. Such giants are Professors: Y.C. Lee (JHU Biology), Kevin Yarema (JHU BME), Anne Le (JHU MED), Tsuan Tsu (Taiwan NIH), Hui Zhang (JHU MED), Lai-Xi Wang (UMCP CHEM), Zachary Gagnon

(JHU ChemBE), Chao Wang (JHU ChemBE) and Carmo Pereira (JHU ChemBE). I will forever remember them for their many stimulating conversations and advice both academically and in thing this called life. Limitless inspiration, countless words of wisdom and the suggestion to study nucleotide sugars my advisor, Michael Betenbaugh, provided a place to shape new ideas into eventual successes in uncharted territories; and for that he will always hold a very dear place.

I would also like to thank the many talented students I've had the pleasure of working with and some of whom having forged life-lasting friendships. They are Dr. Xiaotong Fu, Dr. Markela Ibo, Dr. Andrew Chung, Dr. Quinton Smith, Daniel Lewis, Nick Mavrogianis, Daniel Lewis, Jimmy Kirsch, Qiong Wang, Robert Law, Gayatri Dhara, Swetha Kumar, Dr. Geng Yu, Kevin McFarland, Luis Garcia, Mike Manto, Tienchang Pu, Chien-Ting Li, Matt Gonzalez, Christopher Saeui, Younji Seo, Sandra Chough and Mark Kwok. Through our support network we overcame many obstacles and hurdles that each of us on our own would not have made it. Thanks for the beers, dinners, hugs, smiles and cookies that defines friendship and makes the human experience more bearable.

## Table of Contents

Abstract .....	ii
Acknowledgements .....	v
Table of Contents .....	vii
List of Figures .....	ix
List of Tables .....	xi
<b>Chapter 1. Introduction</b> .....	1
<b>1.1 Biopharmaceuticals, Antibodies and Glycosylation</b> .....	1
<b>Chapter 2. N-Glycan Analysis using HILIC-FD</b> .....	27
<b>2.1 Introduction</b> .....	27
<b>2.2 Materials and Methods</b> .....	32
2.2.1 IgG protein purification using Protein-A Agarose Beads .....	32
2.2.2 Release of Glycans .....	33
2.2.3 Preparation of 2-AB Labeling Solution .....	33
2.2.4 2-AB Labeling Conditions .....	33
2.2.5 Chromatographic Conditions for High-Resolution of N-Glycans .....	34
<b>2.3 Results</b> .....	35
2.3.1 HILIC-FD glycan analysis of gpIgG1F241A from CHOK1 cells .....	37
2.3.2 HILIC-FD glycan analysis of gpIgG1 from CHO23KO cells .....	37
<b>2.4 Discussion</b> .....	37
<b>Chapter 3. Amino Acid Analysis</b> .....	40
<b>3.1 Introduction</b> .....	40
<b>3.2 Materials and Methods</b> .....	46
3.2.1 Preparation of Samples, Cell Media and Biological Fluids .....	47
3.2.2 Preparation of the AccQ•Fluor Derivatization Reagent .....	47
3.2.3 Derivatization of Samples and Standards .....	48
3.2.4 Amino Acid Analysis Chromatographic Conditions .....	49
<b>3.3 Results</b> .....	50
3.3.1 Amino acid profile of F-12K Nutrient medium Formulation. ....	50
3.3.2 Amino acid profile of RPMI 1640 Formulation. ....	52
<b>3.4 Discussion</b> .....	54
<b>Chapter 4. Nucleotide and Nucleotide Sugars Analysis</b> .....	57
<b>4.1. Introduction</b> .....	57
<b>4.2 Materials and Methods</b> .....	59
4.2.1 Cold-Quenching and Extraction of Metabolites .....	59
4.2.2 Purification of by solid-phase extraction .....	60
4.3.3 Fluorescent Assisted Carbohydrate Electrophoresis (FACE) .....	60
4.3.4 IP-RPC chromatographic conditions .....	61
<b>4.3 Results</b> .....	62
4.3.1 FACE of nucleotides and nucleotide sugars .....	62
4.3.2 IP-RPC of nucleotides and nucleotide sugars .....	65
<b>4.4 Discussion</b> .....	70
<b>Chapter 5. A Microfluidic Bio-Reactor for In-Vitro Glyco-Engineering</b> .....	75
<b>5.1 Introduction</b> .....	75
<b>5.2 Materials and Methods</b> .....	81

5.2.1 SDS-PAGE gels.....	81
5.2.2 Liquid chromatography-Mass spectrometry (LC-MS) .....	81
<b>5.3 Results</b> .....	82
<b>5.4 Discussion</b> .....	100
<b><i>Conclusions and Future Work</i></b> .....	102
<b><i>Supplementary Material</i></b> .....	106
<b><i>Bibliography</i></b> .....	108
<b><i>Curriculum Vitae</i></b> .....	119



## List of Figures

Figure 1: Schematic representation of the human IgG structure and glycan composition...	3
Figure 2: Structure and symbolic representations of common carbohydrates. ....	7
Figure 3: Monosaccharide transport and metabolic processing reactions. ....	8
Figure 4: Chemical Structures of some common Nucleotide Sugars. ....	9
Figure 5: Schematic view of N-linked glycosylation processing in mammalian cells....	11
Figure 6: mAb Fc N-linked glycosylation in the Golgi apparatus of mammalian cells...	13
Figure 7: Model for N-glycoprotein biosynthesis in mammals. ....	16
Figure 8: Metabolic details of sialoglycoconjugate biosynthesis.....	18
Figure 9: (A) Sialic acid synthesis pathway; (B) structures of ManNAc and its analog...	21
Figure 10: MALDI-TOF glycoprofile analysis of IgGs from different CHO lines.....	35
Figure 11: HILIC-FD N-glycan analysis of gpIgG1F241A from CHOK1 cells.....	36
Figure 12: Zoom-in of HILIC-FD N-glycan analysis of gpIgG1F241A from CHOK1 cells.....	36
Figure 13: HILIC-FD N-glycan analysis of gpIgG1 from CHO23KO cells.....	36
Figure 14: Zoom-in of HILIC-FD N-glycan analysis of gpIgG1 from CHO23KO cells.....	36
Figure 15: The chemical structures and pKa's of amino acids.....	40
Figure 16: Chemistry of the AccQ-Tag Reaction.....	44
Figure 17: Amino acid profile of F-12K Nutrient medium Formulation.....	50
Figure 18: Amino acid profile of RPMI 1640 Formulation.....	52
Figure 19: FACE gel of monosaccharide standards.....	63
Figure 20: FACE gel of standards 2DG and Arabinose alongside spiked PANC cell extracts.....	64
Figure 21: Overlay of Nucleotides and Nucleotide Sugar Standards.....	66
Figure 22: Comparison of purified Nucleotides and Nucleotide Sugars from CHO cell extracts.....	67
Figure 23: Overlay of NS Standards and of ManNAc-analog-fed CHO cell extract.....	68
Figure 24: Overlay of CMP-Neu5Ac standard and of ManNAc-analog-fed CHO cell extract.....	69
Figure 25: Scanning Electron Microscopy of Silicon Nano-Wires top-view.....	78
Figure 26: Scanning Electron Microscopy of Silicon Nano-Wires zoom-in with 50° tilt.	79
Figure 27: Schematic of Reactor deglycosidating a protein.....	80
Figure 28: Initial structure of the glyco-reactor device.....	82
Figure 29: Dismantled reactor housing.....	83
Figure 30: Copper tape seal of Endo-H enzyme Si-NW Chip.....	84
Figure 31: PDMS sealed reactor.....	85
Figure 32: Endo-H SiNW chip in 24-Well Plate.....	86
Figure 33: SDS-PAGE of Endo-H SiNW chip digest of Alpha-Amylase.....	87
Figure 34: SDS-PAGE gel of RNaseB Reactor Digest.....	89
Figure 35: SDS-PAGE gel of deglycosylated RNaseB Reactor Digest.....	90
Figure 36: TIC and EIC for RNaseB Glyco-Reactor at 14 hour digest.....	90
Figure 37: DMS for RNaseB Glyco-Reactor at 14 hour digest.....	91

Figure 38: TIC and EIC for Intact RNaseB.....	92
Figure 39: DMS for Intact RNaseB.....	93
Figure 40: TIC and EIC for Endo-H digested RNaseB in solution.....	94
Figure 41: DMS for Endo-H digested RNaseB in solution.....	95
Figure 42: TIC and EIC for glyco-chip digestion at 19 hours.....	96
Figure 43: DMS for glyco-chip digestion at 19 hours.....	96
Figure 44: TIC and EIC for glyco-chip digestion at 48 hours.....	97
Figure 45: DMS for glyco-chip digestion at 48 hours.....	98
Figure 46: SDS-PAGE gel of IgG digest using Endo-H Si-NW chip.....	99
Figure 47: Protein-A HPLC Chromatogram.....	106
Figure 48: Protein-A Chromatography IgG Calibration Curve.....	107

## List of Tables

Table 1: Comparison of effectiveness of reported nucleotide sugar feeding experiments.....	24
Table 2: Optimized gradient conditions for n-glycan analysis.....	34
Table 3: Optimized gradient conditions of Amino Acid Analysis.....	49
Table 4: F-12K Nutrient Formulation.....	51
Table 5: RPMI 1640 Formulation.....	53
Table 6: Optimized gradient conditions for nucleotide sugars.....	61

## **Chapter 1: Introduction**

### **1.1. Biopharmaceuticals, Antibodies and Glycosylation**

The past century has seen countless scientific advances that have reshaped the fields of biochemistry and molecular biology. These sophisticated and groundbreaking scientific achievements gave rise to the biopharmaceuticals industry. In contrast to conventional pharmaceuticals that are produced by chemical synthesis, biopharmaceuticals are produced biologically, through recombinant or non-recombinant cell-culture expression systems where manufacturing process conditions dictate the product quality. Biopharmaceuticals currently consist of vaccines, blood, blood components, allergens, gene therapies, tissues, therapeutic proteins, and somatic/live cells. Biopharmaceuticals are composed of sugars, proteins, or nucleic acids or complex combinations of these substances, or may be living cells or tissues. Additionally, they (or their precursors or components) are isolated from living sources, e.g. human, animal, plant, fungal, or microbial, their derivatives, and products of which they are components (e.g., conjugates). Their inherent biological origin endows biopharmaceuticals with greater efficacy, efficiency and selectivity when compared to conventional pharmaceuticals. The biopharmaceuticals market can be segmented into oncology, inflammatory and infectious diseases, autoimmune disorders, metabolic disorders, hormonal disorders, disease prevention, cardiovascular diseases, neurological diseases and other diseases (Mordor Intelligence, 2017). Among these, oncology happens to be the largest segment with 30.5% share in the year 2015 (Mordor Intelligence, 2017). The scope of thesis shall encompass therapeutic proteins, i.e. immunoglobulin G1 (IgG1) monoclonal antibodies (mAbs).

Biopharmaceuticals represent the major source of total company revenue for several major pharmaceutical companies, with the annual global biopharmaceuticals market increasing from \$94 billion in 2007 to \$177 billion in 2015 (Mordor Intelligence, 2017). Amongst biopharmaceutical products, antibody based technologies are the largest market segment, comprising 37% of biopharmaceutical products in the year 2015 (Mordor Intelligence, 2017). Antibodies are over twenty of the fifty highest selling biopharmaceutical products in 2017 (EvaluatePharma, 2017) containing asparagine-linked (N-linked) complex carbohydrates (glycans) at residue Asn297, thus rendering glycosylation a highly prevalent and impactful post-translational modification. Along with a higher approval rate than other biopharmaceutical products, global sales of mAb products have grown faster than other biopharmaceuticals (Ecker, 2015). Corresponding to the increasing sales of mAb products, there has been an increase in the total quantities produced annually to meet market demand, as 10 metric tons of were produced in 2013 (Ecker, 2015). The demand for mAbs has resulted in a significant amount of global biomanufacturing capacity devoted to their production as well as to significant improvements in methods and approaches to monoclonal antibody manufacturing process design and optimization (Ecker, 2015). See Figure 1 for a schematic representation of the human IgG structure and glycan composition.

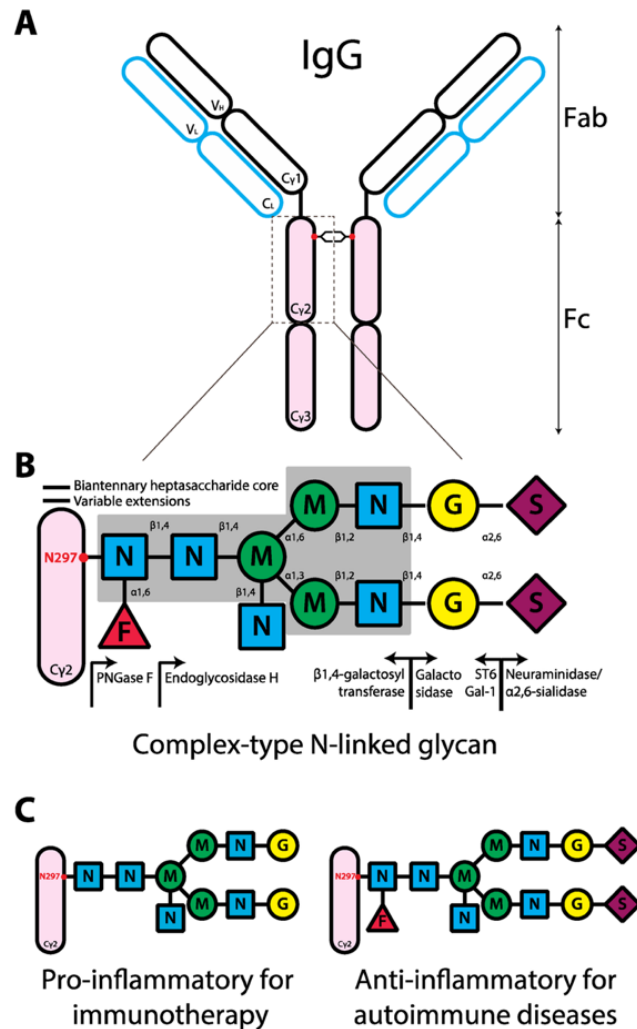


Figure 1. Schematic representation of the human IgG structure and glycan composition. (A) IgG structure. The IgG protein is comprised of two heavy chains (black outline) and two light chains (blue outline). Each IgG heavy chain has the variable region (VH) and the constant region containing three domains (Cγ1-3). The line between Cγ1 and Cγ2 represents the hinge region. Each light chain has variable (VL) and constant lengths (CL). IgG molecule can be divided into antigen-binding fragment (Fab; empty ovals) and fragment crystallizable region (Fc; pink ovals). The red dot represents N-linked glycans of complex-type. (B) Composition of complex-type N-linked glycan on IgG. The glycan has a biantennary heptasaccharide core (solid line and in the gray block) and variable extensions (dash line). Abbreviations: F, fucose; N, GlcNAc; M, mannose; G, galactose; S, sialic acid. The enzymes, glycosyltransferases (left arrow) and glycosidases (right arrow), responsible for the addition or removal of the specific sugar are placed directly underneath of the sugar linkage. (C) Design of glycan composition on IgG Fc for potential antibody therapeutics. This figure was adapted from (Shade, 2013).

Glycosylation is responsible for considerable variation in product quality as current production systems are subject to batch-to-batch variability. As the glycosylation profiles of biopharmaceuticals have a major impact on the bioactivity, bioavailability, biocompatibility and biosafety of the drug (Del Val, 2013), they are deemed glycosylation-associated critical quality attributes (glcCQAs) that require control throughout the biopharmaceutical production campaign (Del Val, 2010). In IgGs, afucosylation and galactosylation play important roles in the antibody-dependent cell-mediated cytotoxicity (ADCC) and complement-dependent cytotoxicity (CDC), two important mechanisms for mAbs to mediate the immune function of killing target cells (Sha, 2016). Fucose levels have been shown to have an inverse relationship with the degree of antibody-dependent cell-mediated cytotoxicity, and high mannose levels have been implicated in potentially increasing immunogenicity and contributing to less favorable pharmacokinetic profiles (Hossler, 2017). The sialic acid content partially determines the mAb anti-inflammatory activity (Sha, 2016). Indeed, as modulation of the glycosylation profile can enhance or attenuate therapeutic properties of the drug, methods towards control of glycosylation therefore are of interest to the research, clinical and industrial communities. However, the identification and control of critical process parameters that pose a risk to glcCQAs remain yet to be elucidated.

Glycosylation is an important post-translational modification involved in a myriad of different cellular processes such as protein folding, cell growth and development, immunity, anti-coagulation, microbial pathogenesis, cancer metastasis (Neelamegham, 2011), cell adhesion, molecular trafficking and clearance, receptor activation, signal transduction and endocytosis (Ohtsubo, 2006), and even during fertilization that initiates

life in multicellular organisms (Yarema, 2001). The type(s) of glycan structures attached to the acceptor gives rise to altered properties of the acceptor molecule as changes in its polarity, conformation, solubility, and/or ligand-receptor interactions, resulting in the ability of the cell to precisely modulate the phenotype of many endogenous compounds. Absent and/or aberrant glycosylation pathways through alterations in glycosylation enzymes have been implicated in over 40 diseases in humans (Jaeken, 2013), such as various cancers, rheumatoid arthritis, autoimmune disease, diabetes as well as an increasing number of disease states related to child development (Ohtsubo, 2006; Varki, 2009), these diseases are grouped under the classification “congenital defects of glycosylation” (Jaeken, 2013).

Glycosylation is defined as the enzymatic process of adding sugars in glycosidic linkages to other molecules generating glyconjugates or complex carbohydrates (Cummings, 2005). The term glycoconjugates includes glycoproteins, glycosylphosphoinositol (GPS) – anchored glycoproteins, glycolipids, glycosaminoglycans and proteoglycans, peptidoglycans, lipopolysaccharides, free oligosaccharides and polysaccharides (Cummings, 2005). Glycans, which refers to the oligosaccharides, polysaccharides and carbohydrates, are considered to be one of the four major components of cells and have been described as one of the most abundant and structurally diverse nature’s biopolymers (Ohtsubo, 2006). Cellulose, a polysaccharide comprising a linear chain of several hundred to over ten thousand  $\beta(1 \rightarrow 4)$  linked D-glucose units, is an important structural component of the primary cell walls of green plants and is the biggest contributor to the production of biomass on the planet (Behmüller, 2014). It is synthesized at the plasma membrane using UDP-Glc as glycosyl



donor, which represents the most prominent nucleotide sugar in plants and which is provided by either photosynthesis or from the cleavage of sucrose by sucrose synthase (Behmüller, 2014). Moreover, many trees contain high amounts of xylans, which are complex polysaccharides synthesized from UDP-xylose, and which account for up to 30 % of the wood biomass (Behmüller, 2014). In mammals, the glycome repertoire is vast and could potentially be larger than the proteome (Ohtsubo, 2006). Additionally, a glycan may be modified with noncarbohydrate substituents, e.g., O-acetyl esters, O-methyl ethers, amino acids, sulfates, and phosphoesters (Bar-Peled, 2011). Despite this potentially enormous diversity, the mechanism of glycan synthesis is highly regulated and constricted, and only a few monosaccharides are used in the enzymatic process of mammalian glycosylation (Ohtsubo, 2006). In general, 10 basic building blocks are used to build mammalian glycoconjugates (Cummings, 2004). These include the 5-carbon pentoses (Xylose – Xyl and Fucose – Fuc), the 6-carbon hexoses (Glucose – Glc, Galactose – Gal, Mannose – Man), the 6-carbon hexosamines (N-acetylglucosamine – GlcNAc and N-acetylgalactosamine – GalNAc), the 6-carbon hexuronic acids (Glucuronic acid – GlcA and Iduronic acid – IdA), and the 9-carbon sialic acids (Sia, including N-acetylneuraminic acid – Neu5Ac and N-glycoylneuraminic acid – Neu5Gc) (Cummings, 2004), some of their chemical structures are depicted in Figure 2.

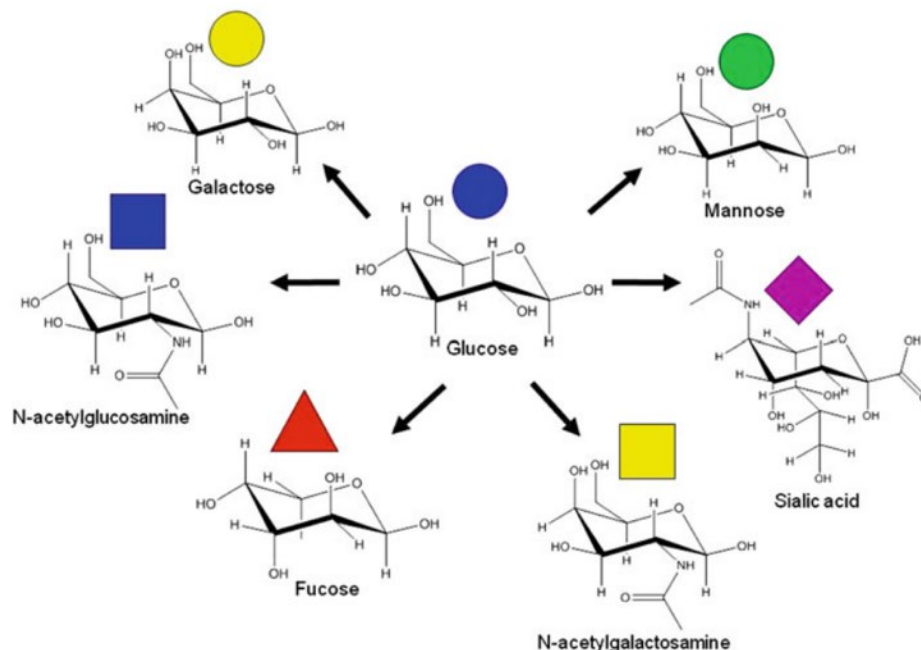


Figure 2: Structure and symbolic representations of common carbohydrates. This figure was adapted from (Dell, 2014).

Glycosylation reactions occur by a sugar donor in the form of an activated, high-energy nucleotide sugar transferring the sugar moiety to an acceptor such as a protein, lipid, or other bioorganic molecule. Protein N- and O-glycosylation (the covalent attachment of carbohydrate sequences to the side-chains of asparagine and serine or threonine, respectively) is a phenomenon shared by all domains of life (Dell, 2014) throughout the entire phylogenetic spectrum, ranging from archaea to eubacteria to eukaryotes (Spiro, 2002). However, the sequences of glycolytic enzymes differ between Archaea, Bacteria and Eukaryotes (Orellana, 2016). Formation of glycosidic linkages and, thus the synthesis of conjugated oligosaccharide(s), requires the availability of the relevant nucleotide sugars (structures shown in Figure 4), which are initially synthesized from monosaccharides and nucleoside phosphates in the cytoplasm and nucleus of cells, with subsequent interconversions through phosphorylation, acetylation and epimerization

[illegible]

8

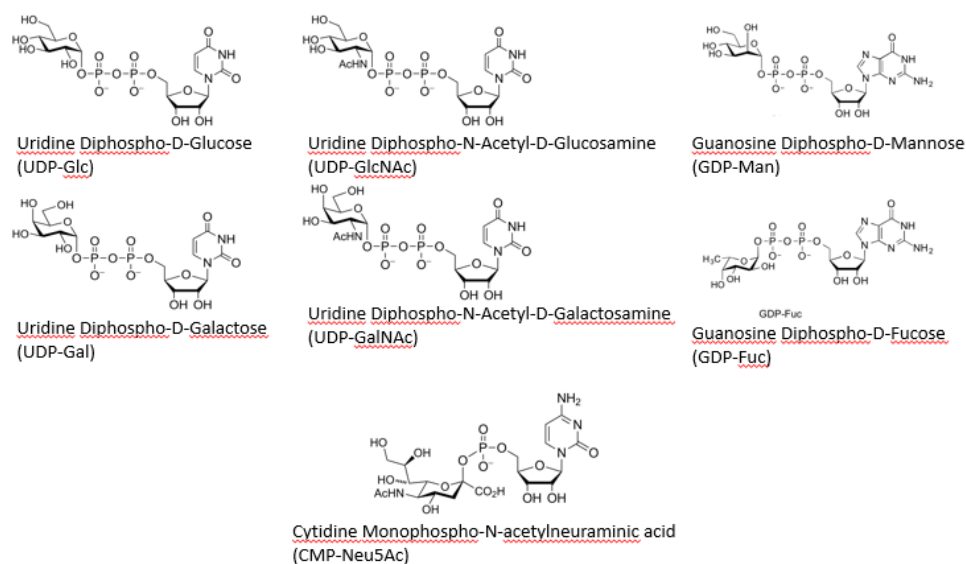


Figure 4: Chemical structures of some common nucleotide sugars.

In contrast to protein isoforms, glycan structures are not directly encoded in the genome (Varki, 2009). The vast glycan diversity exhibited for most proteins is generated as they traverse through the endoplasmic reticulum (ER) and various Golgi compartments due the stochastic nature of interactions between enzymes and oligosaccharide substrates and the variety of glycosyltransferase and glycosidase processing reactions that can act on any one glycan (Wang, 2017). Given its non-template-driven nature, glycosylation heterogeneity arises both from variations in glycosylation site occupancy, i.e. macroheterogeneity, and in the diversity of the final glycan structures attached to glycoproteins, i.e. microheterogeneity, as glycans can emerge from the combinatorial action of exoglycosidases, chain extending and chain terminating glycosyltransferases emerging from the cellular secretory compartments (Wang, 2017). Together, these reactions result in the construction of glycoproteins,

glycosphingolipids, proteoglycans and glycosylphosphatidylinositol-linked protein anchors (Neelamegham, 2011). Schematic view of N-glycosylation processing is illustrated in Figure 5.

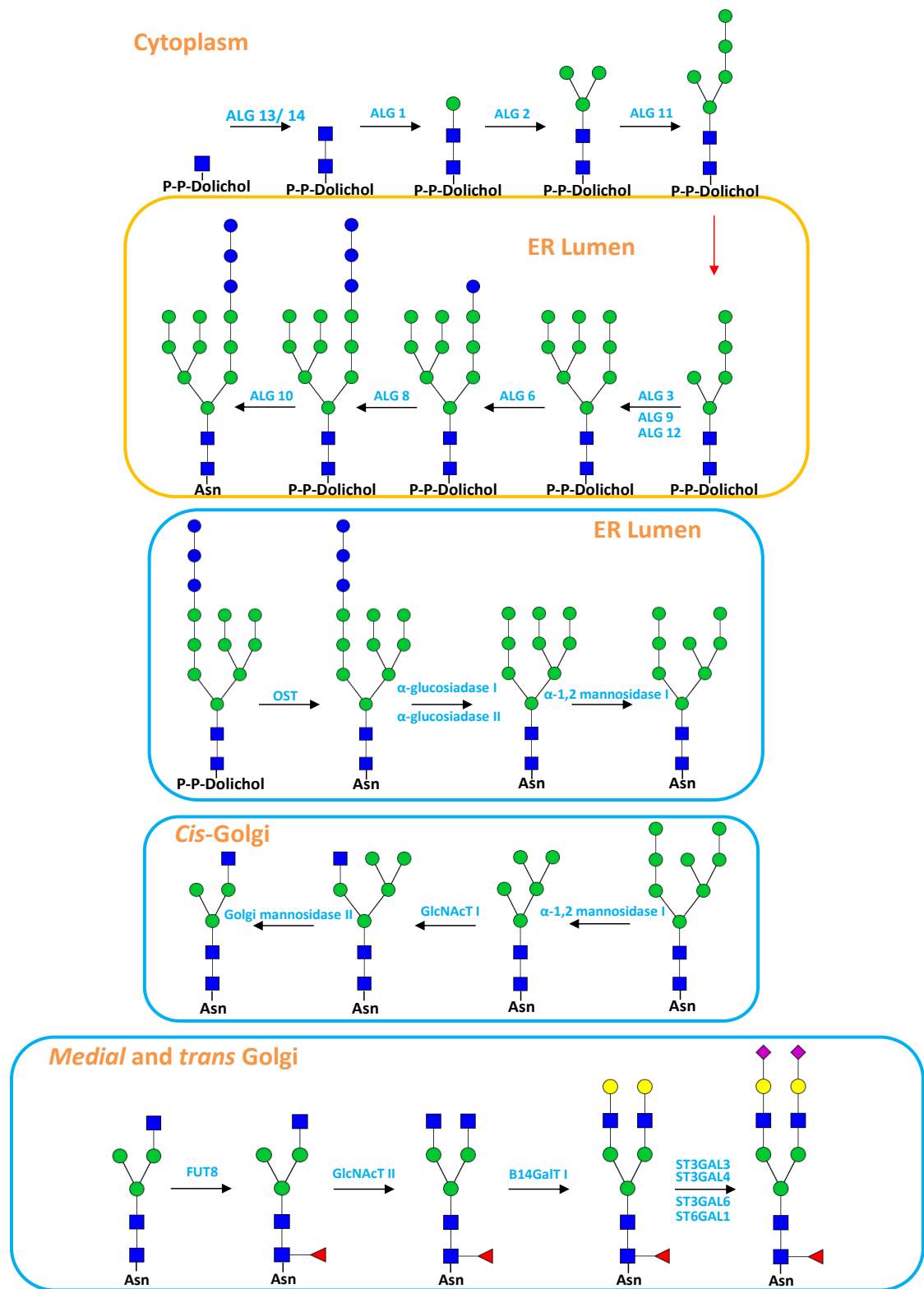


Figure 5: Schematic view of N-linked glycosylation processing in mammalian cells.

Glycosyltransferases utilize an activated donor sugar substrate containing a phosphate leaving group, most commonly as nucleoside diphosphate sugars (e.g., UDP Gal, GDP Man); however, nucleoside monophosphate sugars (e.g., CMP Neu5Ac), lipid phosphates (e.g., dolichol phosphate oligosaccharides), and unsubstituted phosphorylated monosaccharides are also used (Lairson, 2008). Nucleotide sugar-dependent glycosyltransferases are often referred to as Leloir enzymes, in honor of Luis F. Leloir, who discovered the first sugar nucleotide (UDP-Glc) and was awarded the Nobel Prize in chemistry in 1970 for his enormous contributions to our understanding of glycoside biosynthesis and sugar metabolism. The acceptor substrates utilized by glycosyltransferases are most commonly other sugars but can also be a lipid, protein, nucleic acid, antibiotic, or another small molecule (Lairson, 2009). For glycosyltransfer reactions to occur, sugar nucleotides generated in the metabolic reactions must be transported to the ER/Golgi by nucleotide sugar transporters (NSTs) (Neelamegham, 2011), these processes are illustrated in Figure 6 for the glycosylation of a mAb in CHO cells.

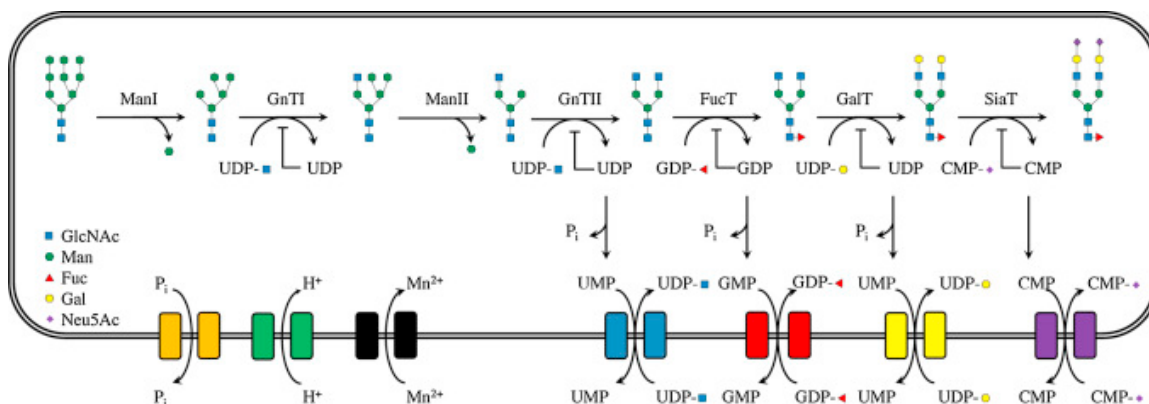


Figure 6: mAb Fc N-linked glycosylation in the Golgi apparatus of mammalian cells. Linear representation of the enzymatic pathway of mAb Fc N-linked glycosylation in the Golgi apparatus of mammalian cells with a simplified illustration of the most important enzymatic reactions, transports mechanism and utilization of nucleotides and nucleotide sugars regarding N-linked glycosylation of monoclonal antibodies. This figure was adapted from (Villiger, 2016).

Protein glycosylation can be either O-linked or N-linked. N-linked glycosylation refers to glycan structure attached to the asparagine residue on proteins with an Asn-Xa-Xb sequence of consensus (sequon) motif (Ohtsubo, 2006), where Xa is any amino acid except Proline (Varki, 2009). O-linked glycosylation refers to glycans attached to serine or threonine residues (Ohtsubo, 2006). In higher organisms, hundreds of genes partake in encoding the enzymes involved in glycosylation which can be divided into five major classes: glycosyltransferases, transglycosylation reverse glycosides, nucleotide sugar transporters, glycan donor transferases and lipid-linked donor transferases (Cummings, 2004). The most common class of enzymes are the glycosyltransferases, which are responsible for sugar addition to the non-reducing (occasionally reducing) end of the glycan (Cummings, 2004). Nascent polypeptides emerging from protein-conducting channels into the ER lumen are often cotranslationally modified with oligosaccharides at selected asparagine residues within the consensus sequence N-X-S/T ( $X \neq P$ ) (Harada, 2013). The native state stabilization and decreased activation barrier for folding



conferred by N-glycosylation enhances both the kinetics and the thermodynamics of protein folding (Hanson, 2009). Furthermore, asparagine (N)-linked glycosylation of nascent polypeptides synthesized in the endoplasmic reticulum regulates the folding, degradation, and intracellular trafficking of the glycoproteins (Harada, 2013). In mammals, N-glycosylation requires preassembly of the lipid-linked precursor, which is composed of three glucose (Glc), nine mannose (Man), and two N-acetylglucosamine (GlcNAc) residues linked to pyrophosphate (PP)-dolichol, Figure 7A. The monosaccharide units that compose the precursor are then donated either directly or indirectly from the nucleotide sugars UDP-Glc, GDP-Man, and UDP-GlcNAc, Figure 7B. Assembly of the precursor is a bipartite process that begins with the synthesis of the Man<sub>5</sub>GlcNAc<sub>2</sub>-PP-dolichol intermediate on the cytosolic side of the ER membrane, the intermediate is transferred with the aid of flippase into the ER lumen, where the oligosaccharide assembly pathway synthesizes Glc<sub>3</sub>Man<sub>9</sub>GlcNAc<sub>2</sub>-PP-dolichol (Harada, 2013). The oligosaccharide thus assembled is transferred to the Asn moiety of nascent polypeptides by oligosaccharyltransferase (OST) forming a GlcNAc-( $\beta$ -N)-Asn bond. The discharged PP-dolichol moiety is then dephosphorylated to form monophosphorylated dolichol (P-dolichol), which can then serve as an acceptor substrate for the next cycle of oligosaccharide assembly (Harada, 2013).

The normal N-glycosylation requires the completely-assembled Lipid-Linked Oligosaccharides (LLO) as the optimal glycan donor substrate, however, genetic and environmental factors greatly influence the highly ordered biosynthesis and transfer of LLOs. The intracellular pool of the nucleotide sugars UDP-GlcNAc, GDPMan, and UDP-Glc, which are essential precursors for the biosynthesis of LLOs, are regulated by

glucose metabolism (Harada, 2013). Under a low-glucose environment induces arrest and the premature degradation of LLOs and release of phosphorylated monosaccharides from the LLO assembly, resulting in the synthesis of extensively truncated premature LLOs, thereby increasing risk of abnormal N-glycosylation (Harada, 2013). Following, the transfer of the oligosaccharide onto the protein, this initiating event is followed by a “trimming” process, in which various glycosidases hydrolytically remove several monosaccharide units from the attached glycan to expose the pentasaccharide core (Khmelnitsky, 2004). The resulting glycoprotein then undergoes further processing by a variety of glycosyltransferases that add back various sugars to the pentasaccharide to produce a wide diversity of oligosaccharide structures (Khmelnitsky, 2004). The whole process occurs co-translationally, i.e., during protein synthesis but before the final protein molecule is formed and adopts its final conformation (Khmelnitsky, 2004). N-glycan branching produced in the Golgi is dependent upon the sequential yet incomplete action of the Golgi  $\alpha$ -mannosidases and N-acetylglucosaminyltransferases I, II, IV, and V (encoded by Mgat1, 2, 4, and 5), along with hexosamine pathway production of the substrate uridine diphosphate N-acetylglucosamine (UDP-GlcNAc) (Grigorian, 2012). Additionally, the UDP-GlcNAc synthetic pathway is complex as it is a nexus of glucose, nucleotide, fatty acid and amino acid metabolic pathways. Thus, the metabolic flow of glucose modulates the branching patterns of N-glycans via UDP-GlcNAc concentrations because many of the key GlcNAc transferases that determine the branching patterns have widely different  $K_m$  values for UDP-GlcNAc ranging from 0.04 mM to 11 mM (Nakajima, 2013).

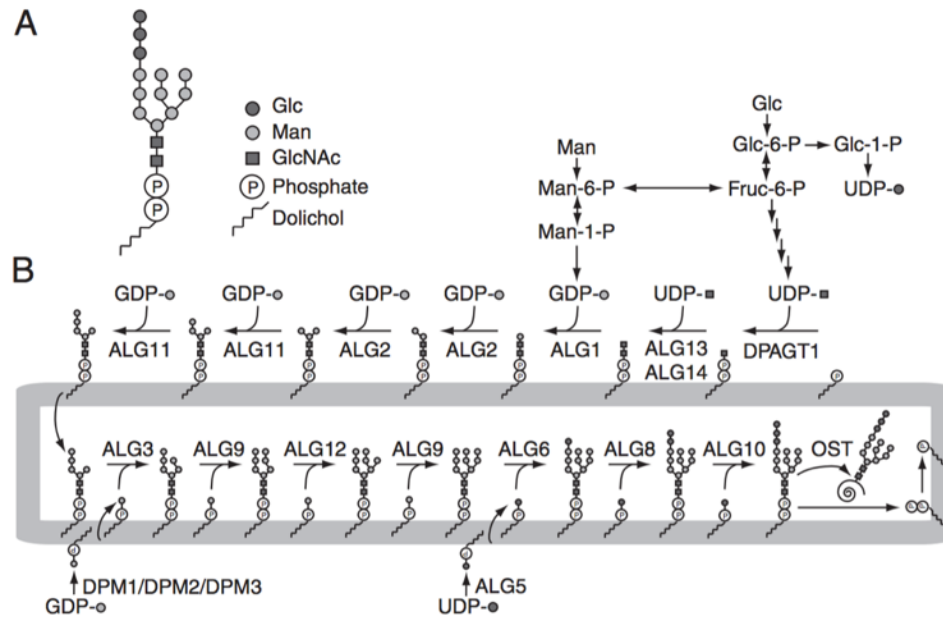


Figure 7: Model for N-glycoprotein biosynthesis in mammals. (A) Structure of fully assembled Glc<sub>3</sub>Man<sub>9</sub>GlcNAc<sub>2</sub>-PP-dolichol. (B) Model for the biosynthetic pathway and transfer of DLOs to proteins. Fruc-6-P, fructose 6-phosphate; Glc-1-P, glucose 1-phosphate; Glc-6-P, glucose 6-phosphate; Man-1-P, mannose 1-phosphate; Man-6-P, mannose 6-phosphate. This figure was adapted from (Harada, 2013).

Sialic acids are a family of nine carbon alpha-keto acids involved in a wide variety of biological functions in nature (Tanner, 2005). These sugars are major determinants of cellular recognition and adhesion events, often found at the distal ends of cell surface glycoconjugates (Tanner, 2005) and secreted glycoproteins (Tangvoranuntakul, 2003). In certain strains of pathogenic bacteria, they are found in capsular polysaccharides that mask the organism from the immune system by mimicking the exterior of a mammalian cell (Tanner, 2005). Their negative charge at physiological pH, a result of their low acid-base disassociation constant, endows sialic acids with unique properties among other sugar moieties and has proven to be very important for several biological processes (Inoue, 2010). Protein sialylation is the penultimate of a very complex process involving numerous glycosyltransferases, following specific sugars being trimmed in the Golgi, the terminal sialic acid is finally added by a sialyltransferase

in the Golgi (Li, 2012). In nature, sialic acids are subject to a remarkable number of modifications, generating a diverse repertoire of more than 50 structurally distinct forms (Angata, 2001), but the most common ones are N-acetylneuraminic acid (Neu5Ac) and N-glycolylneuraminic acid (Neu5Gc) (Li, 2012). Most mammals express both of these sialic acid structures, except humans only possess Neu5Ac (Kavaler, 2011). Humans cannot synthesize Neu5Gc due to an inactivating mutation of a gene occurring in the human species around 3 million years ago (Tangvoranuntakul, 2003). In mammalian organisms, CMP-Neu5Ac is generated in the nucleus in a multi-step process by the action of three enzymes, UDP-N-acetylglucosamine 2-epimerase, Sialic acid synthase and NeuNAc-9-phosphatase (Li, 2012). The biosynthesis of the most common sialic acid, NeuNAc, begins with the formation of N-acetylmannosamine (ManNAc) from UDP-N-acetylglucosamine (UDP-GlcNAc) (Angata, 2002). In the following step, ManNAc is then phosphorylated to yield ManNAc 6-phosphate (ManNAc-6P) (Angata, 2002). Then condensation of either ManNAc or ManNAc-6P with phosphoenolpyruvate occurs to give NeuNAc or NeuNAc-9P (Angata, 2002, Li, 2012). In mammals, NeuNAc-9P is then dephosphorylated to generate NeuNAc by NeuNAc-9-Phosphatase (Tanner, 2005). Dephosphorylation of Neu5Ac-9-P allows the Neu5Ac to then be transported into the nucleus. CMP-sialic acid synthase catalyzes the conjugation of Neu5Ac onto the activated nucleotide cytidine triphosphate forming CMP-Neu5Ac and diphosphate (Tanner, 2005). CMP-sialic acid transporters then shuttle the CMP-Neu5Ac into the Golgi. Refer to Figure 8 for a schematic of the synthesis and reactions of CMP-Neu5Ac.

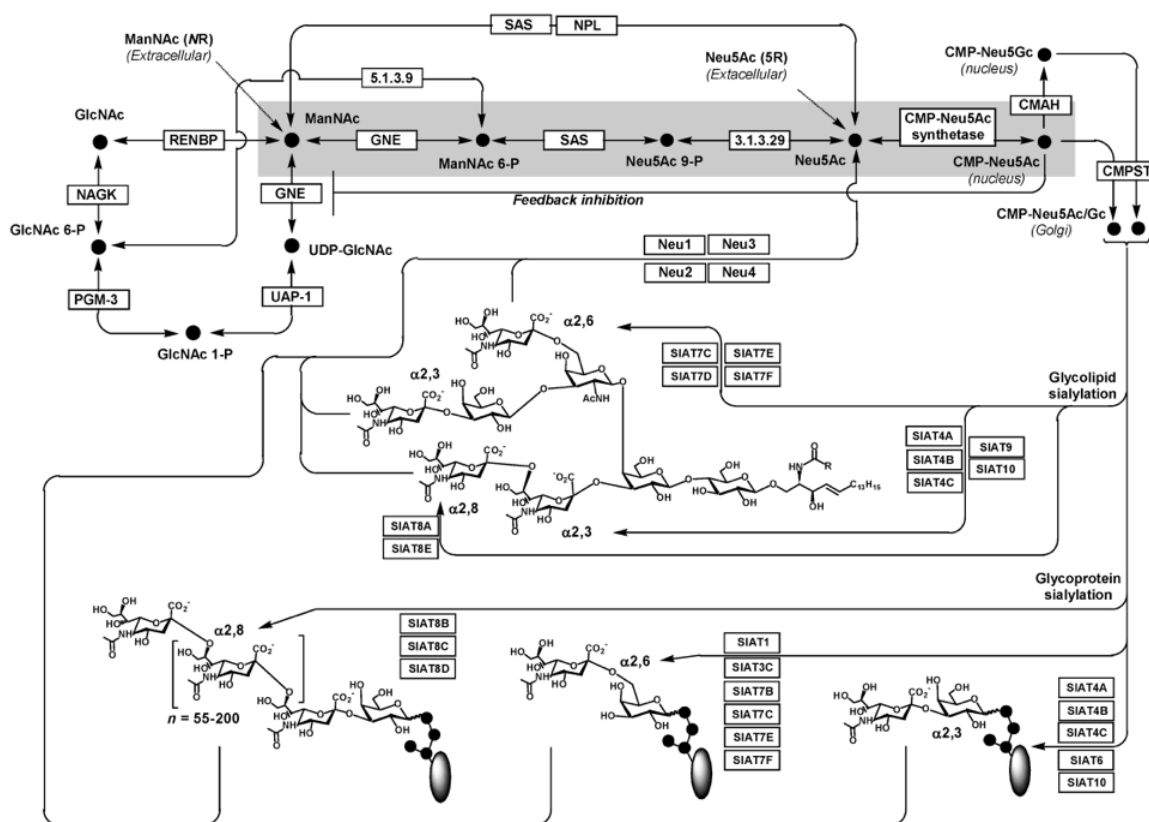


Figure 8: Metabolic details of sialoglycoconjugate biosynthesis. Upon production of the CMP-Neu5Ac “building blocks”, these compounds contribute a sialic acid residue during the assembly of sialoglycoconjugates. The final biosynthetic step is catalyzed by a suite of sialyltransferases (SIATnx) that work in parallel to provide  $\alpha$ 2,3-,  $\alpha$ 2,6-, or  $\alpha$ 2,8-linked sialoglycoconjugates. This figure was adapted from (Murrell, 2004).

CMP-sialic acid is the substrate for all sialyltransferases that incorporate these keto acid into glycoproteins and glycolipids (Tanner, 2005). Increased attention has been given to sialic acids as they have been shown to be important in a wide range of cellular functions and human disease states. Sialylation is associated with several physiological and pathological processes such as nervous system embryogenesis, cancer metastasis, immunological regulation and bacterial and viral infection (Li, 2012). Given this importance, certain enzymes related to sialic acid metabolism, such as sialic acid synthases, sialyltransferases, sialidases and sialic acid modification enzymes, are all potential targets for drug development (Li, 2012). While the activation and transfer

processes of sialic acids are conserved across bacteria to humans, the location of these enzymes differs between the two organisms (Li, 2012). The sialic acid content of proteins was found to be related to the proteins' circulatory retention time (Fukuda et al. 1989; Goldwasser et al. 1974; Higuchi et al. 1992). The proposed mechanism was that when exposed galactose residues of the glycan are recognized by the asialoglycoprotein receptor (ASPR), this induces binding of the protein and initiation of a protein degradation process (Morell et al. 1968). Thus, glycoproteins with sialic acid can evade the capture of the ASPR. Since then, the strategy of increasing the total sialic acid content of proteins was employed to prolong several biotherapeutics' circulation retention time such as acetylcholinesterase (Chitlaru et al. 2002), butyrylcholinesterase (Schneider et al. 2014), tissue plasminogen activator (Weikert et al. 1999) and erythropoietin (Egrie et al. 2003).

Modifying medium and feed, optimizing culture process, and engineering genetic elements of the cell are three major approaches for fine-tuning N-glycosylation patterns of recombinant proteins leading to the possibility of controlling protein N-glycosylation in cell culture (Fan, 2015). Modification of the medium and feed has the advantage of achieving successful N-glycosylation modulation in a relatively fast and easy process independent of cell line genetics (Fan, 2017). It is therefore often favored to be applied in the later stage of industrial bioprocess development when a production cell line has already been developed (Fan, 2017). Classical culture components such as glucose, galactose, amino acids,  $\text{NH}_4^+$ , and many feed additives, such as manganese, sodium butyrate, and nucleotide and nucleotide sugar precursors, have been shown to be able to modulate protein N-glycosylation in cell culture (Fan, 2017). Hills et. al

(2001), proposed that Fc N-glycan processing, specifically galactosylation and sialylation, can be improved by metabolic control of the level of the respective nucleotide sugar substrate in cells. As similar studies utilizing other recombinant glycoproteins produced by animal cells in culture demonstrated that N-glycosylation can be altered through the addition of nucleotide sugar precursors to the cell culture medium (Hills, 2001). With respect to the control of N-glycan processing in animal cells in culture, the latter concept is based on the general hypothesis that addition of specific metabolic intermediates involved in nucleotide sugar biosynthesis to the culture medium will promote metabolic flux toward a specific nucleotide sugar (Hills, 2001). Consequently, the altered transport and availability of that nucleotide sugar substrate within the Golgi lumen would promote specific alterations in nucleotide sugar availability and subsequent N-glycan processing (Hills, 2001). Recently, Yin et. al (2017), have discovered a novel sugar analog, 1,3,4-O-Bu<sub>3</sub>-ManNAc, capable of enhancing sialic acid production and biotherapeutic sialylation in CHO cells. This analog was used to stimulate sialic acid production discussed later in chapter 4. The molecular structure and its incorporation into the metabolic pathway is shown in Figure 9.

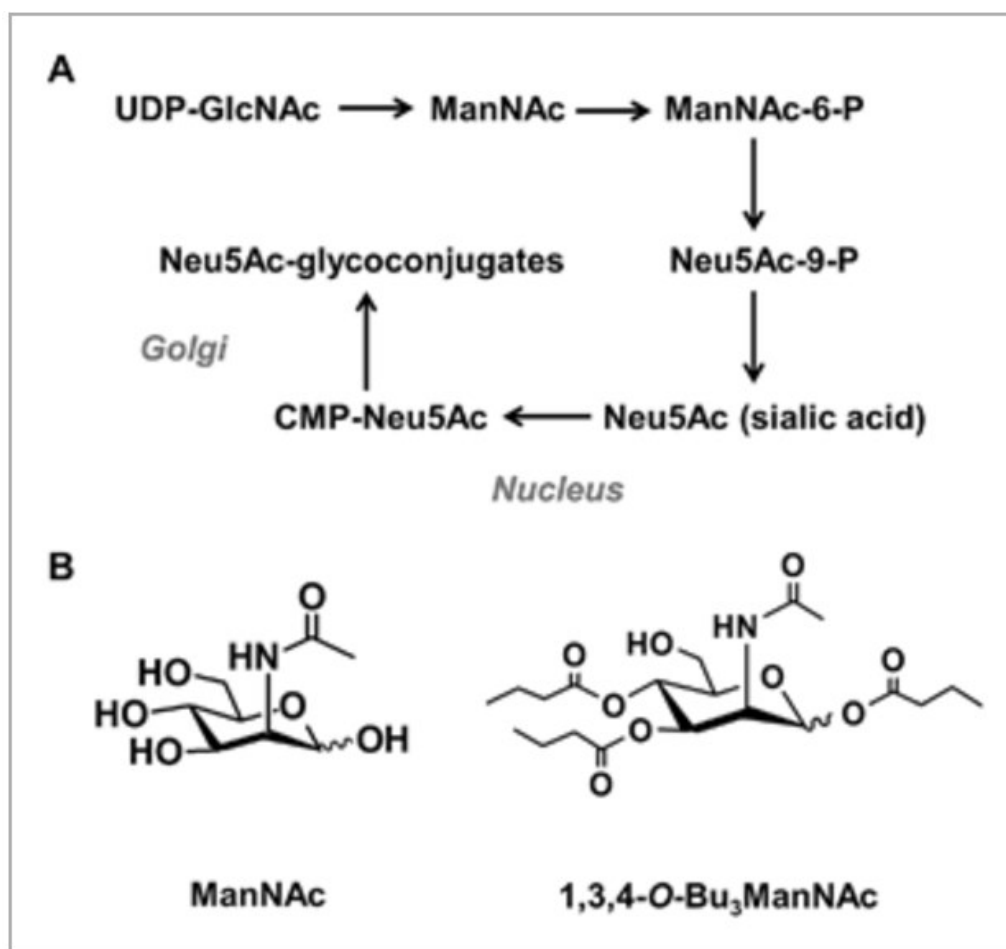


Figure 9: (A) Sialic acid synthesis pathway; (B) structures of ManNAc and its analog. This figure was adapted from (Yin et. al, 2017)

Chinese hamster ovary (CHO) cells have emerged as the predominant platform for the heterologous production of biotherapeutic proteins mainly due to their well characterized molecular biology, unparalleled adaptability, the ability to grow in both adherent and serum-free suspension cell cultures, long-term success in industrial scale production, and most importantly in their ability to generate appropriate post-translational modifications most similar to that of humans (Fan, 2017). Furthermore, studies in the late 1980's revealed that human viral contaminations such as HIV, polio, herpes, and measles, do not replicate in CHO, thus outweighing the use of human cells as biological production hosts (Wiebe, 1989). CHO cells are thus an ideal platform capable



of the biosynthetic complexity required to produce biopharmaceuticals. Fed-batch CHO cell culture is the most commonly used process for IgG production in the biopharmaceutical industry (Templeton, 2013). Amino acid and carbohydrate composition, cell growth, metabolism, titer, and glycosylation patterns have always been the major concerns during upstream process optimization, especially media optimization (Fan, 2015). Thus, being able to monitor these parameters would be of great asset to understand the impact of each towards concerted efforts to direct the glycosylation pattern. However, the adaptability of the CHO line also has its drawbacks, as each production target requires the selection of clones that exhibit the necessary phenotypic properties, such as product quality/uniformity, doubling time and long term viability, under the used bioprocess conditions (Jadhav, 2013). Even when an appropriate CHO production clone has been identified, phenotypic drift (i.e. changes in the previously selected characteristics) is not uncommon and remains a challenge (Jadhav, 2013). Glycosylation is subject to changes during fed-batch cultures by disturbing the complex interaction of multiple components including metal cofactors, nucleotides, nucleotide sugars and the acceptor sugars itself (Villiger, 2016). Manipulation of these components using various cell culture supplementations is a cost- and time-effective way to modulate and fine-tune glycosylation, since the degree of glycosylation is mainly changed through a shift of intracellular compounds or glycosyltransferase activities while maintaining consistent process performance. Metal cofactors such as manganese have been applied to enhance the enzymatic activity leading to more processed glycan structures (Villiger, 2016). Supplementing cell culture media with glucosamine, galactose or N-acetylmannosamine has been shown to increase the corresponding intracellular levels of

nucleotide sugars uridine diphosphate N-acetylglucosamine (UDP-GlcNAc), uridine diphosphate galactose (UDP-Gal) or cytidine diphosphate N-acetylneuraminic acid (CMP-Neu5Ac), respectively (Villiger, 2016). As nucleotides are precursors to nucleotide sugars, their nucleotide synthesis is an energy intensive process that uses multiple metabolic pathways across different cell compartments and several sources of carbon and nitrogen (Lane, 2015). These processes are regulated at the transcription level by a set of master transcription factors but also at the enzyme level by allosteric regulation and feedback inhibition, and at different stages of the cell cycle, during which these events are regulated at multiple levels (Lane, 2015). The nucleotide pools play an ambivalent role in terms of glycosylation since they can either increase the concentration of nucleotide sugar donors or act as enzyme inhibitors in their (di)-phosphorylated forms inside the Golgi as shown in Figure 6 (Villiger, 2016). Furthermore, combinations of different factors such as galactose, uridine and manganese have been found to have synergistic effects on N-linked glycosylation (Villiger, 2016). Refer to Table 1 for a comprehensive examination of how precursor feeding affects the nucleotide sugar levels.

Table 1: Comparison of effectiveness of reported nucleotide sugar feeding experiments. This table was adapted from (Wong, 2010).

Cell line/product	Nucleotide sugar precursor	Culture summary <sup>a</sup>	Effect on nucleotide sugar/nucleotide levels	Effect on glycosylation	Refs. <sup>b</sup>
BHK-21/IL-2 variant	Glucosamine (10 mM)	Bioreactor; 2.5 L; continuous	3× increase in UDP-HexNAc	11% and 12% increase in tri- and tetra-antennary branching respectively	Gawlitzek et al. (1998)
BHK-21/IL-2 variant	Glucosamine (12.5 mM) + uridine (2 mM)	Bioreactor; 2.5 L; continuous	26× increase in UDP-HexNAc; 9× increase in UTP; maintenance in ATP levels	4% and 8% increase in tri- and tetra-antennary branching respectively No change in sialylation	Grammatikos et al. (1998)
CHO/IFN-γ	ManNAc (0.2–40 mM)	Shake flask; 20–50 mL; batch	Up to 30× increase in CMP-sialic acid (SA)	Up to 15% increase in sialylation	Gu and Wang (1998)
CHO/none; small cell lung cancer/none	Glucosamine (3.5 mM) ± uridine (1 mM)	Well-plates; 1.25–4 ml; batch	Not reported; 6–25× increase in UDP-HexNAc	Between 55% and 75% decrease in polysialylation; between 20% and 90% decrease in polysialylation	Zanghi et al. (1998)
CHO/TNFR-IgG	Glucosamine (5 mM)	Bioreactor; 1.8 L; batch	1.7× increase in UDP-HexNAc	No change in sialic acid content or % terminal galactosylation	Gawlitzek et al. (2000)
NS0/TIMP-1; CHO/TIMP-1	Glucosamine (10 mM) + uridine (2 mM)	Spinner flask; 400 ml; batch	18–60× increase in UDP-HexNAc; 3–8× increase in UDP-Hex; 2–5× increase in CMP-SA	Up to 14% increase in mean antennae per <i>N</i> -glycan and 8% decrease in sialylation	Baker et al. (2001)
	ManNAc (20 mM)		12–28x increase in CMP-SA; 2× decrease in UDP-Hex (NS0)	No change in mean antennae per <i>N</i> -glycan and % sialylation	
GS-NS0/humanized IgG	Galactose (10 mM)	Spinner flask; 200 ml; batch	No increase in UDP-HexNAc and UDP-Hex	6% increase in mean galactosylation	Hills et al. (2001)
	Glucosamine (10 mM)		17× increase in UDP-HexNAc; 3× decrease in UDP-Hex	56% decrease in mean galactosylation	
	ManNAc (20 mM)		13× increase in CMP-SA; 3× increase in UDP-HexNAc; 2× decrease in UDP-Hex	9% decrease in mean galactosylation	
CHO/EPO	Glucosamine (10 mM)	Spinner flask; 250 ml; batch	18.5× increase in UDP-HexNAc pools	~19% decrease in tetra-antennary branching; 41% decrease in tetra-sialylated glycans	Yang and Butler (2002)
CHO/IL-4/13 cytokine trap fusion	Galactose (20 mM)	Spinner flask; 1 L (flask volume); batch	Not reported	No change in sialylation	Clark et al. (2005)

<sup>a</sup> Culture summary includes details of culture system, working volume (unless otherwise specified) and mode.

<sup>b</sup> References are mainly limited to reports of nucleotide sugar precursor feeding in cell lines which produce recombinant proteins.

When culture medium and feed supplement medium are chosen, modification of these media can be done by addition of different amounts of feed additives or feed

additive combinations, including, but not limited to, glucose, glutamine, other amino acids, galactose, sodium butyrate, uridine, manganese, and other nucleotide sugar precursors (Fan, 2017). In particular, extracellular and intracellular metabolic analysis is very commonly used in exploring metabolic bottlenecks in cell culture and provides guidance for further optimizing the medium and feed (Fan, 2017). Towards this goal, development of a toolset to provide inputs to defining such acceptable criteria during the manufacturing campaign, through HPLC-based methods to determine the amino acid composition, glycosylation patterns, nucleotide sugar distributions and titer were established.

Numerous factors influence cellular carbohydrate composition, and the combination of biochemical and metabolism-based approaches in conjunction with omic's methods will accelerate efforts towards understanding glycosylation (Yarema, 2001). Integration of cellular engineering (through enzyme knockout/knock-ins), feeding strategies, detailed metabolic analysis, and glycan analysis may uncover the fundamental intricacies in cellular physiology. As the intracellular metabolism directly impacts glycosylation and biologic activity at scale, gaining knowledge on a systems level interaction network would provide insight into obtaining higher IgG titers and better control of glycosylation-related product qualities. Furthermore, this systems biology approach may provide clues to enhance production capabilities by revealing rational strategies for cell line selection and process development. Towards this goal a more in-depth physiological understanding of cellular responses to particular process conditions and subsequent detailed glycoprotein characterization is presented with the aim of increasing the sialic acid content on mAbs through use of (Yin et. al, 2017) high-flux

ManNAc analog. This work embarks on a multipronged approach towards achieving uniform, consistent and specified protein glycosylation through development of analytical methodologies to monitor glcCQAs (Chapters 2-4), and by construction of a cell-free bioreactor for In-Vitro Glyco-Engineering (Chapter 5).

## **Chapter 2: N-Glycan Analysis using HILIC-FD**

### **2.1 Introduction**

The status of a protein's glycosylation can reveal highly valuable diagnostic information. For instance, glycomics studies may reveal disposition to diseases such as sialuria and the identification of protein glycans as biomarkers of life-threatening diseases such as cancer. In the biopharmaceutical industry, glycan analysis is of paramount importance, as it has a profound impact on many properties of proteins that can alter the physicochemical properties of the therapeutic such as efficacy, safety and PK/PD profiles (Zhang, 2016). According to the International Conference on Harmonization (ICH) ICH Q5E, ICH Q6B, the FDA's Guidance for Industry; the structure, content, and glycosylation sites should be investigated as thoroughly as possible. However, the assessment of glycan structures is challenging due to the isomeric and branched nature of oligosaccharides (Cook, 2010). Moreover, no method reported can determine the glycosylation site, glycan structure and abundance in a single run. Therefore, the use of complementary and orthogonal methods for appropriately assessing specific glycosylation attributes is required to ensure comprehensive and accurate coverage of glycosylation, thereby providing corroboratory information to clarify instances of inconclusive data. High-performance liquid chromatography (HPLC), High pH Anion Exchange Chromatography-Pulsed Amperometric Detection (HPAEC-PAD), capillary electrophoresis (CE), mass spectrometry (MS), isoelectric focusing (IEF), and lectin-based microarray (Zhang, 2016), are typical methods employed to study glycan attributes, each with specific advantages and disadvantages, and are industry standards in glycan analysis (Cook, 2015). Prior to separation and detection, glycans enzymatically or chemically released from the protein. A drawback of this approach is that it captures a

protein's global glycosylation pattern, as opposed to site-specific profiling, which results in an average determination of glycans present. Following release, the complex mixture of oligosaccharides present then requires high-efficiency separation techniques prior to characterization, typically accomplished by mass spectrometry (MS). Detection by light absorption, i.e. Ultraviolet (UV) detection, cannot be used at this stage because glycans lack chromophores. To circumvent this limitation, HPAEC-PAD combines a unique mode of separation with a selective detective strategy through oxidation of functional groups by specifically applied voltages on an electrode that is sensitive only to carbohydrates. However, MS and HPAEC-PAD equipment is expensive, requires substantial maintenance, and highly-trained personnel to operate and interpret data. The more commonly used approach is to label the glycans with a fluorescent molecule, followed by HPLC with fluorescence detection. Among the fluorescent molecules that can be used for tagging carbohydrates, 2-aminobenzoic acid and 2-aminobenzamide (2-AB), are the most commonly used when HPLC is the selected separation technique (Cook, 2016). The tagging protocol with 2-AB is relatively simple, results in negligible desialylation, and is quantitative (Cook, 2016). Moreover, glycans and 2-AB are strongly bound through an amide bond, thus the tagged molecules have excellent stability (Cook, 2016).

Variations in the N-linked glycan profile (macro- and micro-heterogeneity) can occur during the mAb production process. Studying the impact of various environmental factors and process conditions will increase understanding of the glycosylation machinery and provide the potential to control and target desired mAb glycoforms. Multiple cell culture conditions during upstream processing such as different feeding regimes, media

supplementation, as well as waste metabolite accumulation can affect glycosylation (Ivarsson, 2014). Limiting glucose concentrations in fed-batch culture showed a reduction in terminal galactosylation for a chimeric heavy chain antibody (Ivarsson, 2014). Moreover, supplementation with manganese chloride, galactose and uridine can provide control over galactosylation during fed-batch cultivation (Ivarsson, 2014). Aside from metabolic control, bioreactor process parameters such as pH, temperature, dissolved O<sub>2</sub> and CO<sub>2</sub> levels, and shear stress through agitation and sparging can lead to variability in the glycoform profile and thus, play an important role in manipulating and actively controlling the product quality (Ivarsson, 2014). While the impact of process parameters on N-linked glycosylation has been summarized in literature (Butler, 2006; Hossler, 2009), the effects shown are often incoherent and incomplete, and therefore do not allow general conclusions. This is partly due to the fact that glycosylation is dependent on the 3-dimensional structure of the protein, the enzyme repertoire of the host cell, the transit time in the Golgi and the availability of intracellular sugar-nucleotide donors (Butler, 2006).

IgG plays important roles in both innate and adaptive immunities, in which the state of glycosylation provides the capacity to regulate the intrinsic underlying IgG functions through glycan-dependent structural effects in the receptor-binding regions of the hinge/CH2 and CH2/CH3 domains (Jefferis, 2009). These IgG glycoform conformational variants differentially interact with the FcγRs and other receptors variously expressed on immune cells and other cells throughout the body. Therefore, the absence or modification of Fc glycans can profoundly affect the therapeutic performance of mAbs by modulation or loss of intended functions, greater immunogenicity, and



unfavourable pharmacokinetic profiles (Jefferis, 2009). The glycans of IgG Fc are incomplete structures with varying amounts of branch N-acetylglucosamine and terminal galactose, and generally minimal sialylation (Jefferis, 2009). Human IgG Fc N-glycans have a very high degree of core fucosylation and a low degree of bisecting N-acetylglucosamine (Jefferis, 2009). Immunoglobulin G (IgG) with  $\alpha$ -2,6 sialylation has been reported to have an impact on antibody-dependent cellular cytotoxicity and anti-inflammatory efficacy (Chung, 2017). Due to the inaccessibility of sialyltransferases for the heavy chain N-glycan site, production of antibodies with  $\alpha$ -2,6 sialylation from CHO cells is challenging, since CHO cells exclusively possess  $\alpha$ -2,3 sialyltransferases (Chung, 2017). Chung et. al demonstrated through combining mutations on the Fc regions to allow sialyltransferase accessibility in combination with overexpression of  $\alpha$ -2,6 sialyltransferase, IgGs were produced with significant levels of both  $\alpha$ -2,6 and  $\alpha$ -2,3 sialylation as determined by MS.  $\alpha$ -2,3 sialylation was disrupted by CRISPR/Cas9 targeting the ST3GAL4 and ST3GAL6 genes (Chung, 2017). Resulting in  $\alpha$ -2,3 linked sialic acids not detected on IgG produced from the  $\alpha$ -2,3 sialyltransferase knockout- $\alpha$ -2,6 sialyltransferase overexpression pools (Chung, 2017). Glycoprofiling of IgG with four amino acid substitutions expressed from an  $\alpha$ -2,3 sialyltransferase knockout- $\alpha$ -2,6 sialyltransferase stable clones resulted in more than 77% sialylated glycans and more than 62% biantennary disialylated glycans as indicated by both MALDI-TOF and LC-ESI-MS (Chung, 2017). In this study, the N-glycans from three of the genetically engineering mAbs (Chung, 2017) were analyzed by HILIC-FD. This chapter describes a complete workflow for the analysis of Immunoglobulin G (IgG) protein N-glycans. The sample-preparation procedure, consisting of IgG purification, then release of the N-

glycans by PNGase-F, followed by fluorescence labeling with 2-aminobenzamide (2-AB), removal of excess label, and separation and detection by HILIC-FD. Because 2-AB-glycans are hydrophilic compounds, the HPLC separation technique most frequently chosen is hydrophilic interaction liquid chromatography (HILIC) with fluorescence detection. The results were shown to distinctive elution profiles in each antibody studied, thus verifying the effects of the applied protein and cellular engineering strategies. To demonstrate the accuracy of the method the antibody samples were additionally analyzed by an orthogonal method, MALDI-ToF. The consistency of the results between these two methods demonstrates the reliability of the glycan analysis method introduced herein.

## 2.2 Methods & Materials

2-Aminobenzoic Acid (2-AB, Sigma Aldrich)  
Dimethylsulfoxide (DMSO, Sigma Aldrich)  
Acetic Acid (Sigma Aldrich)  
Milli-Q H<sub>2</sub>O (house tap)  
Trifluoroacetic acid (TFA), Fisher #A116-05amp or equivalent  
Acetonitrile, HPLC grade, Fisher #BPA998-4  
1-Propanol: Fisher #A414-4  
Ammonium Hydroxide 21%, Fisher #A470-250  
Formic Acid, Proteochem #LC6201-10amps  
Hydrochloric Acid, Fisher #SA49  
Carbograph Column (3.0mL, Grace)  
MabSelect SuRe protein A resin (Sigma Aldrich)  
Waters Xbridge Amide column, 3.5  $\mu$ m, 2.1 x 150 mm (# 186004861)  
Acetic acid (Fisher Scientific, Cat. # AC222140010)  
Dimethyl sulfoxide (DMSO) (Fisher Scientific, Cat. # AC397600010)  
2-Aminobenzamide (2-AB) (Sigma-Aldrich, Cat. # A89804)  
Sodium cyanoborohydride (NaBH<sub>3</sub>CN) (Sigma-Aldrich, Cat. # 156159)  
Maltotetraose (DP4) (Sigma-Aldrich, Cat. # 47877)  
PNGase F (Promega Corporation, Cat. # V4831)  
Tris-HCl (Sigma Aldrich)  
Glycine (Sigma Aldrich)  
Speedvac  
Agilent 1260 quaternary solvent delivery with FLD, PDA, and Column Oven

### 2.2.1 IgG protein purification using Protein-A Agarose Beads

1. Samples from cell culture are centrifuged at  $4500 \times g$  for 20 min.
2. Filter the supernatant through a 0.22  $\mu$ m low protein-binding filter.
3. Then apply onto a MabSelect SuRe ProteinA column, into which 200  $\mu$ L of MabSelect SuRe protein A resin slurry is packed.
4. Equilibrate the column with 2 mL of  $1 \times$  PBS.
5. Load the filtered supernatant into the column and repeat for at least two times to ensure sufficient binding of IgG to the column.
6. Wash the column with 4 mL of  $1 \times$  PBS, perform twice.
7. Elute IgG by 500  $\mu$ L of 0.1 M citrate pH = 3.5.
8. Neutralize the pH of eluate by adding 1 M Tris-HCl, pH 9.0.
7. Separate the IgG from the beads by performing a centrifugation step at 3000rpm for 5 minutes.
8. Collect the supernatant, as this contains the purified IgG, being careful not to disturb the pellet.
9. Dialyze the IgG into an appropriate buffer for next steps, e.g. 10mM Ammonium Bicarbonate using Amicon Ultra flow filter unit with molecular weight cut-off (MWCO) 30 kDa (Millipore).

### **2.2.2 Release of Glycans**

1. Release the N-Glycans by adding 1uL PNGase F (New England Biolabs) per 50µg protein.
2. Incubate the reaction overnight in a 37°C incubator.
3. Purify the released glycans using Extract-Clean SPE Carbograph columns (Grace).
4. Add 3 mL of acetonitrile (100%) to carbograph cartridge.
5. Add 3 mL of 1% TFA, repeat once.
6. Load sample to Carbograph, allow sample solution penetration to cartridge by gravity.
7. Re-load the flow-through to Carbograph for an additional time.
8. Wash cartridge with 3 mL of 0.1% TFA, repeat four additional times.
9. Wash cartridge with 3mL of 0.1% TFA in 10% acetonitrile.
10. Elute sample with 400 µL of 0.1% TFA in 80% acetonitrile, repeat once.
11. Dry sample solution in SpeedVac at 37°C.

### **2.2.3 Preparation of 2-AB Labeling Solution**

1. To make 400 µl 2-AB labeling solution, add 20 mg 2-aminobenzamide into 200 µl solvent (150 µl glacial acetic acid + 350 µl Dimethyl sulfoxide).
  2. Add 25 mg NaBH<sub>3</sub>CN into 200 µl solvent (as above).
  3. Combine equal volumes of both solutions.
  4. Total volume can be adjusted based on the amount of 2-AB ingredient weighted.
- CAUTION: NaBH<sub>3</sub>CN should be handled in a fume hood. Less toxic 2-picoline borane with same molar concentration can be used as alternative to NaBH<sub>3</sub>CN.

### **2.2.4 2-AB Labeling Conditions**

1. Add 5µl of the 2-AB labeling Solution to each dried glycan sample. Cap and mix thoroughly. Tap or spin down to collect the dissolved sample in the bottom of each vial.
2. Incubate glycan samples for 3 hours at 65°C in a heating block, dry oven, or sand tray.  
Note: Incubation periods of 2–4 hours will not significantly affect results.
3. If insoluble particulates are present, vortex the pre-heated samples from step 5 for 30 minutes.
4. Following incubation, briefly spin the vials to recollect each sample at the bottom of the reaction vial.
5. Allow the samples to cool to ambient temperature prior to proceeding with post-labeling analysis.
6. Purify the labeled glycans using Extract-Clean SPE Carbograph columns (Grace).
7. Elute the glycans was eluted with 80% acetonitrile (0.1% formic acid).
8. Dry the purified glycans in a Speedvac.
9. Reconstitute the labeled glycans in 25uL H<sub>2</sub>O and mix with acetonitrile for a final concentration of ~75% organic to facilitate binding.

### 2.2.5 Chromatographic Conditions for High-Resolution of N-Glycans

HPLC System: Agilent 1260 quaternary solvent delivery

Detectors: FLD (Excitation 330nm and Emission 420nm) and PDA (Abs. 215nm)

Column Thermostat: 45°C

Column: Waters Xbridge Amide column, 3.5 µm, 2.1 x 150 mm

Mobil Phase A: 100mM Ammonium Formate pH 4.50

Mobil Phase B: 80% 1-Propanol, 10% AcN, 10% H<sub>2</sub>O, 0.05% TFA

Flow Rate: 0.5 mL/min

Injection Volume: 25µL

Gradient Conditions:

Table 2: Optimized Gradient Conditions for N-Glycan Analysis

<b>Time (min)</b>	<b>A %</b>	<b>B %</b>
0	5	95
3	5	95
59	25	75
60	100	0
61	100	0
62	5	95
70	5	95

## 2.3 Results

In (Chung, 2017), two different anti-grass pollen IgGs (gpIgG1) were developed to enhance certain glycosylation features, in addition to maintaining the wild-type. Specifically, gpIgG1 (wild-type), gpIgG1F241A from CHOK1 cells (incorporating a mutation of F->A to enhance glycosyltransferases accessibility to N297), and gpIgG1 from a CHO 2,3-sialyltransferase knock-out cell line. In (Chung, 2017) MALDI-TOF glycoprofile analysis of these IgGs from different CHO cell lines were performed to observe the glycosylation profile of each type, shown in Figure 10.

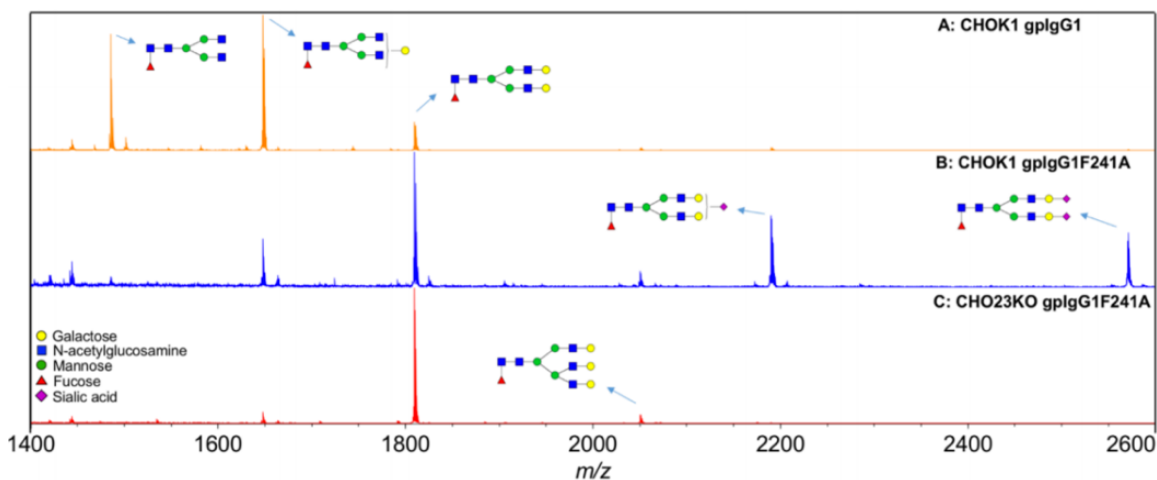


Figure 10: MALDI-TOF glycoprofile analysis of IgGs from different CHO lines. (a) Glycoprofile analysis of gpIgG1 and single amino acid mutants expressed from CHOK1 and CHO23KO cells. N-glycan analysis of gpIgG1 from CHOK1 cells from a previous study (Chung et al. 2016) (Panel A), gpIgG1F241A from CHOK1 cells (Panel B), and gpIgG1 from CHO23KO cells (Panel C). This figure was adapted from (Chung, 2017).

Each mAb type was then subjected to n-glycan analysis via HILIC-FD, as described in the methods section. However, the wild-type sample (shown in Figure 10a) was apparently too old ~4 years, and resulted in no glycan peaks observed. Data not shown. The results of the analyses are shown in Figures 11-14. The relative abundance of each glycoform was calculated by measuring peak area of a certain glycoform and

dividing by the total of all identified glycan peaks using the ChemStation software.

However, as results were not able to identify due to lack of standards, no conclusions could be drawn as to the ratios of which peaks corresponded to what area, therefore this data was omitted.

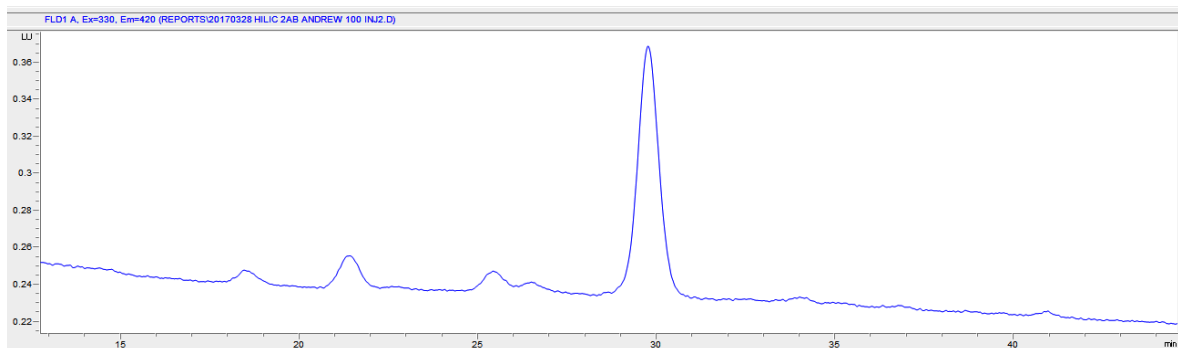


Figure 11: HILIC-FD N-glycan analysis of gpIgG1F241A from CHOK1 cells.

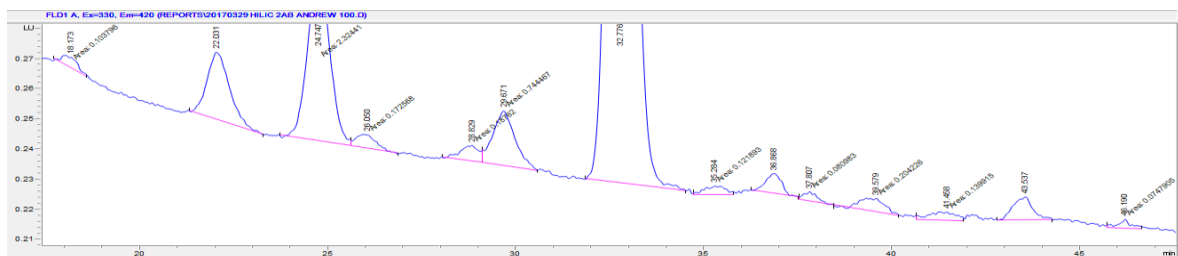


Figure 12: Zoom-in of HILIC-FD N-glycan analysis of gpIgG1F241A from CHOK1 cells.

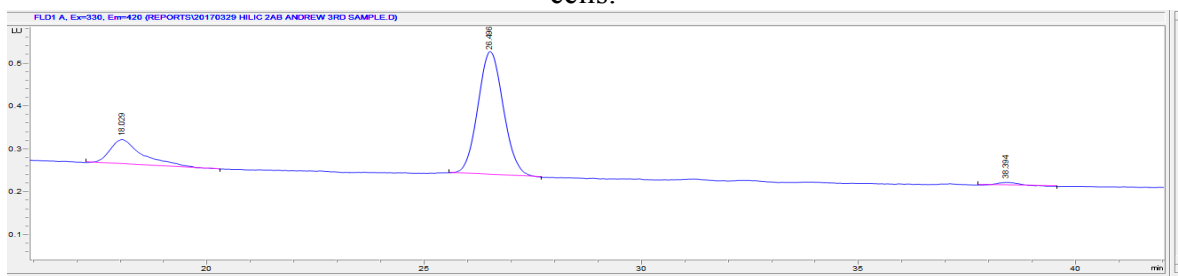


Figure 13: HILIC-FD N-glycan analysis of gpIgG1 from CHO23KO cells.

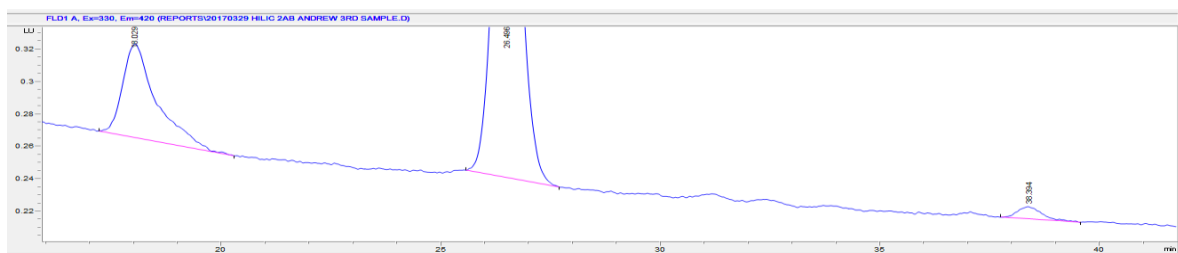


Figure 14: Zoom-in of HILIC-FD N-glycan analysis of gpIgG1 from CHO23KO cells.

2.3.1 HILIC-FD glycan analysis of gpIgG1F241A from CHOK1 cells.

2.3.2 HILIC-FD glycan analysis of gpIgG1 from CHO23KO cells.

Through comparison of Figures 10-14, some interesting observations can be made. It is unfortunate that the wild-type IgG glycoprofile shown in Figure 10a, did not generate usable data as the other samples clearly show similar glycoprofiles across both methods. The sample shown in Figure 10B does match the profile of Figures 11-12. Similarly is the case for the sample shown in Figure 10C matching the profile of Figures 13-14. MALDI-ToF is a semi-quantitative method thus rendering only relative quantification on the basis of sample comparison. It was the goal of this method to establish a quantitative n-glycan analysis method, however, without standards to identify each glycoform, and then to construct standard curves for each sample, this work must be carried out at a later time.

## **2.4 Discussion**

The glycosylation status of proteins is an inherent source of heterogeneity, where cell line selection, process parameters and production scale all contribute to affecting the glycoform distribution (i.e. the story Genzyme's Myozyme). Therefore, analysis of the glycan pattern is an important issue for characterization studies and quality control in research and biopharmaceutical industries. Pharmaceutical regulatory agencies worldwide have established the general principles for process- and quality-control and risk management in biopharmaceutical manufacturing. The glycan method developed is to address and determine the appropriate limits, ranges (e.g. tolerances) and distributions (e.g. required features) of the N-linked glycosylation profiles of biotherapeutic



glycoproteins to ensure the desired product quality, safety and efficacy. Through careful inspection of glycosylation profiles during product development, scale up, process changes and production may allow the identification of factors or methods that affect glycan patterns or heterogeneity. These observations may in turn isolate potential glycosylation control points to selectively enable production of preferred glycoforms for specific functional purposes.

In this study, glycans were derivatized with the 2-AB fluorescent label producing a neutrally charged, highly stable amide bond between the label and glycan. The labels charge neutrality helps to enhance separation of neutral and negatively charged glycans, and furthermore allows stoichiometric detection, as each N-linked glycan is derivatized on the reducing terminus with one fluorescent tag, thereby reducing the complexity of data interpretation. A drawback of this technique is that it requires additional steps to attach the label and clean-up the glycans prior to chromatography, unlike MS or PAD. Following labeling, HILIC-FD was employed for separation of the glycoforms. HILIC separations are based on a variation of normal-phase chromatography in which the mobile phases consist of polar aqueous and miscible aprotic organic character with the stationary phase being of polar hydrophilic amine/amide-derivatized silica, polymeric or “hybrid-type”. The mechanism of HILIC is such that the eluents pH and ionic strength affect the separation as an increasingly aqueous gradient then separates the analytes on the basis of their relative polarity and solvation. However, the selectivity of this method is hindered by compounds of similar polarity. In the study of glycoanalysis presented here, HILIC separations of glycans was achieved through progressive gradient of 80% 1-Propanol, 10% AcN, 10% H<sub>2</sub>O, 0.05% TFA into 100mM ammonium formate pH 4.5 on

a amide-derivatized silica column. Through comparison of the N-glycan chromatograms to the MALDI-ToF data, the results from the two orthogonal analysis methods demonstrate a strong measure of consistency in the types and amounts of N-linked glycans in the mAbs tested. Thus validating the accuracy and sensitivity of the method presented herein. Future studies would need to incorporate a standard panel of typically observed N-glycans, alternatively use of a Glucose Unit (GU) ladder would aid in the identification of glyco-forms through comparison of their retention times with the ladder, and correlating this with known glyco-databases. Additionally, through construction of calibration curves, absolute quantification of each glycoform could be performed provided availability of each glycoform standard.

## Chapter 3: Amino Acid Analysis

### 3.1 Introduction

Naturally occurring L-amino acids are required for protein synthesis and are precursors for essential molecules, such as co-enzymes and nucleic acids (Bushan, 2001). These molecules exhibit a wide spectrum in their chemical and physical properties such as polarity, hydrophobicity and solubility (Rahman, 2014), see Figure 15 below for their chemical structures and pKa's.

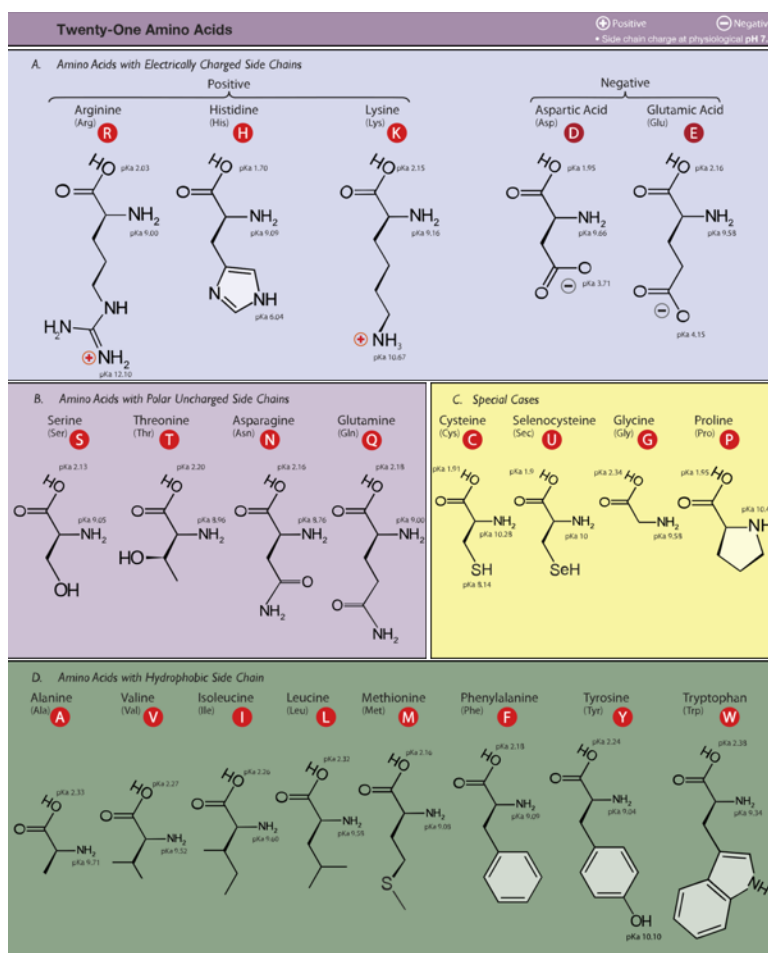


Figure 15: The chemical structures and pKa's of amino acids.

This molecular diversity is the main challenge in achieving quantitative analytical chemistry in a single method with minimal technical variations (Rahman, 2014).

Metabolic profiling on cells (the metabolic fingerprint) and on the cell growth medium (the metabolic footprint) are the complimentary approaches to study pathway(s) and inter-conversion(s) of compounds such as amino acids or carbohydrates (Rahman, 2014). Amino acid analysis (AAA) is a fundamental biochemical technique used in peptide, protein and bio-active metabolites across research, clinical facilities and industrial processes. AAA allows for the determination of the amino acid composition or content of proteins, peptides, tissues, biological fluids, and other samples containing amino groups within their molecular structure. AAA allows for amino acid quantitation of free amino acids such as those found in cell media, as well as amino acids released from macromolecules or cell hydrolysates. As this analytical tool may be used to monitor or detect the topology and operation of cellular metabolism (Millard, 2017), it is highly useful in a metabolic engineering laboratory for the determination of amino acid fluxes, biomass composition, and mass isotopomer distributions (MID) (Millard, 2017). Metabolic Flux Analysis (MFA) experiments require accurate and precise isotopomer measurements (Antoniewicz, 2017), as the mass isotopomer distributions provide additional equations through atom mapping matrices in stoichiometric material balances. Metabolic flux analysis (MFA) provides a powerful approach to map intracellular carbon flows of cultured cells and thereby elucidate the functional behavior of entire biochemical networks, as opposed to studying individual reactions or nodes in isolation (Sauer, 2006). However, it's progress is stifled due to lack of better analytical chemistry methodologies discussed below.

Among the various chromatographic methods for the analytical separation and quantification of amino acids; ion chromatography, gas chromatography, and liquid

chromatographic techniques are the most frequently used (Peace, 2005). AAA methods based on precolumn derivatization procedures have become a popular alternative to the traditional postcolumn derivatization techniques based on ion-exchange separation of the underivatized amino acids (Cohen, 2003). The major reasons for this include greater sensitivity, faster analyses, and the ability to use less expensive, more flexible HPLC instrumentation rather than dedicated amino acid analyzers (Cohen, 2003). Gas Chromatography (GC) can also be used, and in certain cases instrumentation availability or operation costs can make it a better choice. However, the polar nature of amino acids requires derivatization prior to GC analysis. For GC analyses, a silylation reagent N-tert-butyldimethylsilyl- N-methyltrifluoroacetamide (MTBSTFA) is used for the derivatization of amino acids. MTBSTFA, forms tert-butyl dimethylsilyl (TBDMS) derivatives when reacted with polar functional groups containing an active hydrogen, resulting in the substitution of the active hydrogen atoms of OH, NH, and SH groups by a TBDMS moiety. The consequent reduction of the dipole–dipole interaction of the target molecules results in their transformation into molecules of low polarity, increased volatility, and high thermal stability, rendering them amenable to study by GC-MS. Under certain reaction conditions, the majority of the amino acids produce one derivative, however, some amino acids under certain reaction conditions can produce multiple derivatives. Specifically, the amino acids asparagine, glutamine, and tryptophan can produce multiple adducts, rendering their quantitation difficult (Stenerson, 2011). In the case of these amino acids, a modification in the reaction conditions, such as, lowering the temperature or changing the reaction time, may prevent this from occurring (Stenerson, 2011). Asparagine, glutamine and tryptophan

produce multiple reaction products as a result of the TBDMS derivatization, which prevents accurate determination of MID's. As the majority of MFA labs employ GC-MS, they are only able to measure 16 of the 20 natural amino acids. This why current Metabolic Flux Laboratories, despite immense mathematical progress, do not possess the analytical chemistry capability for determining all 20 amino acids.

To overcome the limitations in GC based analyses and because HPLC instrumentation is more versatile to various work flows, this work focuses on HPLC-based AAA. Among the more widely employed derivatization reagents are orthophthalaldehyde (OPA) and Edman's reagent, phenylisothiocyanate (PITC), for which there are numerous publications illustrating their utility. OPA, however, has the significant drawback in that it does not react with secondary amino acids, and some of the derivatives, notably those with Gly and Lys, are unstable (Cohen, 2003). PITC, while reactive with the secondary amino acids, also produces somewhat unstable derivatives, notably with Asp and Glu, which slowly cyclize from the desired phenylthiocarbamyl moieties to their respective phenylthiohydantion derivatives (Cohen, 2003). In addition, excess PITC must be removed, typically by evaporation, prior to HPLC analysis to avoid column contamination and poor chromatographic separation (White, 1986). A noteworthy feature of the analysis with PITC is the quantification of secondary amino-acids, such as proline and hydroxyproline. In contrast to post-column ninhydrin detection or ortho-phthalaldehyde (OPA) derivatization, the proline and hydroxyproline PTC derivatives have the same chromophore and approximately the same molar response as other amino-acids (White, 1986). There is thus no need to suffer reduced sensitivity or to employ a second detector for these secondary amino-acids (White, 1986). Cohen and

Michaud introduced 6-aminoquinolyl-N-hydroxysuccinimidyl carbamate (AQC) for precolumn derivatization (Cohen, 1993). This reagent reacts smoothly with primary and secondary amines to produce stable unsymmetrical urea derivatives that are highly fluorescent, see reaction scheme in Figure 16.

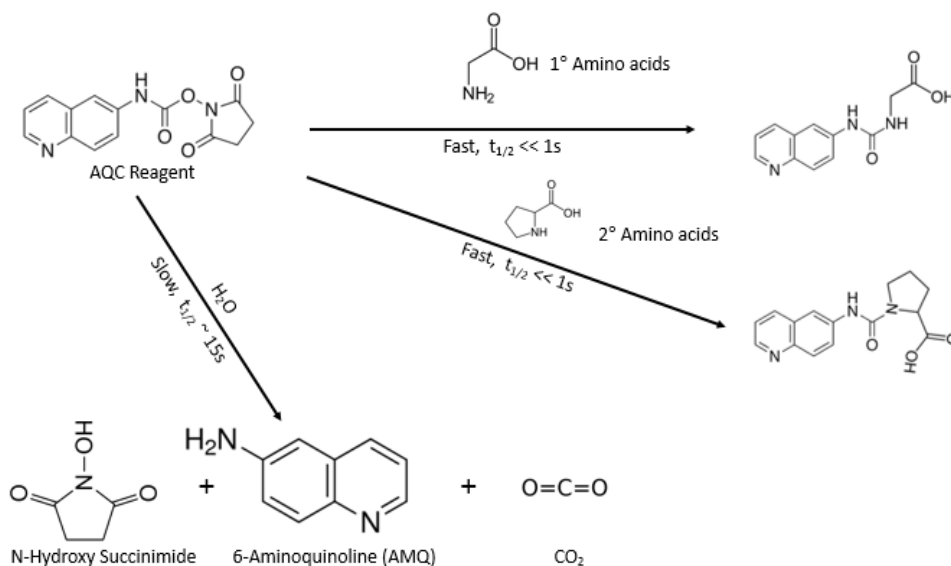


Figure 16: Chemistry of the AccQ-Tag Reaction. Derivatization of AQC with primary (1°) and secondary (2°) amines with AQC, and hydrolysis reaction of excess reagent.

The reaction products are generated within seconds, and in a somewhat slower reaction, excess reagent is hydrolyzed to yield 6-aminoquinoline (AMQ), carbon dioxide, and N-hydroxysuccinimide (NHS) (Cohen, 2003). Key to the design and implementation of this method are the fluorescence properties of the derivatized amino acids and AMQ. While both have excitation maxima approx 248 nm, they have radically different emission maxima, with the AMQ near 520 nm, and the amino acid products at 395 nm (Cohen, 2003). This shift in emission maximum allows the derivatization mixture to be injected onto the HPLC column without need for excess reagent removal. Studies on derivatization conditions demonstrate excellent derivative yield over the pH range 8.2-

10.0 (Cohen, 2003). Maximal yields are observed with a molar reagent excess of approximately three or greater. The reaction is extremely tolerant of common buffer salts and detergents, with no discernible decrease in reaction yield with well-buffered samples (Cohen, 2003). Fluorescence detection permits highly sensitive analyses with detection limits ranging from 50–300 fmol (Cohen, 2003). Combination of HPLC with mass spectrometry makes analyses very reliable in instances of co-eluting compounds, where optical detection fails to discriminate between these co-eluting species (Bhushan, 2001). Use of stable isotopes as internal standards also enhances sensitivity of the method (Bhushan, 2001). Although there are many techniques available for AAA, and the sample can be analyzed quickly, accurately, and sensitively, several precautions need to be taken in order to obtain reliable data on the concentration of amino acids. These include the sample collection, centrifugation, storage conditions, and most importantly the deproteinization method. The presence of remaining proteins can introduce artifacts into the analysis that interfere with the resolution and quantitation of species present in the sample (Bhushan, 2001).

Calculation of amino acid flux is described below by the method of (Glacken, 1988). In general, the flux of any compound can be calculated by first experimentally determining: the growth rate,  $\mu$  ( $\text{hr}^{-1}$ ), the change in cell count or dry weight over a specified time interval,  $dX$  ( $\text{cells} \cdot 10^6/\text{hr}$ ), and the change in the compound over that same specified time interval,  $dC_i$  ( $\text{moles}/\text{hr}$ ). Then dividing the change in compound concentration in time by the change in cell count/dry weight in time and multiplying by the specific growth rate, gives the flux of compound  $J_i$ , giving units of  $\text{mol}/\text{cell}\cdot\text{hr}$  or  $\text{mole}/\text{gDW}\cdot\text{hr}$ , see equation below.



$$\text{Flux of Compound} , J_i = \frac{dC_i}{dx} \mu$$

The flux is the rate of change in substrate or product concentration (-d[S] and d[P], respectively) per unit time (dt) per cell number or mass basis. The specific rates of production of amino acids, Nova metabolites, product titer and biomass are then combined with carbon material balances via a reaction network (coupled, linear differential equations) to estimate the metabolic fluxes at steady state using an appropriate software such as INCA (Young, 2014) or METRAN (Yoo, 2008).

### 3.2 Materials and Methods

Waters AccQ•Fluor™ Reagent Kit (WATERS, Pn: WAT052880)

\*The Waters AccQ•Fluor Reagent Kit contains sufficient reagent for up to 250 analyses.

Heat Block

Vortexer

Acetonitrile (Fisher Scientific, LC grade)

Ammonium Hydroxide (Fisher Scientific)

Formic Acid (Fisher Scientific)

Hydrochloric Acid (Sigma Aldrich)

pH Meter

Milli-Q H<sub>2</sub>O on house tap

Wattman 0.22µm Filter, and suction unit

2x Agilent Eclipse EC-C18 2.7µm 150x2.1mm HC columns

Agilent 1260 HPLC with quaternary solvent delivery with FLD, PDA, and Column Oven

#### 3.2.1 Preparation of Samples, Cell Media and Biological Fluids

1. Remove Media from culture flask using a serological pipette.
2. If suspension culture, centrifuge at 3000g for 5 minutes at 4°C to pellet cells, and collect supernatant.
3. Combine fluid with 100% Acetonitrile in 1:1 mixture to pellet the proteins.
4. Centrifuge the fluid at 16000g for 30 minutes at 4°C.
5. Carefully collect the supernatant without disturbing the protein pellet.
6. Filter the supernatant through a 0.22µm filter.

#### 3.2.2 Preparation of the AccQ•Fluor Derivatization Reagent

1. Preheat a heating block to 55 °C.
2. Tap Vial 2A lightly before opening to ensure all AccQ•Fluor Reagent Powder is at the bottom of the vial.
3. Rinse a clean micropipette by drawing and discarding 1 ml of AccQ•Fluor Reagent Diluent from Vial 2B.
4. Transfer 1.0 ml of AccQ•Fluor Reagent Diluent From Vial 2B to the AccQ•Fluor Reagent Powder In Vial 2A.
5. Cap Vial 2A lightly and vortex for 10 seconds.
6. Heat Vial 2A on top of heating block, vortex occasionally, until the powder dissolves. Do not heat longer than 10 minutes. Reconstituted AccQ•Fluor Reagent is approximately 10 mM

AQC in acetonitrile.

Note: You can store the reconstituted AccQ•Tag reagent in a desiccator at room temperature for up to one week. The AccQ•Tag reagent reacts with atmospheric moisture so seal the container tightly when not in use and DO NOT refrigerate.

7. Amino acid calibration stock solution (2.5 mM in 0.1M HCl) (Pierce Chemical Co. or Sigma Chemical Co.).
8. Working calibration mixture: Mix 40 µL of amino acid stock solution (2.5 mM) with 960 µL of water to give a solution with 100 pmol/µL of each AA.
9. 20 mM HCl: Mix 10 µL of constant boiling HCl with 3 mL of HPLC-grade water.

Note: 20 mM HCl is used to reconstitute protein hydrolysates or dried amino acid powders.

### **3.2.3 Derivatization of Samples and Standards**

1. Preheat a heating block to 55 °C.
2. Add 60 µl of AccQ•Fluor Borate Buffer to the reconstituted sample in the 6 x 50 mm sample tube and vortex.
3. Add 20 µl of AccQ•Fluor reagent. Vortex immediately for several seconds.
4. Allow to incubate for one minute at room temperature.
5. Transfer the contents of the tube to an autosampler vial low volume insert (LVI). Cap with a silicone-lined septum.
6. Heat the vial In a heating block for 10 minutes at 55 °C.
7. Inject 5 µL or perform a 1:4 dilution and inject 10uL for enhanced resolution.

### 3.2.4 Amino Acid Analysis Chromatographic Conditions

HPLC System: Agilent 1260 quaternary solvent delivery

Detectors: FLD (Excitation 250nm and Emission 395nm) and PDA (Abs. 254nm)

Column: 2x Agilent Eclipse EC-C18 2.7 $\mu$ m 150x2.1mm, connected in series

Flow Rate: 0.475 mL/min

Column Oven: 37°C

Injection Volume: 5 $\mu$ L

Mobil Phase A: 100mM Ammonium Formate pH 4.40

Mobil Phase B: Acetonitrile (Fisher HPLC grade)

Mobil Phase C: H<sub>2</sub>O (Mili-Q house tap)

Mobil Phase D: 60% Acetonitrile / 40% H<sub>2</sub>O (HPLC grade)

Gradient Conditions:

Table 3: Optimized gradient conditions of AAA

Time (min)	%A	%B	%C	%D
0	100	0	0	0
0.5	96.5	3.5	0	0
11	95.4	4.6	0	0
13	89	11	0	0
25	86	14	0	0
25.1	93.3	0	0	6.7
28.2	91.9	0	0	8.1
38	70	0	0	30
58	20	0	0	80
60	0	0	0	100
62.5	0	95	5	0
74.5	0	95	5	0
85	0	0	0	0

### 3.3 Results

#### 3.3.1 Amino acid profile of F-12K Nutrient medium Formulation.

F-12K Nutrient media was spiked with 13.5mg/L of Norvaline for use as an internal standard. Following derivatization with the AQC, the resulting HPLC chromatogram for F-12K is shown in Figure 17. The concentrations of the F-12K amino acid components are listed in Table 4, these values were taken from Corning cellgro.

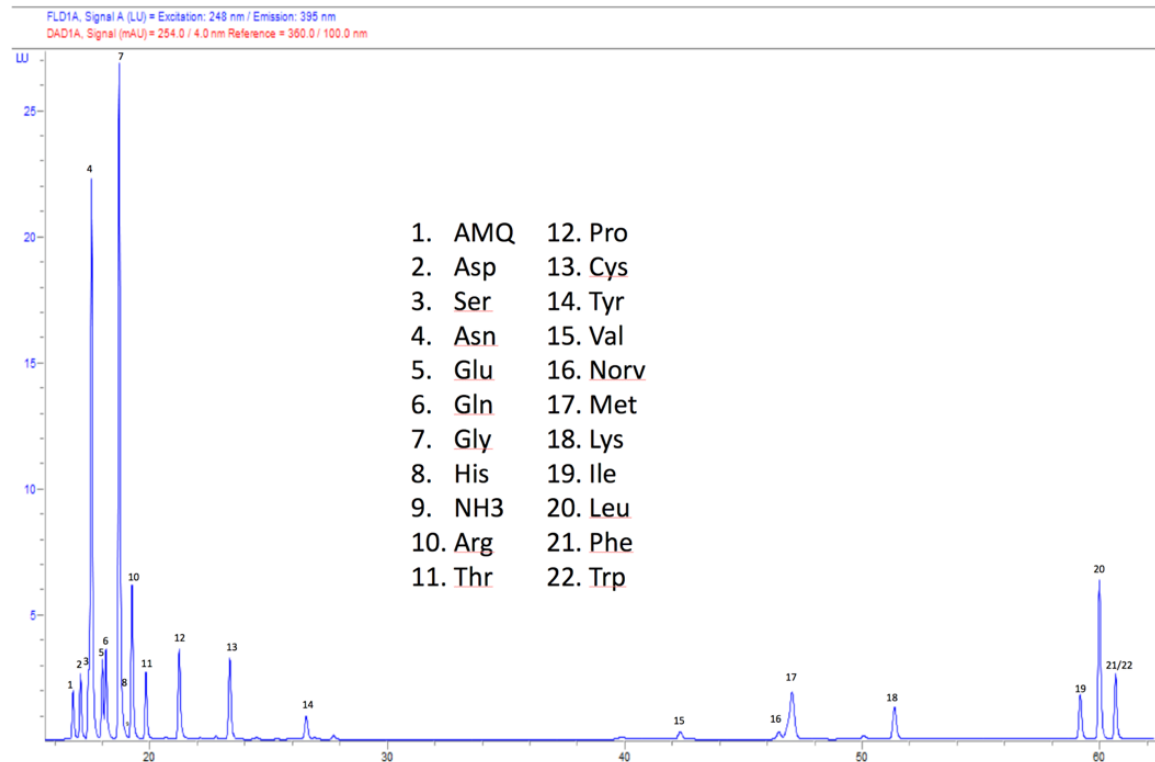


Figure 17: Amino acid profile of F-12K Nutrient medium Formulation.

Table 4: F-12K Nutrient Formulation, taken from  
[http://cellgro.com/media/docs/files/items/file\\_83.pdf](http://cellgro.com/media/docs/files/items/file_83.pdf)

<b>F-12K Formulation in mg/L</b>	
Aspartate	30
serine	9.92
asparagine	422
glutamate	70
Glutamine	29
Glycine	292
Histidine	15
NH <sub>3</sub>	
Arginine	18
Threonine	69
Proline	69
Cysteine	26.6
Tyrosine	23
Valine	4.1
norvaline	13.5
Methionine	73
Lysine	26.2
Isoleucine	45.8
leucine	7.88
phenylalanine	8.96
Tryptophan	21

### 3.3.2 Amino acid profile of RPMI 1640 Formulation.

RPMI 1640 formulation media was spiked with 13.5mg/L of Norvaline for use as an internal standard. No standard was available for hydroxyproline however comparison of Water's elution order for the AccQ derivatized amino acids established that Hyp elutes prior to Pro. Following derivatization with the AQC, the resulting HPLC chromatogram for RPMI 1640 is shown in Figure 18. The concentrations of the RPMI 1640 amino acid components are listed in Table 5, these values were taken from Corning cellgro.

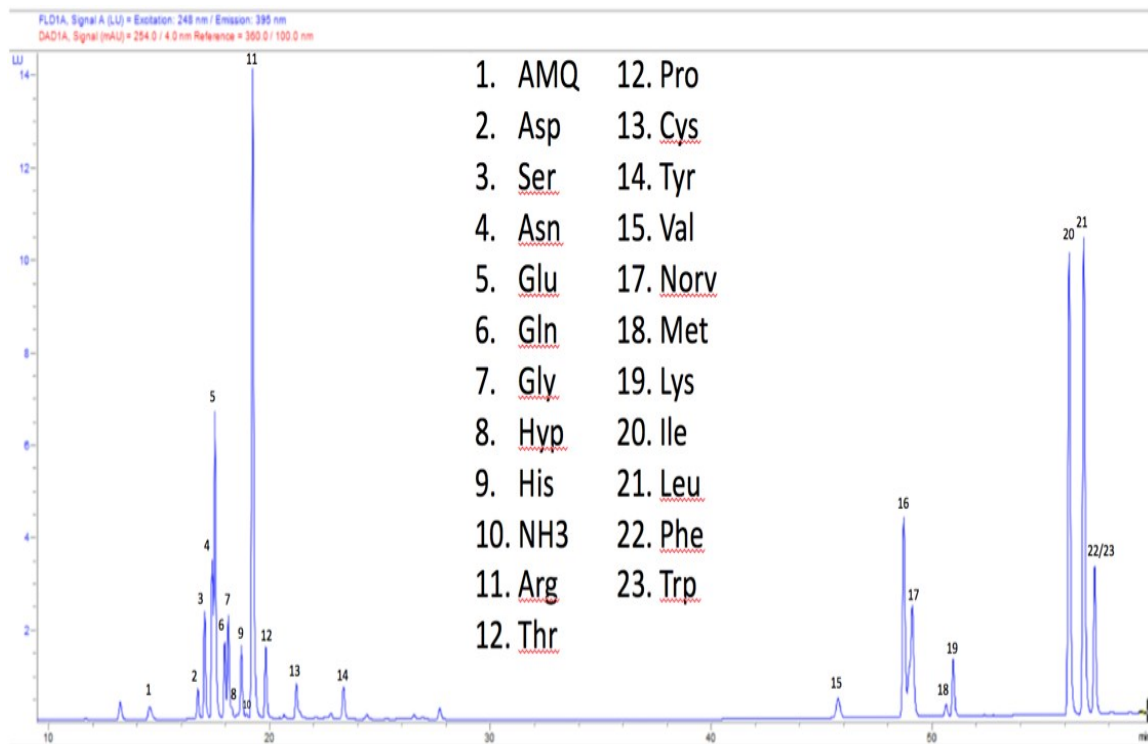


Figure 18: Amino acid profile of RPMI 1640 Formulation.

Table 5: RPMI 1640 Formulation, taken from  
[http://cellgro.com/media/docs/files/items////////10-041\\_3.pdf](http://cellgro.com/media/docs/files/items////////10-041_3.pdf)

<b>RPMI 1640 Formulation in mg/L</b>	
Aspartate	20
serine	30
asparagine	56.82
glutamate	20
Glutamine	300
Glycine	10
Hydroxy Proline	20
Histidine	15
NH <sub>3</sub>	
Arginine	200
Threonine	20
Proline	20
Cysteine	65.2
Tyrosine	28.83
Valine	20
norvaline	13.5
Methionine	15
Lysine	40
Isoleucine	50
leucine	50
phenylalanine	15
Tryptophan	5



The results demonstrate that the method is able to not discern differences in the concentrations of medias but also their composition. Future work would establish calibration curves for each individual amino acid component and then use this calibration to determine changes in the media composition of cell culture over time. This data would then allow fitting of fluxes to each amino acid component.

### **3.4 Discussion**

A drawback of some pre- and post-column derivatization assays is the requirement of an automated pretreatment multi-functions autosampler. This is an autosampler that is able to perform injector programming that mixes desired functions of solutions, and enables consistent sample preparation. Use of o-phthalaldehyde (OPA) and 9-fluorenyl methyl chloro formate (FMOC) to derivatize primary and secondary amino acids, respectively, requires a constant reaction time be maintained with the automated autosampler derivatization. Manual operation of the derivatization reaction results in repeatability issues over intra- and inter-day RSD's. Thus the advantage of using the Waters' AccQ reagent is clear, as the reactants can simply be mixed without concern of reaction time due their short half-life. Furthermore, unlike OPA/ FMOC, ninhydrin and other labels, AccQ derivatives have the same chromophore and approximately the same molar response as other amino-acids. AAA using AccQ resulted in the separation of complex amino acid mixtures, such as free amino acids present in cell culture fluids. Precise control of eluent pH and organic solvent gradient slopes were determined to be essential for optimum resolution, particularly in the preparation mobile phases. The sensitivity, calibration, inter- and intra-day precision, reproducibility and molecular stability of each targeted metabolite still remains to be assessed under the experimental

conditions. Furthermore, the choice of volatile mobil phases makes this method readily amenable to ESI-MS for molecular weight verification and obtaining the MIDs in isotope labelling experiments. This AAA method also has advantages to studying cellular metabolic responses to media composition changes and the corresponding impact on glycosylation during the culture (Gillmeister, 2009). Several amino acids have been known for the effects on N-linked glycosylation and used for glycan modulation. Raising glutamine concentrations or adding ammonia directly to the culture led to decreased galactosylation (Gillmeister, 2009). Increased consumption of glutamine is shown by many cell lines, but much of the nitrogen provided by this substrate is lost to the production of ammonia and alanine (Sha, 2016). Resultantly the ammonia byproduct can be detrimental to sialylation and galactosylation (Gillmeister, 2009; Sha, 2016). Supplementation with threonine, proline, or glycine was found to result in an increase in the glycan galactose and sialic acid content (Sha, 2016). A correlation was reported between the distribution of galactosylated glycoforms and the concentration of Asn in the media (Sha, 2016). Changing nutrient availability and cell densities give rise to transitions between distinct growth phases (i.e., exponential, stationary, and decline). During early growth phases concentrations of lactate, ammonia, and other waste products accumulate to concentrations that inhibit cell growth and antibody production and impact protein glycosylation during later phases. While minimizing wasteful byproduct accumulation has always been a goal of the biopharmaceutical industry, it still remains an unresolved and challenging issue. Furthermore, many production cultures will shift from net production to net consumption of these byproducts during the bioprocess run (Nolan and Lee, 2011); however, the regulatory mechanisms that control these changes remain

elusive. Hence the need to accurately monitor amino acid expression levels as a function of cellular condition, stress, or other perturbation of the cell and how those changes correlate to altered glycan composition. While substantial improvements in bioprocess rates and titers have been made, the ability to precisely quantify cell metabolism throughout the production run is essential to further understand and optimize the industrial fed-batch production process in relation to the glycosylation status of the biotherapeutic.

## **Chapter 4: Nucleotides and Nucleotide Sugars Analysis**

### **4.1 Introduction**

Nucleotide Sugars are ubiquitous metabolites that are the activated substrates for the biosynthesis of carbohydrate molecules. Furthermore, the interconversion of one monosaccharide to another, e.g. glucose to galactose, occurs in their activated forms (Ramm, 2004). As obligate precursors of glycosylation, the presence of nucleotide sugar pools provides strong evidence for cellular glycosylation reactions (López-Gutiérrez, 2017). To date, 30 different nucleotide sugars have been identified in plants, at least 70 are known in bacteria, 12 in humans, and up to 16 in fungi (Bar-Peled, 2011). Previous studies have found that the availability of nucleotide sugar donors determines the macroheterogeneity and also the microheterogeneity of the carbohydrates bound to the protein (del Val, 2015). Investigations into the metabolism of nucleotide sugars requires a generally applicable, rapid and robust analytical assay which should enable the separation, unambiguous structural characterization and quantitation of substrates, intermediates and end products (Ramm, 2004). Several attempts have been made to extract and quantify these compounds from cells in culture using analytical techniques such as high-performance anion-exchange chromatography, reverse-phase ion-pairing high-performance liquid chromatography, and capillary electrophoresis (del Val, 2015). Despite encouraging results, many of the available analytical techniques have limitations such as the length of analysis time (>50 min), detection of certain species, based on sophisticated detection or separation methods, or laborious preparation of the mobile phase(s) (del Val, 2015). Prior to performing the analytical method, recent reports suggest that cell culture sample treatment prior to extraction (washing and quenching), as well as the metabolite extraction protocol, may greatly influence the measurement of

intracellular metabolite pools (Del Val, 2015). This is due to the fact that some intracellular metabolites are turned over on a short time scale, where rapid cold-quenching is necessary to capture an accurate snapshot of intracellular metabolism (Templeton, 2009; Sellick, 2009). Ideally, tedious sample preparation should be avoided which could result in loss of analytes and decomposition of labile compounds. The objective of these procedures are to ensure that (i) the extraction method allows for reproducible retrieval of the desired metabolites, (ii) the metabolite pools to be extracted are representative of the metabolic state of the cells at the moment of extraction, and (iii) components from the cell culture medium do not contaminate the intracellular samples (del Val, 2015). This chapter describes an optimized method for nucleotide and nucleotide sugar extraction and identification from CHO cells, which in principle is amenable to other cell types, in the case of plants/algae/fungi following disruption of the cellular membrane.

## 4.2 Methods & Materials

PBS (cat # 70011-044; ThermoFisher, Grand Island, NY, USA)

Milli-Q Water, house tap

75.0% ice cold ethanol (cat # 459836; Sigma, St. Louis, MO, USA)

ENVI-Carb SPE column (cat # 57109-U; Sigma, St. Louis, MO, USA)

Acetonitrile (cat # 34998; Sigma, St. Louis, MO, USA)

Methanol (Sigma-Aldrich)

Trifluoroacetic acid (cat # 302031; Sigma, St. Louis, MO, USA)

Potassium Phosphate (Sigma-Aldrich)

tetrabutylammonium hydrogensulphate (Fisher)

Ammonium Bicarbonate (cat # A6141; Sigma, St. Louis, MO, USA)

Triethylamine (Fisher)

Acetic Acid (Sigma-Aldrich)

Quenching Solution: 0.85% (w/v) of the aqueous portion which is a 60/40 mixture of methanol/AMBIC pre-cooled to  $-40^{\circ}\text{C}$

The purified monosaccharides, nucleosides and nucleotide sugars: N-Acetylgalactosamine (GalNAc), Mannose (Man), Sialic Acid (NeuAc), N-Acetylglucosamine (GlcNAc), Glucuronic Acid (GlcUA), Galactose (Gal), Glucose (Glc), Adenosine Monophosphate (AMP), Adenosine Diphosphate (ADP), Adenosine Triphosphate (ATP), Uridine Monophosphate (UMP), Uridine Monophosphate (UDP), Uridine Monophosphate (UTP), Guanosine Monophosphate (GMP), Guanosine Diphosphate (GDP), Guanosine Monophosphate (GTP), Cytosine Monophosphate (CMP), Cytosine Diphosphate (CDP), Cytosine Triphosphate (CTP), UDP-Gal, UDP-Glc, UDP-GalNAc, UDP-GlcNAc, CMP-Neu5Ac, GDP-Man, GDP-Fuc, and GDP-Glc were all purchased from Sigma Aldrich, St. Louis, MO, USA.

Buffer A for HPLC analysis: 100 mM potassium phosphate buffer ( $\text{K}_2\text{PO}_4$ ) (pH 6.40) supplemented with 8 mM tetrabutylammonium hydrogensulphate (TBAHS)

Buffer B for HPLC analysis: 70% buffer A plus 20% acetonitrile

Handy Sonic Disruptor (Tomy Seiko Co. Ltd., Tokyo, Japan)

Speed Vac Concentrator (Labconco Co., Kansas City, MO)

Lyophilizer

Shimadzu LC-10ai binary HPLC system equipped with a UV & FLD detector (Shimadzu Corp., Kyoto, Japan)

Inertsil ODS-2 (particle size: 3  $\mu\text{m}$ ; 150  $\times$  4.6 mm; GL Science, Tokyo, Japan)

### 4.2.1 Metabolite Cold-Quenching and Extraction of Aqueous Phase Metabolites

1. At each sample time point, transfer an aliquot of culture medium containing approximately 9 million CHO cells (cell counting performed by hemotocytometry, see supplemental information for details) into a 15mL falcon tube.
2. Rapidly place into the quenching solution at a ratio of 1:5 cells to quench solution.
3. Following the cold-quench, metabolite extraction is performed using the Folch method (Folch, 1957) with use of a sonicator to help disrupt the cell membrane.
4. Remove the aqueous portion of the metabolite extraction, as this phase contains the nucleotides and nucleotide sugars.

5. Lyophilize the aqueous extract.

#### **4.2.2 Purification of sugar nucleotides by Solid-Phase Extraction (SPE)**

##### **Chromatography**

1. Place a 1 mL/100 mg ENVI-Carb SPE column in a 15 mL conical tube.
2. Equilibrate the column by adding 1 mL of 80% acetonitrile in 0.1% trifluoroacetic acid and spin at  $60 \times g$  for 45 s (room temperature). Repeat twice.
3. Add 1 mL of ultrapure water to the column and spin as described in step 1. Repeat once.
4. Reconstitute the dried cell samples (generated from extraction from step 5) in 2 mL of 10 mM ammonium bicarbonate.
5. Add 1 mL of the dissolved sample to the column and spin as in step 1. Repeat with the other half of the sample.
6. Collect flow-through and enrich by re-applying the sample to the ENVI-Carb column in 1 mL fractions (same as step 5).
7. Wash the column with 2 mL of ultrapure water, 2 mL of 25% acetonitrile, 1 mL of ultrapure water, and 2 mL of 10 mM TEAA buffer (pH 7) and spin after each wash as described in step 2.
8. Collect SPE Envi-Carb column(s) and place into a new 15 mL conical tube.
9. Elute the bound sugar nucleotides with 2 mL of 25% acetonitrile in 50 mM TEAA buffer (pH 7). Spin and pool as described in step 2.
10. Transfer the purified sugar nucleotides to a 2 mL eppendorf tube.
11. Lyophilize the samples to remove the TEAA.
12. Reconstitute the samples in 100uL H<sub>2</sub>O.

#### **4.3.3 Fluorescent Assisted Carbohydrate Electrophoresis (FACE)**

1. Refer to (Barnes, 2016) for an excellent step-by-step detailed procedure.

#### 4.3.4 Ion Pair Reverse Phase Chromatography (IP-RPC) Conditions for High-Resolution of Nucleotide Sugars

HPLC System: Shimadzu LC-10ai binary HPLC system equipped with a UV & FLD detector (Shimadzu Corp., Kyoto, Japan)

Detector: PDA (Abs. 254nm)

Column Thermostat: Ambient

Flow Rate: 1 mL/min

Injection Volume: 20µL

Column: Inertsil ODS-2 (particle size: 3 µm; 150 × 4.6 mm; GL Science, Tokyo, Japan)

Mobil Phase A: 100 mM potassium phosphate buffer (K<sub>2</sub>PO<sub>4</sub>) (pH 6.40) supplemented with 8 mM tetrabutylammonium hydrogensulphate (TBAHS)

Mobil Phase B: 70% buffer A plus 30% Acetonitrile

Gradient Conditions:

Table 6: Optimized Gradient Conditions for Nucleotide Sugars

Time (min)	A %	B %
0	100	0
15	100	0
37	23	77
38	0	100
42	0	100
45	100	0
70	100	0



## **4.3 Results**

### **4.3.1 FACE technique results**

Pancreatic cancer cells were used to establish the FACE techniques ability to handle cellular extracts. Briefly,  $10^6$  cells were isolated, washed, then spiked with 10 $\mu$ g 2-Deoxy-Glucose (2DG) immediately prior to cell extraction (2DG is an unnatural monosaccharide that was used to determine the efficiency of the subsequent nucleotide sugar purification steps from free monosaccharides, e.g. any 2DG left over in the final sample would indicate that clean-up steps could not remove free monosaccharides and hence give false signal on the FACE gel), then samples were dried, and reconstituted and spiked with 100 nmol of UDP-Arabinose (UDP-Ara) (to test for nucleotide sugar extraction efficiency of purification), then acid hydrolyzed to release sugars from nucleotide sugars, then labelled with 2-aminoacridone, and lastly ran on a 30% acrylamide gel. Figure 18 shows the FACE gel of a panel of typically observed monosaccharides.

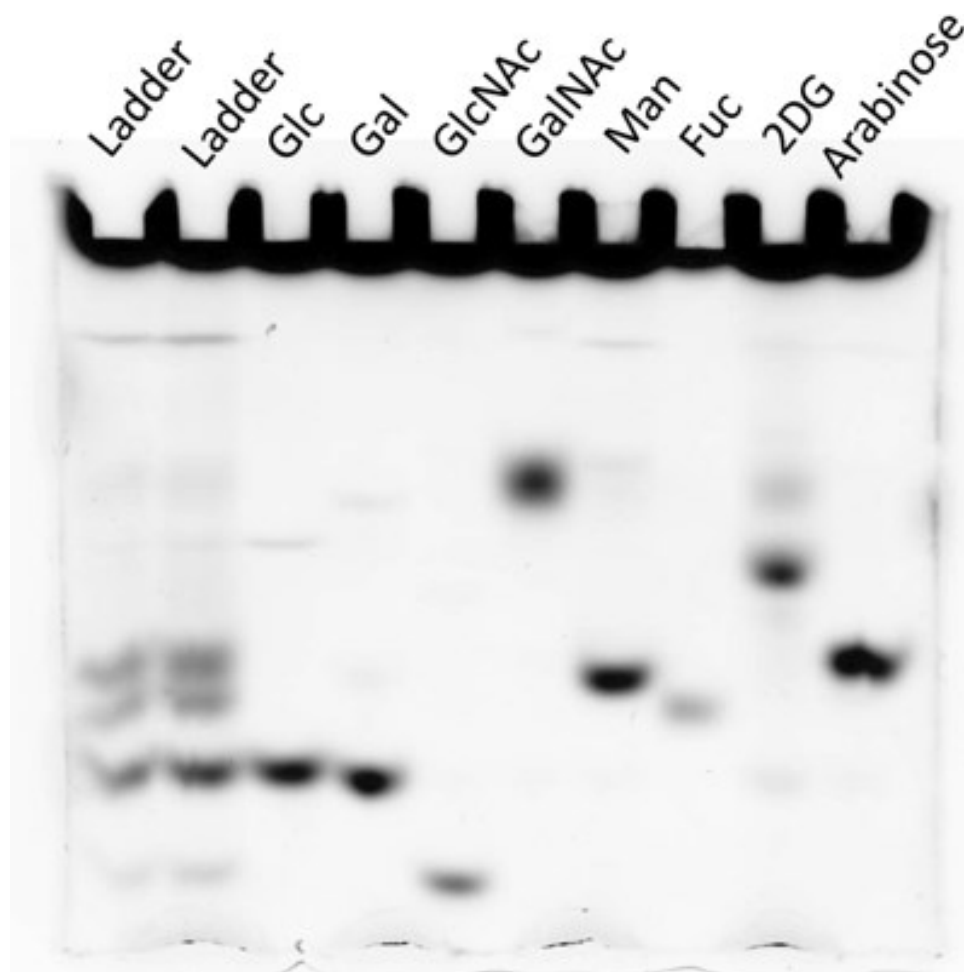


Figure 19: FACE gel of monosaccharide standards.

One of the most remarkable things about the FACE technique is the high resolution observed between UDP-GlcNAC and UDP-GalNAC as seen in Figure 19. Indeed no other method comes anywhere near this resolution. However, Glc and Gal appear very near each other. The sharpness of the bands could also use improvement, apparently the casting of the gel is very critical.

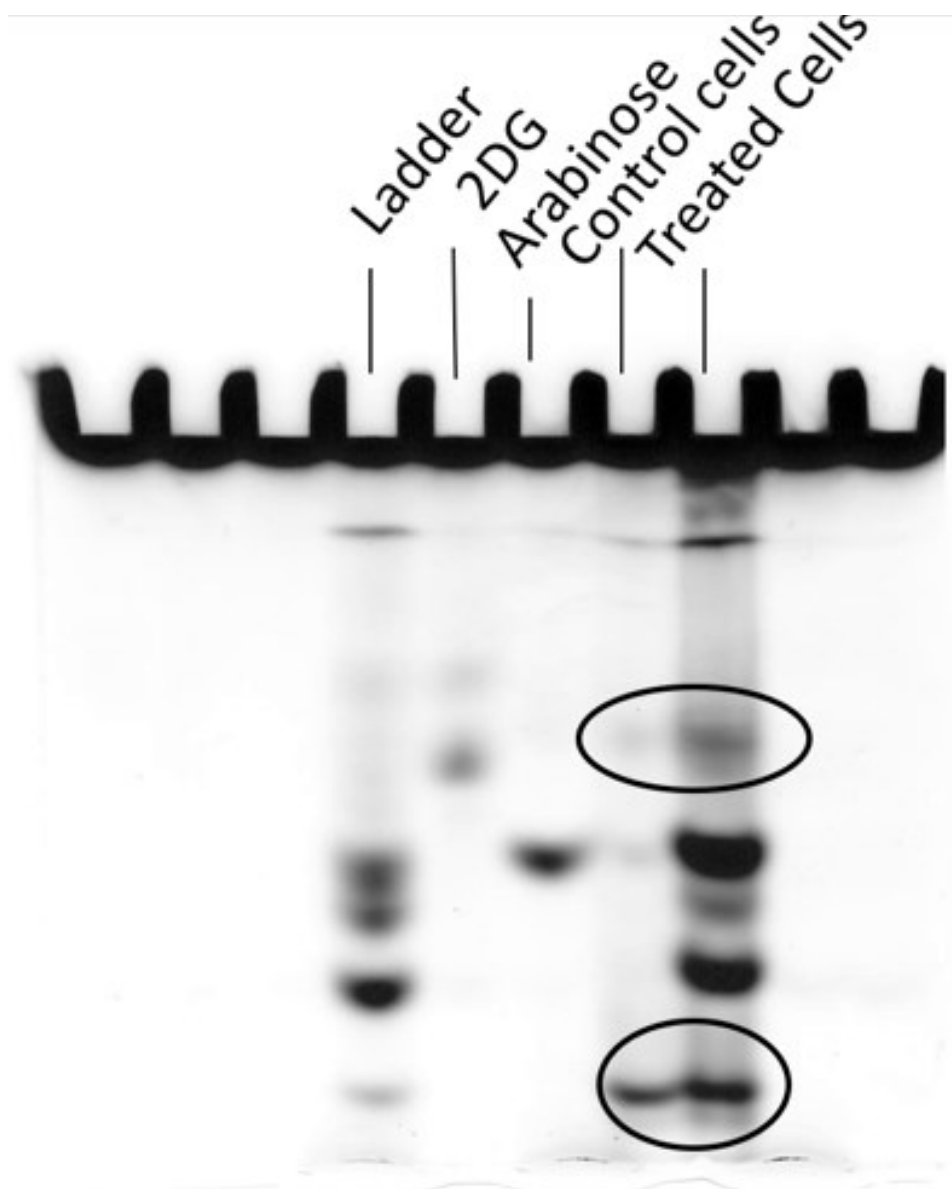


Figure 20: FACE gel of standards 2DG and Arabinose alongside spiked PANC cell extracts. Upper circle shows the presence of some 2DG in extracts indicating washes not able to 100% purify out free monosaccharides . As a result, the lower circle (Glc-NAC band) is a superposition of both free Glc-NAC and UDP-GlcNAc. The UDP-Arabinose internal standard was not spiked into the control cells which is why the band is absent.

Figure 20 shows the comparison of standards used as internal controls in the assay alongside cell extracts, with the control sample not being spiked with UDP-Ara. The slight presence of 2DG in the samples means that the carbo-column was not able to 100% purify out free monosaccharides. Therefore, there is probably some contamination of the

all bands present with some small amount of free monosaccharides. However, quantification of free monosaccharide versus activated sugar was not accomplished in these studies. The UDP-Arabinose spike in shows that nucleotide sugars are indeed recoverable in a complex matrix such as a cell extract. The blurring of the bands renders them difficult to quantitatively measure, instead this technique offers a more qualitative look at the cellular status of nucleotide sugars at the time of extraction. This limitation in quantitation provided the impetus for development of an HPLC based method.

#### **4.3.2 IP-RPC Results of Nucleotides and Nucleotide Sugars**

All nucleotides, nucleoside and nucleotide sugars standards were previously reconstituted by Yuzhou Fan in 2013, and kept frozen at -80C prior to use. Unfortunately, even though vials listed 100nmol/ $\mu$ L, the samples did not appear to have consistent dilutions (data not shown), presumably, the molar response ratios are different resulting in different peak areas, however no confirmation of concentrations could be made thus preventing quantitation. None the less, the standards did give excellent qualitative results in terms of observed retention times, refer to Figure 21 for an overlay chromatogram of available standards.

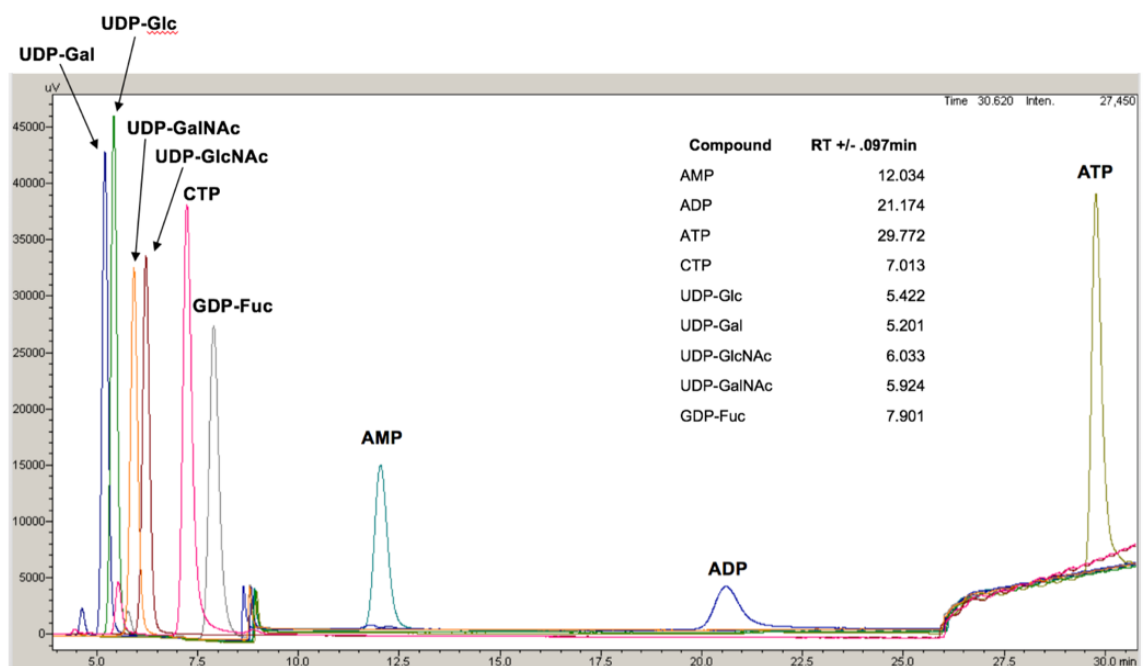


Figure 21: Overlay of Nucleotides and Nucleotide Sugar Standards. The retention times of the compounds are listed on the right.

Since the method was shown to have resolution, reproducibility, and analyte retention, CHO cell extracts were then examined. To be able to see a large difference between cells, one CHO cell line was treated with the high-flux analog 1,3,4-O-Bu<sub>3</sub>-ManNAc at a concentration of 100μM, and a control sample was fed glucose as standard carbon source at a concentration of 15mM, refer to “Treatment of Cultures With 1,3,4-O-Bu<sub>3</sub>ManNAc and ManNAc” in supplemental material. The results of the CHO cell feed comparison are shown in Figure 22.

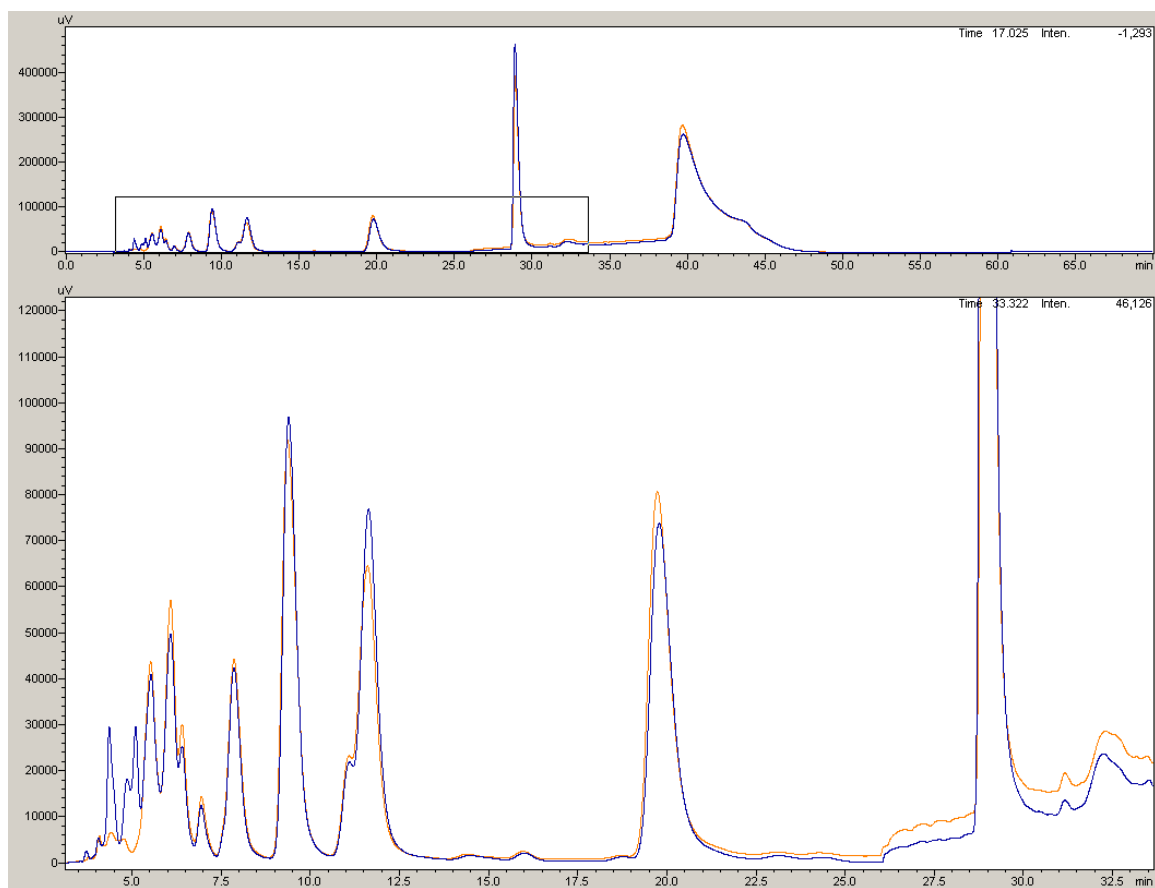


Figure 22: Comparison of purified Nucleotides and Nucleotide Sugars from CHO cell extracts. CHO cells were ManNAc-analog-fed (blue) vs non-fed (gold).  $\sim 9.5 \times 10^6$  CHO cells were subjected to extraction and purification of Nucleotide Sugars.

To determine the peak identities of the CHO cell extracts, the nucleotides and nucleotide sugars standards were overlaid with the analog fed nucleotide sugar extract, shown in Figure 23. However, as can be seen there appeared co-elution of the UDP-GalNAc and UDP-GlcNAc peak, which even though the standards separated, additional molecules could be co-eluting there as well. Without additional standards to establish their retention times, the identities of these other compounds proved difficult to determine.

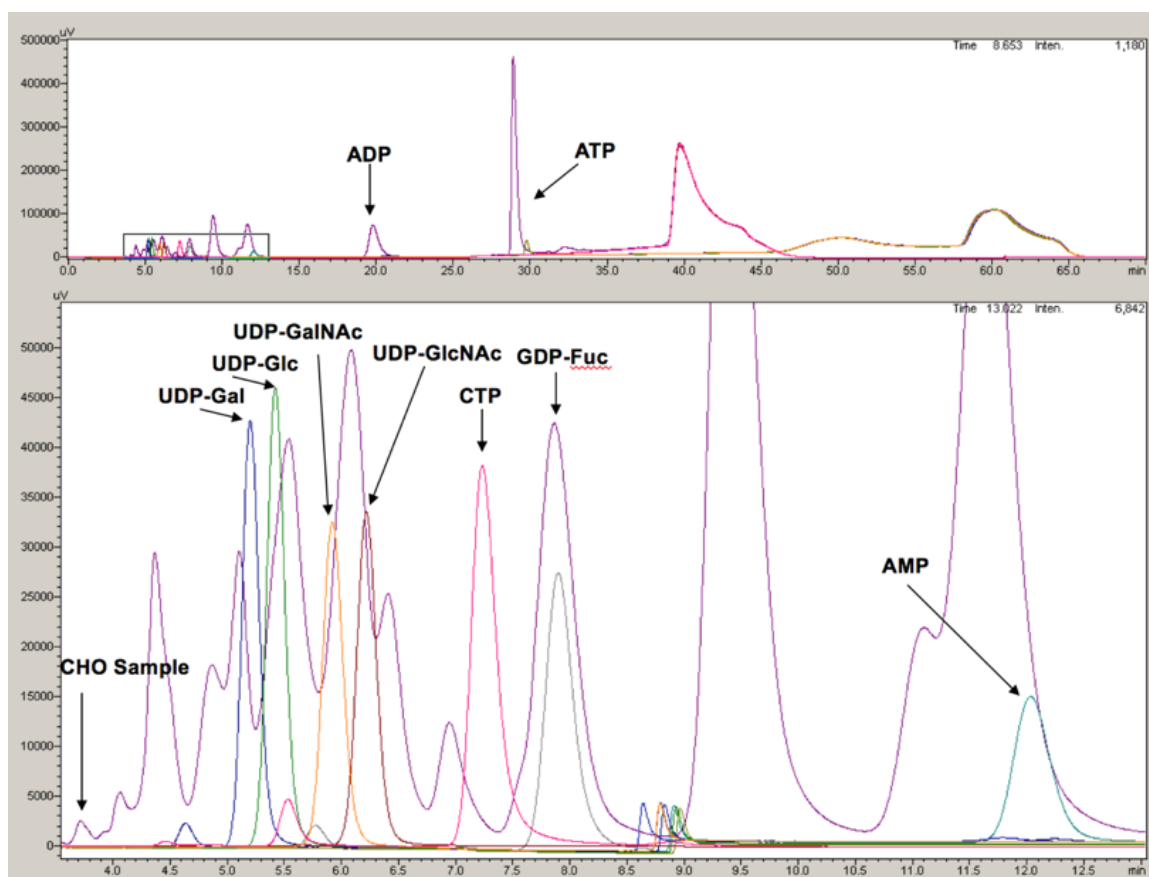


Figure 23: Overlay of Nucleotides and Nucleotide Sugars Standards and of ManNAc-analog-fed CHO cell extract (purple).

To observe if the high-flux analog feeding strategy had any effect on the levels CMP-Neu5Ac in CHO cells, a CMP-Neu5Ac was run to determine its' retention time. CMP-Neu5Ac eluted at ~3.75 min., as shown Figure 24. Figure 24 also shows the overlay of the CMP-Neu5Ac standard with the fed and non-fed CHO cell extracts.

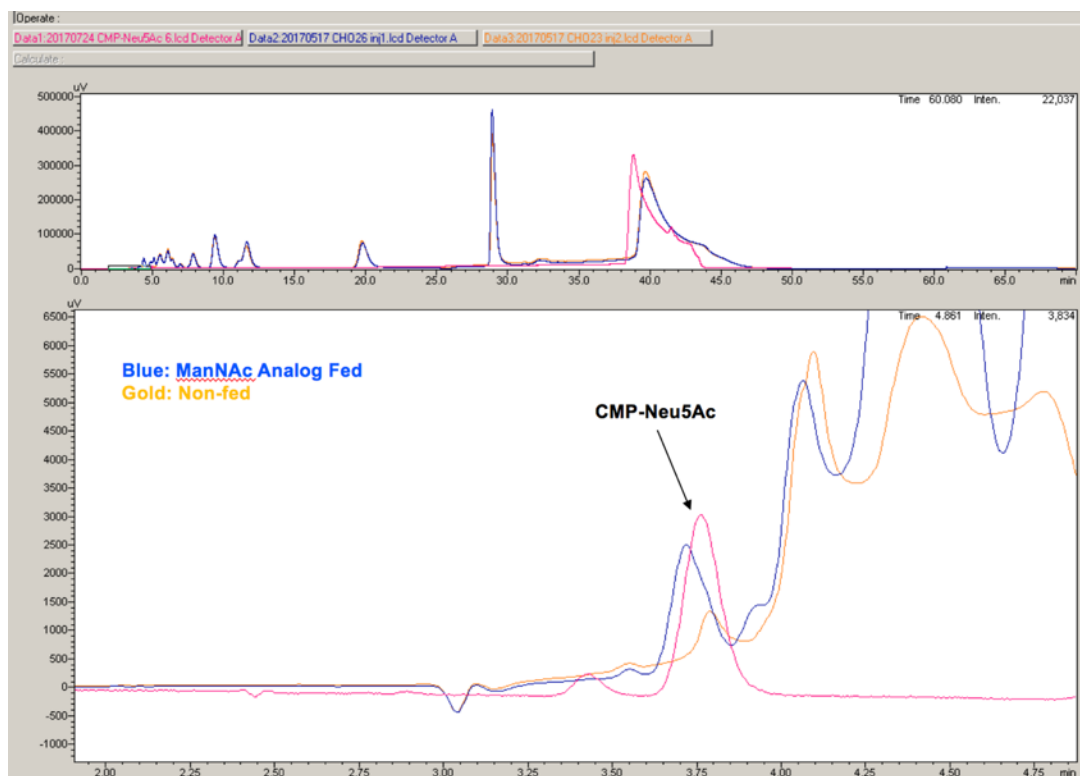


Figure 24: Overlay of CMP-Neu5Ac standard (pink) and of purified Nucleotides and Nucleotide Sugars from CHO cell extracts that were ManNAc-analog-fed (blue) vs non-fed (gold).

Having established some of the peak identities, some observations can be noted from Figures 21-24. Figure 22 clearly shows substantial remodeling of nucleotide and nucleotide sugar cellular metabolism as shown by the difference in peak heights between treated vs non-treated CHO cells. Clearly, the levels of nucleotides and nucleotide sugars were perturbed following the change in carbon source to the high flux analog. Furthermore, substantial differences appear in the levels of UDP-Gal and UDP-Glc at ~5 min., as well as alterations in the levels of UDP-GlcNAc and UDP-GalNAc at ~6 min. The most exciting finding of these results is the alteration of CMP-Neu5Ac levels in treated vs non-treated CHO cells. When coupled to the glycan analysis method these results correlate with increased sialylation of the protein molecules.



#### 4.4 Discussion

Analysis of intracellular nucleotide and nucleotide sugar contents is essential to glycosylation as nucleotides are involved in the metabolism and regulation of cellular energy and nucleotide sugars are the donor substrates of glycosyltransferases. Multiple reasons hamper the analysis and quantitation of sugar nucleotides, including the difficulty in isolation and purification as well as the required expensive instrumentation such as a high performance liquid chromatograph (HPLC), mass spectrometer (MS), or capillary electrophoresis (CE). This was the initial motivation behind establishing the Fluorescence Assisted Carbohydrate Electrophoresis (FACE) technique, as the simplicity of use, combined with the ability to run multiple samples at one time, gave this technique a distinct advantage over other established methods for the isolation and analysis of nucleotide sugars from cell culture models. However, several drawbacks also plague the FACE technique from suitability to the requirements of the project goal. Firstly, in terms of quantitation, the technique relies on densitometry, which is semi-quantitative at best, especially in light of the band smearing that would occur on most standards and samples. Secondly, the hydrolysis of the nucleotide sugar to liberate the sugar for subsequent fluorophore derivatization loses all information on which nucleotide the monosaccharide moiety was initially conjugated, e.g. UDP-Glc or ADP-Glc, as the observed signal of Glucose would be the combination of both in this example. Despite the FACE techniques cost effective, simple, and robust attributes, the method was abandoned in favor of HPLC-based ion-pair reverse phase chromatography (IP-RPC).

A sensitive and reproducible ion-pair reverse-phase high-performance liquid chromatography (IP-RP-HPLC) method has been developed, allowing for the direct and simultaneous determination of several essential nucleotides and nucleotide sugars in a

single chromatographic run. After a Folch extraction, then solid phase extraction of the aqueous metabolites onto Carbo-Graph column purification, 10 molecules (4 nucleosides and 6 nucleotide sugars) were separated, such as AMP, ADP, ATP, CTP, UDP-Glc, UDP-Gal, UDP-GlcNAc, UDP-GalNAc, GDP-Fuc and CMP-Neu5Ac. The HPLC method was then applied to quantify intracellular levels of nucleotides and nucleotide sugars of CHO cells cultivated in a bioreactor batch process. Due to the hydrophilic and polar character of the nucleotide sugars, chromatographic separations require the aid of an ion-pair reagent for providing the desired chromatographic resolution. Presumably caused by almost identical pKa values, charge numbers, and polarizabilities of the structurally-similar nucleotide sugars, as they are diastereoisomers, attempts to separate the compounds proved challenging. Especially challenging are UDP-Glc and UDP-Gal, UDP-GlcNAc and UDP-GalNAc, for which numerous reports cannot achieve baseline chromatographic resolution of these molecules. A combinatorial approach through various stationary phases, column dimensions, mobile phases and pH adjustment, was used to optimize the separation. Stationary phases such as Porous Graphitic Carbon (PGC), C4, C8 and C18, were attempted, whilst keeping constant the mobile phase and pH. Although the literature reports enhanced nucleotide sugars separation using PGC, this was not observed in experiments, due perhaps to the column being purchased in 1992 (~25 years old, with unknown contents ran previously despite multiple 0.1% Tri-Fluoro Acetic Acid in Acetonitrile cleaning washes), and its 100mm length. Furthermore, because carbon is conductive, linking this stationary phase to a positively charged Electro-Spray Ionization source Mass Spectrometer (ESI-MS) resulted in redox processes occurring on the stationary phase, leading to charge accumulation on the column (which

in future studies requires purchase of a grounding splitter prior to the ESI). The altered stationary phase properties on a run-to-run basis prevented consistent chromatography. As the alkyl chains on C4 and C8 stationary phases have smaller surface area available for adsorption compared to C18, results demonstrated poor retention and separation of analytes, as their limited hydrophobicity prevents the detachment of the double-layer around these phases when analytes undergo mass transfer onto the stationary phase. Due to the extreme hydrophilicity of nucleotides and nucleotide sugars they require more hydrophobic stationary phases. Hence, C18 columns, being the most hydrophobic column available, provided the best peak shape, separation and retention. However, successful chromatography required use of an ion-pair reagent to buffer the mobile phase at suitable pH to control analyte ionization and avoid analyte acid-base equilibrium that would be deleterious for peak shape. The ion-pair reagent functions to increase the dielectric strength of the mobile phases and thereby shielding the analytes electrical surface potential which mitigates the electrostatic interactions of the sample ions with the stationary phase. Additionally, the ion reagent helps to lower the surface tension of the eluent as chaotropic agents help to disrupt the double layer surrounding the stationary phase, facilitating enhanced mass transfer through increasing accessible adsorption sites on the column by the analyte. Paramount to the method, was its ability to be mass spectrometry compatible, which requires use of volatile additives to the mobile phase, as salts would not only suppress ionization but cause contamination of the MS source, adduct formation, which all will have significant consequences for the robustness of the method. Tri-Fluoro Acetic Acid (TFA), Tri-Ethyl Ammonium Acetate (TEAA), Formic Acid (FA), were tried but none proved to offer the desired peak shape and resolution,

however, this could be a vendor specific issue of materials used. Instead, the method of (Nakajima, 2010), resulted in the best chromatographic performance with improvements to the gradient conditions, column choice and column oven temperature. Unfortunately, this method incorporated high salt concentrations, 100mM Potassium Phosphate and 8mM Tert-Butyl Ammonium Hydrogen Bisulfate. A WATERS ODS2 column proved best, as these columns are end-capped reversed-phase columns with higher hydrophobicity (surface area: 450 m<sup>2</sup>/g) than a conventional column. Under these conditions, the differences in the retention times of the nucleotide sugars were remarkable, facilitating the detection of even trace concentrations of analytes, i.e. CMP-Neu5Ac, in the presence of a great excess of analyte, i.e ATP. The methods superior separation of the peaks, then would allow fraction collection followed by desalting of the samples prior to ESI-MS analysis or alternatively no desalting would be required if MS detection was done using a MALDI-ToF. As light absorption is a non-selective detector, the possibility that some of the peaks observed contained certain contaminants in various samples or were subject to co-elution of compounds cannot be ruled out. Thus, it is recommended that additional analyses of the same samples be done by LC-ESI-MS/MS and NMR to verify the absolute identities of each peak. Future work would be to validate the analytical parameters, reproducibility, generate calibration curves of all detected molecules, identify detection limits, and establish recovery for standard mixtures and cell extracts.

This method proved able to detect cellular metabolic differences due to changes in feed and media composition. Specifically, by using the high-flux analog 1,3,4-O-Bu<sub>3</sub>-ManNAc, where ManNAc is a precursor to the sialic acid CMP-Neu5Ac, was shown to enhance sialic acid production in CHO cells. This analytical method could also be used

to observe species-specific differences in the concentrations and identities of nucleotide sugars. This last point is highly desired by metabolic engineering laboratories who seek to construct missing metabolic pathways in other organisms, such the sialic acid pathway in insects or fungi, and wish to observe the effects of their strategies. Certainly this method allows for opening up the cell from a black box to an open, fertile field; this insightful view will most certainly allow new ideas and paths to ripen.

## **Chapter 5: A Microfluidic Bio-Reactor for In-Vitro Glyco-Engineering**

### **5.1 Introduction**

The composition and relative abundance of monosaccharides within the glycoform greatly influences the bioactivity, bioavailability, and biocompatibility of the therapeutic protein. Thus, methods towards controlling the glycoform are of critical importance to the biopharmaceutical industry and research organizations. However, even when a certain glycan variant is known to have a positive impact on biological activity, it remains challenging to consistently produce such a glycosylation pattern. Whilst cell line engineering or bioprocess optimization enable the increase of glycosylation homogeneity or to at least partially achieve a certain glycan pattern (Yamane-Ohnuki, 2004; Jassal, 2001, Imai-Nishiya, 2007), these activities are time-consuming and might compromise other key parameters, e.g. antibody yield, and due to regulatory issues, it is normally only applicable at the early stages of bioprocess development (i.e., production cell line generation and selection) (Fan, 2017). Additionally, the production of mAbs with a certain glycan pattern in analytical amounts remains uneconomical using such tedious approaches (Thomann, 2015). Such drawbacks provide the motivation behind the development of In Vitro Glyco-Engineering (IVGE). IVGE represents an attractive and facile approach to providing consistent and homogeneous glycosylation. Despite enormous progress in this field, many technical problems remain. There is yet no practical chemical and biological means to discriminate different specific-sites for introducing distinct glycans with natural linkages (Wang, 2012).

Using IVGE, certain glycoforms can be enriched in downstream processing using discrete enzymatic reactions with clear kinetics and predictable outcomes (Thomann,

2015). Using IVGE, a sample itself might still exhibit glycan heterogeneity but selective changes can be introduced, e.g. conversion from low levels to high levels of galactose (Thomann, 2015). Furthermore, since it can be applied on therapeutic proteins during downstream processing, the technology is independent from the cell line and the bioprocess used, uncoupling glycosylation management from the entangled processes of cell culture and subsequent processing, granting greater control over each. No more resources wasted on uncertain tweaking of the bioprocess, leading to faster development as well as improved control of the manufacturing process (Thomann, 2015). Besides the common use of enzymes in solution, the immobilized enzymes (enzyme reactors) have recently gained attention for such studies (Palm, 2005). In contrast to the free enzymes, an enzyme reactor is reusable and can be connected on-line to other analytical techniques, such as liquid chromatography (LC) and mass spectrometry (MS), as a part of an integrated sample investigation and as part of an automated process (Palm, 2005). Enzyme reactors can thus increase the throughput of analytical assays and enhance productivity (Palm, 2005). The immobilized enzymes can be classified as either support (carrier)-bound or support (carrier)-free. Support-free immobilized enzymes whilst creating a high density of enzymes (for a rapid substrate-to-product conversion), lose the ability to retain effective enzymatic activity in combination with good hydrodynamic flow properties (i.e., high perfusion flow rate of substrate) is not always preserved (Palm, 2005). Alternatively, the enzymes immobilized at high density on highly permeable supports can be a convenient and efficient route to rapid digestion provided low concentrations of protein (Palm, 2005). To overcome these difficulties, this work has developed a chemo-enzymatic method for *in vitro* glycosylation remodeling

(glycoremodeling) of natural and recombinant glycoproteins to provide structurally defined, homogeneous glycoforms. This work is objective (2) of this thesis through implementation of a novel and transformative scalable biofabrication process applying In-Vitro Glyco-Engineering (IVGE) of a lab scale quantity of natural and recombinant glycoproteins to produce structurally well-defined, homogeneous n-glycans. Gains from performing IVGE: time- and cost-saving generation of glycan variants to develop improved and optimized glycosylation profiles without compromising other CQAs or product yield, improved lot-to-lot consistency which reduces risk of product quality variation and resulting delays, the generation of glycoprofiles which may not otherwise be generated and streamlined analytics in comparability studies (Thomann, 2015). Since it can be applied on therapeutic proteins during downstream processing, the technology is independent from the cell line and the bioprocess used. This chemo-enzymatic approach utilizes the deglycosidation activity of Endo-H for cleavage of heterogeneous n-glycans from the glycoprotein by hydrolysis of the glycosidic bond in the chitobiose core leaving only the innermost GlcNAc still attached at the Asn glycosylation site, a schematic of the reaction can be seen in Figure 27.

The choice of endoglycosidase is dictated by the glycoforms present on the protein, such as high-mannose (Endo-H/A/M), hybrid (Endo-H/S/M) or complex N-glycans (Endo-S/M)(Wang, 2012), but for exploratory purposes of the technology Endo-H was chosen out of convenience. This chemo-enzymatic approach utilizes Endo-H (containing activatable tyrosine “pro” fusion tags) covalently coupled to amine-terminated groups of pre-functionalized native oxides of silicon nano-wires (SiNW), Figures 25 and 26, to perform the glycoremodeling reaction in a biologically compatible



environment. The dimensions of the SiNWs are about 400 nm in diameter and 7 microns tall. As the SiNWs are capable of developing a capacitance  $\sim 100$  farads, this build of charge could be used to bring proteins in solution nearer to the surface for enhanced catalytic rates, in addition, this charge could solid phase capture proteins from solution, and thereby provide a unique mechanism of separation after the reaction is done. In addition, if connected the device is connected to a lock-in amplifier, using impedance spectroscopy one could functionalize the device into a nano-sensor to detect protein binding events to the surface. It is therefore critical to keep the architecture of the device capable of being electrically compatible.

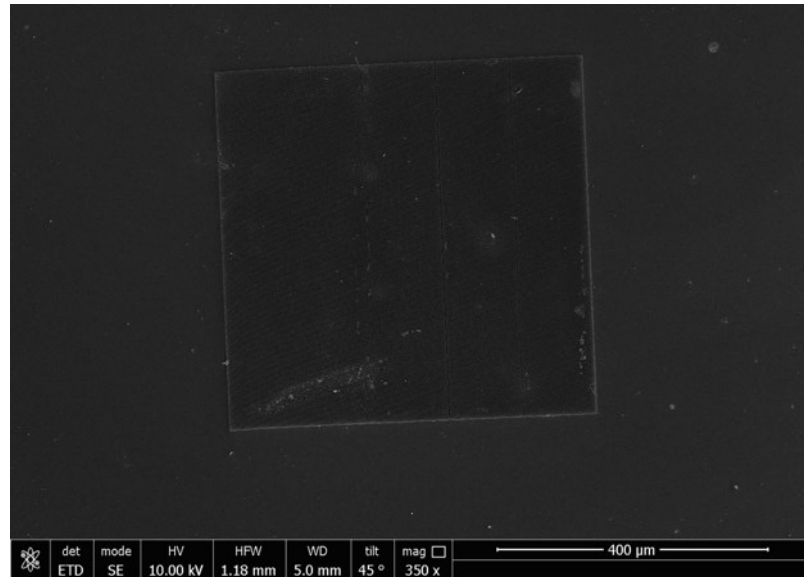


Figure 25: Scanning Electron Microscopy of Silicon Nano-Wires top-view. SEM images provided by Erdong Song, New Mexico State University.

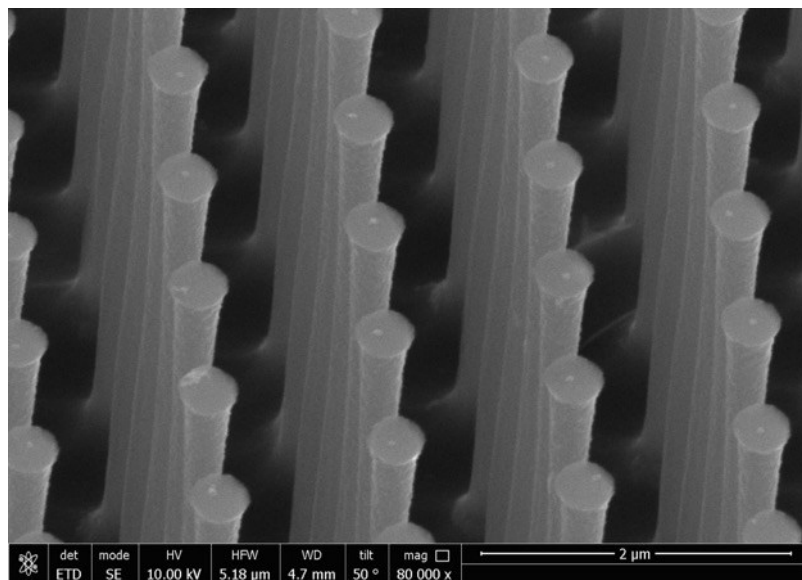


Figure 26: Scanning Electron Microscopy of Silicon Nano-Wires zoom-in with 50° tilt. SEM images provided by Erdong Song, New Mexico State University.

Using a top-down bio-fabrication method via dry etch Bosch process from a silicon single crystal wafer, these devices were elaborated by our collaborators at New Mexico State University/Sandia National Laboratories in New Mexico. Detailed description of the fabrication process will be included in a publication that is in preparation. This facile process then generates a “nanostructured forest” of enzymes onto the bioreactor surface, characterized by a large surface to volume ratio thereby offering enhanced reaction rates. In contrast to traditional in vitro methods using bulk enzymes, which are subsequently irrecoverable, this technology is re-usable; adding economic value to the process.

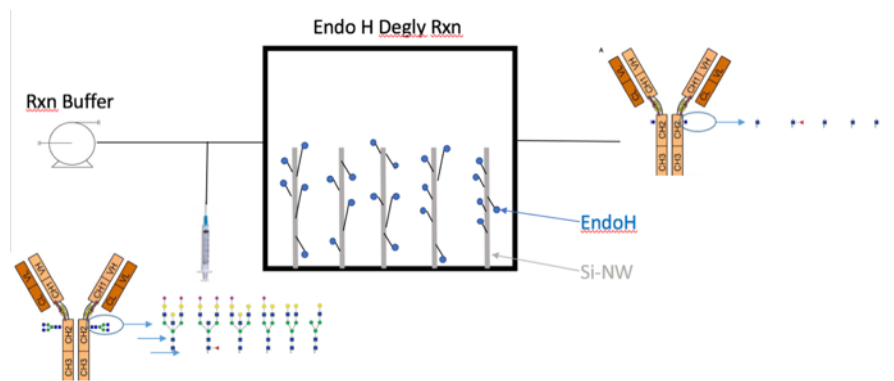


Figure 27: Schematic of Reactor deglycosidating a protein.

As Figure 27 shows, a pump would flow a protein compatible fluid such as PBS or buffered solution, then a diverter valve could be opened to allow entrance of protein solution via a syringe. As the glycoproteins enter the reaction chamber, the Endo-H enzyme would then deglycosidate the proteins, generating a terminal GlcNAc (where the GlcNAc moiety is either Fucosylated or not, Endo-H is reactive towards both species). Then the deglycosylated protein would be collected for subsequent analytical characterization. In order to demonstrate the flexibility of the method select model proteins: RNaseB, alpha-amylase and IgG, were subjected to treatment, with results demonstrating active glycoremodeling.

## 5.2 Materials and Reagents

Micro-Liter Syringe Pump (Cole-Palmer)  
Syringes (Thermo-Fisher)  
SDS-PAGE equipment (Bio-Rad)  
Endo-H conjugated silicon wires chip (Provided J.A. Martinez, NMSU Chemical Engineering)  
PDMS wet-glue (Provided Z. Gagnon, JHU Chemical Engineering)  
IgG standard 10mg (Pn I2511-10MG, Sigma-Aldrich)  
RNaseB (Provided courtesy of L.X. Wang, UMCP Chemistry & Biochemistry)  
Alpha-Amylase (Provided courtesy of Y.C. Lee, JHU Biology)  
Copper Conductive Tape, Double Sided (Pn 77802-22, Emsdium)  
Scotch 665 Double Sided, 3/4", no liner (Pn 77102, Emsdium)  
Endo-H Deglycosidase, 10000 units (Pn P0702S, New England Biolabs)

### 5.2.1 SDS-PAGE gels

Protein samples were subjected to polyacrylamide gel electrophoresis (Bio-Rad) under reducing conditions. For Coomassie blue staining, the polyacrylamide gel was soaked into the staining solution (1% w/v Coomassie blue, 50% v/v methanol, 10% v/v glacial acetic acid and 40% v/v of H<sub>2</sub>O) for 3 h and then transferred the gel to destain solution (50% v/v methanol, 10% v/v Glacial acetic acid and 40% v/v of H<sub>2</sub>O) for overnight destaining. Gels were then imaged using Bio-Rad gel imager.

### 5.2.2 Liquid chromatography-Mass spectrometry (LC-MS)

The LC-MS was performed on a LXQ system (Thermo Scientific) with a Hypersil GOLD column (1.9  $\mu$ m, 50  $\times$  2.1 mm). The samples were treated with 0.5% beta-mercaptoethanol and heated at 60 °C for 15 min. then subject to LC-MS measurement. The analysis was performed at 60 °C eluting with a linear gradient of 10–40% MeCN containing 0.1% formic acid within 10 min. at a flow rate of 0.25 mL/min. Total Ion Chromatogram (TIC), Extracted Ion Chromatogram (EIC) and Deconvoluted Mass Spectrum (DMS) are shown in the results section 5.3. Performed in the lab of Lai-Xi Wang, Chemistry Department at University Maryland College Park.

### 5.3 Results



Figure 28: Initial structure of the glyco-reactor device.

To determine the volume of the reactor housing, the reactor was first weighed dry on scale, and subsequently zeroed. After achieving steady state liquid flow of H<sub>2</sub>O across the reactor, the liquid was stopped, and the reactor was again weighed. By the difference in weight, DI water weighed .1490g, this translated to an approximate volume of fluid in the reactor as 0.1490mL, or ~150uL of liquid volume across the surface of the reactor. It was also found that in it's current configuration the reactor reservoir does not fill completely, it merely forms a lake across surface of the chip contained by the PDMS housing that flows via the tubing. This could result in limited fluid mixing, as the device is of micro-scale, it would be difficult to install a small propeller or stirrer to keep fluid moving around in the chamber to ensure continuous mixing. Perhaps at higher temperatures thermal convection could more rapidly transport analytes within the

chamber, however care must be taken to avoid denaturation of the protein and evaporation of the sample.

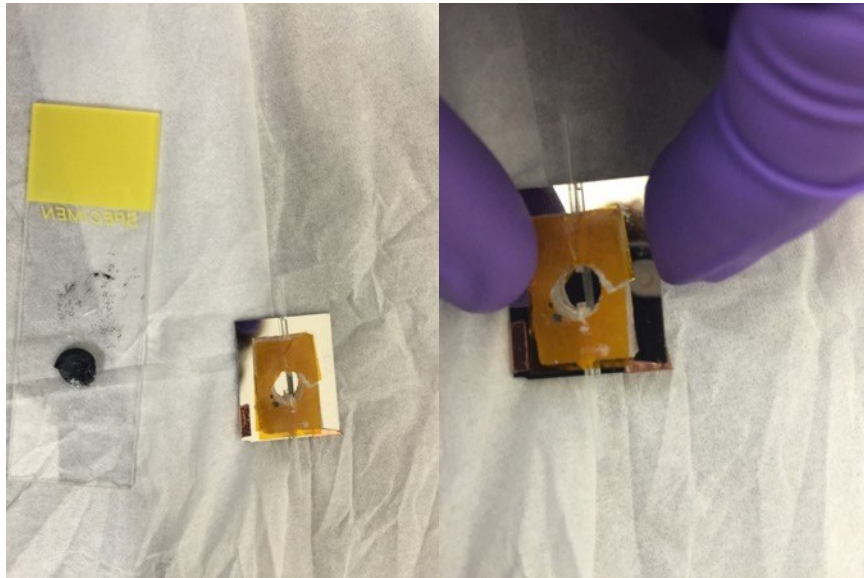


Figure 29: Dismantled reactor housing.

Figures 28 and 29 shows what the outside and inside of the reactor housing looked like. In this configuration, the device had numerous leaks, no matter what low flow rate was used 5-200  $\mu\text{L}/\text{min}$ . The inlet and outlet tubes cause protrusion of the PDMS base plan around them resulting in a not flat surface, this irregularity prohibits a good seal. The initial use of double-sided tape does not form a seal capable of withstanding the pressure of fluid flow. So the thought to switch to a thicker tape that was also conductive was done. Double sided copper tape then provided a much thicker plane to ease the unevenness of the other part geometries, as copper is malleable it would bend to the distortions inherent to the construction of the reactor housing. The base plane is a lab-glass slide, which would not conduct current. The copper tape proved a very useful tool to seal the deck of the Endo-H SiNW chip to the glass slide, result is shown in

Figure 30. However, copper tape provided better seal than the plastic tape as it was more maleable, but still leaked at 25uL/min.

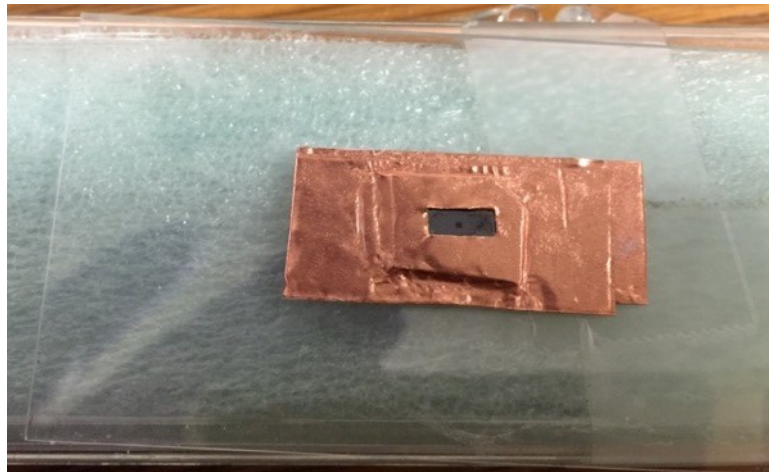


Figure 30: Copper tape seal of Endo-H enzyme SiNW Chip.

Using ‘wet PDMS’ was found the most practical way to seal, however cannot incubate in quick bake, or use plasma torch to dry as the surface enzymes will be degraded. So the copper tape with chip sealed inside and then reactor housing top was then sealed with wet PDMS. To avoid the quick bake or plasma torch, a long wait time for wet PDMS to fully cure while constantly keeping enzyme surface wet through minimal addition of solvent directly onto chip during drying at room temperature in the dark, allowed the PDMS to cure and thus seal the reactor housing. With this modification was able to achieve sealed reactor with Chip inside with ZERO LEAKS at flow rates up to 50 $\mu$ L/min. Figure 31 shows the sealed reactor connected to a syringe pump delivering protein solution into the chamber.

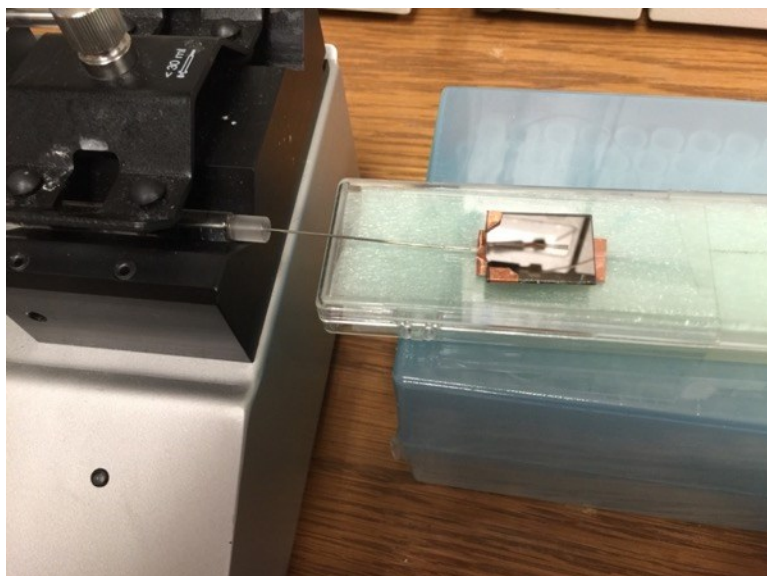


Figure 31: PDMS sealed reactor. This shows the sealed reactor with Endo-H SiNW inside connected to a syringe pump delivering protein solution into the chamber.

Although no fluid was leaking, another issue with the architecture of the reactor design arose. Namely, an issue of head-space above the chip caused by the fluid lake formed across it as discussed earlier, resulted in evaporation of the fluid during incubation at 37°C within the chamber resulting in no recoverable sample. Collection of the sample was attempted by flushing 150 $\mu$ L of DI H<sub>2</sub>O across the reactor and then removing the fluid in an attempt to resolubilize the protein. Instead it was found that a 24-Well plate had sufficient diameter to allow placement of the Endo-H SiNW chip within a well, shown in Figure 32. The appropriate volume of fluid placed above the chip was determined to be 300-400 $\mu$ L. This allowed sealing of the plate with lid attached using parafilm wrap.



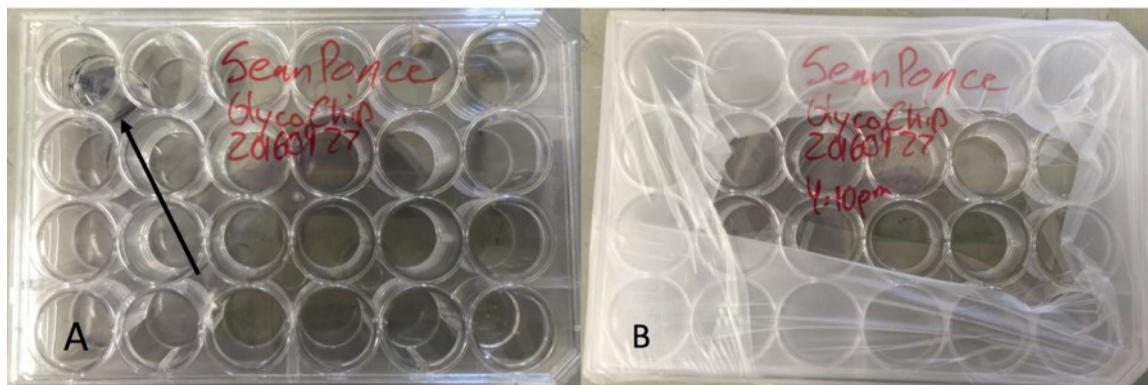
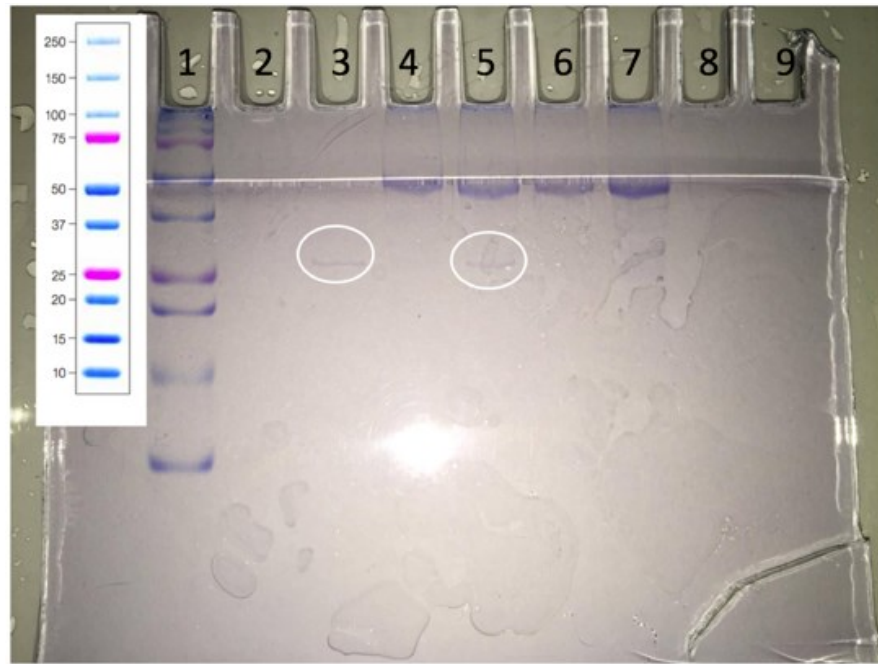


Figure 32: Endo-H SiNW chip in 24-Well Plate. Figure A shows the chip placed in upper left corner and immersed in 400 $\mu$ L of H<sub>2</sub>O. Figure B shows the plate with lid wrapped in parafilm to prevent evaporation.

Now that conditions were optimized to assess the activity of the Endo-H SiNW chip, a target protein was attempted. Alpha-Amylase (MW 51kDa) with one n-glycan site with Man5 (MW 1235 Da) was chosen because of its unique glycosylation pattern. As Endo-H enzyme has limited reactivity towards certain glycoforms, alpha-amylase is a high-mannose type glycoform, therefore amenable to digestion by Endo-H. As a control experiment, 1.5 $\mu$ L of Endo-H purchased from NEB, was digested with 5 $\mu$ g of alpha-amylase in a 37°C oven for 1 hour according to NEB protocol. The Endo-H SiNW chip placed in a 24-well plate was then incubated with 350 $\mu$ L of 0.1mg/mL intact, non-reduced, non-denatured alpha-amylase in a 37°C oven. At 4 hours a 25 $\mu$ L aliquot was removed for analysis. Then at 30 hours the plate was removed from the oven, the sample removed, however, the sample had evaporated 2/3 of its original volume, resulting in an increase of the protein concentration within the sample, this was evident on the gel image shown in Figure 29. Figure 29 shows a 15% Polyacrylamide SDS-PAGE gel run in reducing conditions as protein has disulfide bonds. The high acrylamide percentage was needed to be able to resolve +/- 1235 Da shift in mass. The molecular weight of alpha-amylase is 51kDa and the molecular weight of Endo-H NEB Cat # P0702S is 29kDA. As

Figure 33 shows, the chip's Endo-H enzyme is catalytically active, 4 hours shows no real shift in shift, at 30 hours showing complete population shift to deglycosylated state.



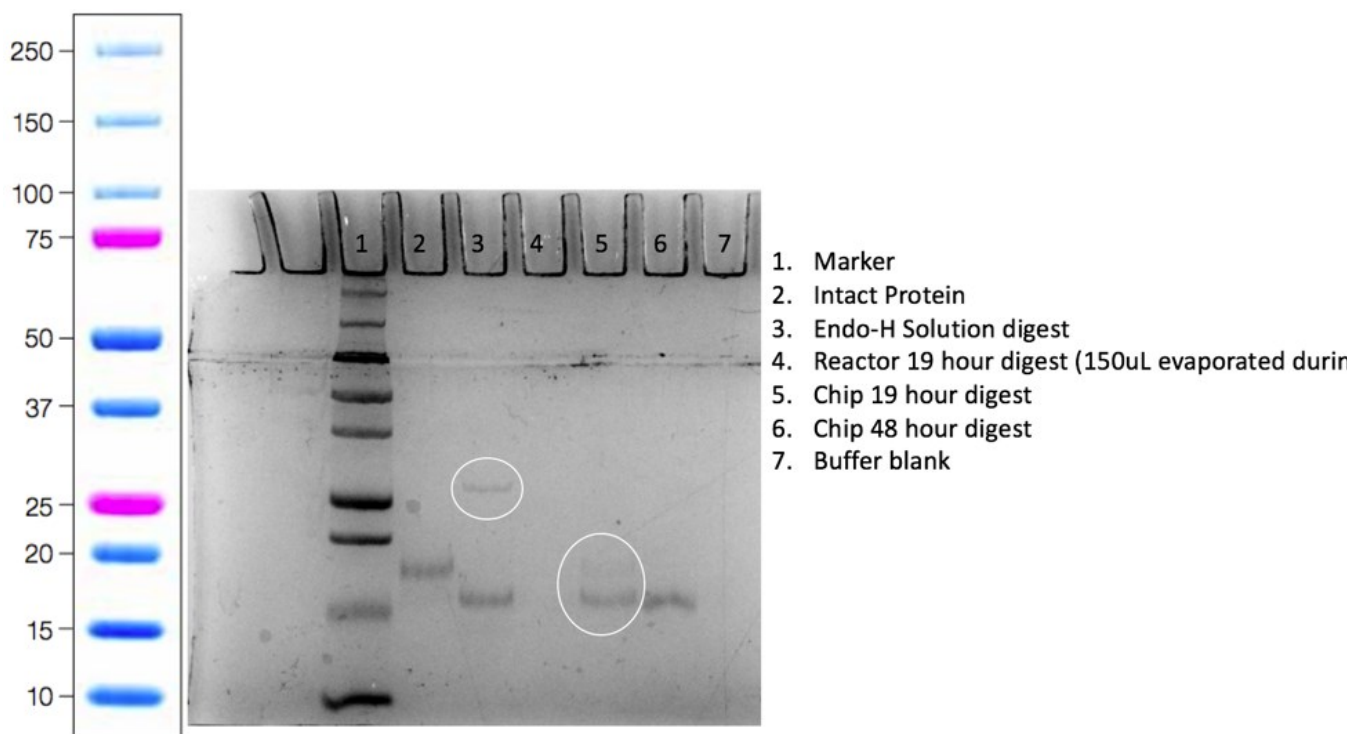
1. Precision Plus Dual Color Standard
2. Assay Reagent Blank (just buffers)
3. Endo-H enzyme only (to see enzyme on gel)
4. Alpha-Amylase Protein only (negative control)
5. Endo-H enzyme and Alpha-Amylase Digest (NEB protocol 1hr)
6. Glyco Chip Reaction at t=4hr
7. Glyco Chip Reaction at t=30hr
8. Loading Dye
9. Loading Dye

\* White circles show location of Endo-H enzyme on gel

Figure 33: SDS-PAGE of Endo-H SiNW chip digest of Alpha-Amylase. 0.7 $\mu$ g load of protein.

Now that the enzyme chip was found catalytically active another target enzyme was chosen. RNaseB, is a widely used glycoprotein standard, it has high-mannose glycan structures from Man5-Man9. As a control experiment, 5 micrograms of RNaseB was digested with 1.5 $\mu$ L Endo-H enzyme in a 37°C oven for 1 hour according to NEB protocol. Previous attempts at using the PDMS sealed glyco reactor all resulted in

evaporative loss of the sample, to overcome this, the reactor inlet and outlet tubes were sealed with parafilm to try to prevent escape after placement of 150 $\mu$ L of 0.1mg/mL intact, non-reduced, non-denatured RNaseB into the reaction chamber, the reactor was then placed into in a 37°C oven overnight for 14 hours. Separately, an Endo-H SiNW chip was placed in a cut-out well from a 24-well plate, then 500 $\mu$ L of 0.1mg/mL intact, non-reduced, non-denatured RNaseB was added and wrapped in parafilm to prevent evaporation and placed in a 37°C oven. At 19 hours a 50 $\mu$ L aliquot was removed for subsequent analysis. Then at 48 hours the well containing chip was removed from the oven. Even when wrapping the ends of the inlet and outlet tubes of the sealed glyco-reactor evaporation occurred. During the RNaseB reactor digest the ~150 $\mu$ L sample evaporated during the 37°C incubation, the protein was reconstituted in 150 $\mu$ L of H<sub>2</sub>O to remove and collect the sample for subsequent analysis by SDS-PAGE and mass spec. Figure 34 shows a 15% Polyacrylamide SDS-PAGE gel of the samples ran in reducing conditions, the high acrylamide percentage was needed to be able to resolve the shift in mass from Man<sub>9</sub>-Man<sub>5</sub> to GlcNAc stump.



\*White circle show location of Endo-H enzyme on gel  
 \*\* Note at 19 hours both degly and gly species present!

Figure 34: SDS-PAGE gel of RNaseB Reactor Digest. 0.7 $\mu$ g load of protein.

In Figure 34, it can be seen that both the glycosylated and deglycosylated forms of RNaseB exist in the Endo-H SiNW chip digest at 19 hours. This indicates a rather slow reaction time, due to limited amounts of enzymes on the surface, limited enzyme activity and/or limited interaction of the substrate and enzyme due to poor fluid mixing. Figure 30 again confirms that the Endo-H SiNW chip is catalytically when compared to the Endo-H solution digest control. At 48 hours showing complete population shift of RNaseB to deglycosylated state.

To prove that the reverse reaction of spontaneous re-glycosylation of the deglycosylated RNaseB material was not occurring, the samples were then subjected to the time incubation scheme shown in Figure 35. It can be seen that no shift in molecular

weight can be observed for the RNaseB in all cases, thus proving that the deglycosylation reaction was not proceeding in the reverse direction.

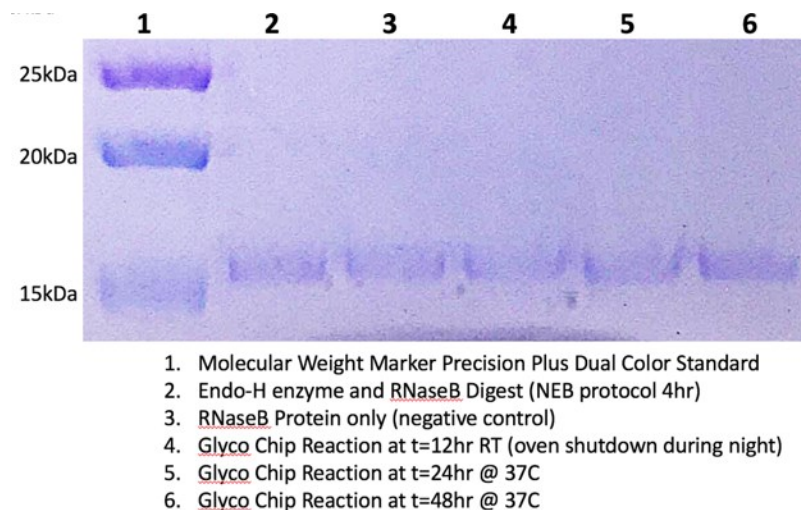


Figure 35: SDS-PAGE gel of deglycosylated RNaseB Reactor Digest. 0.7 $\mu$ g load of protein.

To prove absolutely certain that the Endo-H SiNW chip was performing deglycosylation, the samples from the RNaseB experiment were subjected to LC-MS.

Each protein sample was loaded onto the column at 1  $\mu$ g.

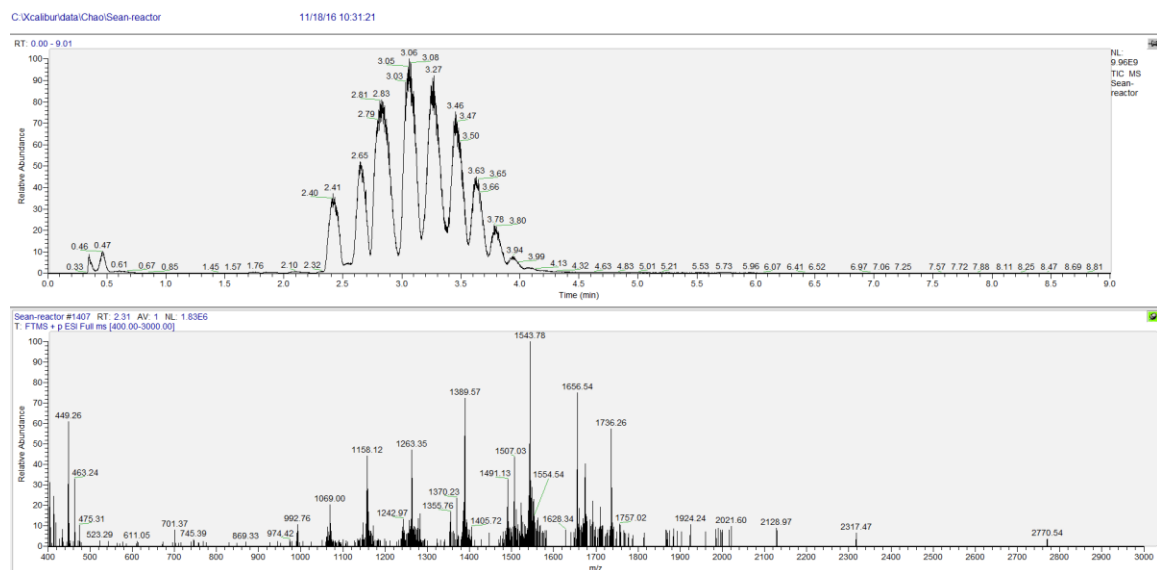


Figure 36: TIC and EIC for RNaseB Glyco-Reactor at 14 hour digest.

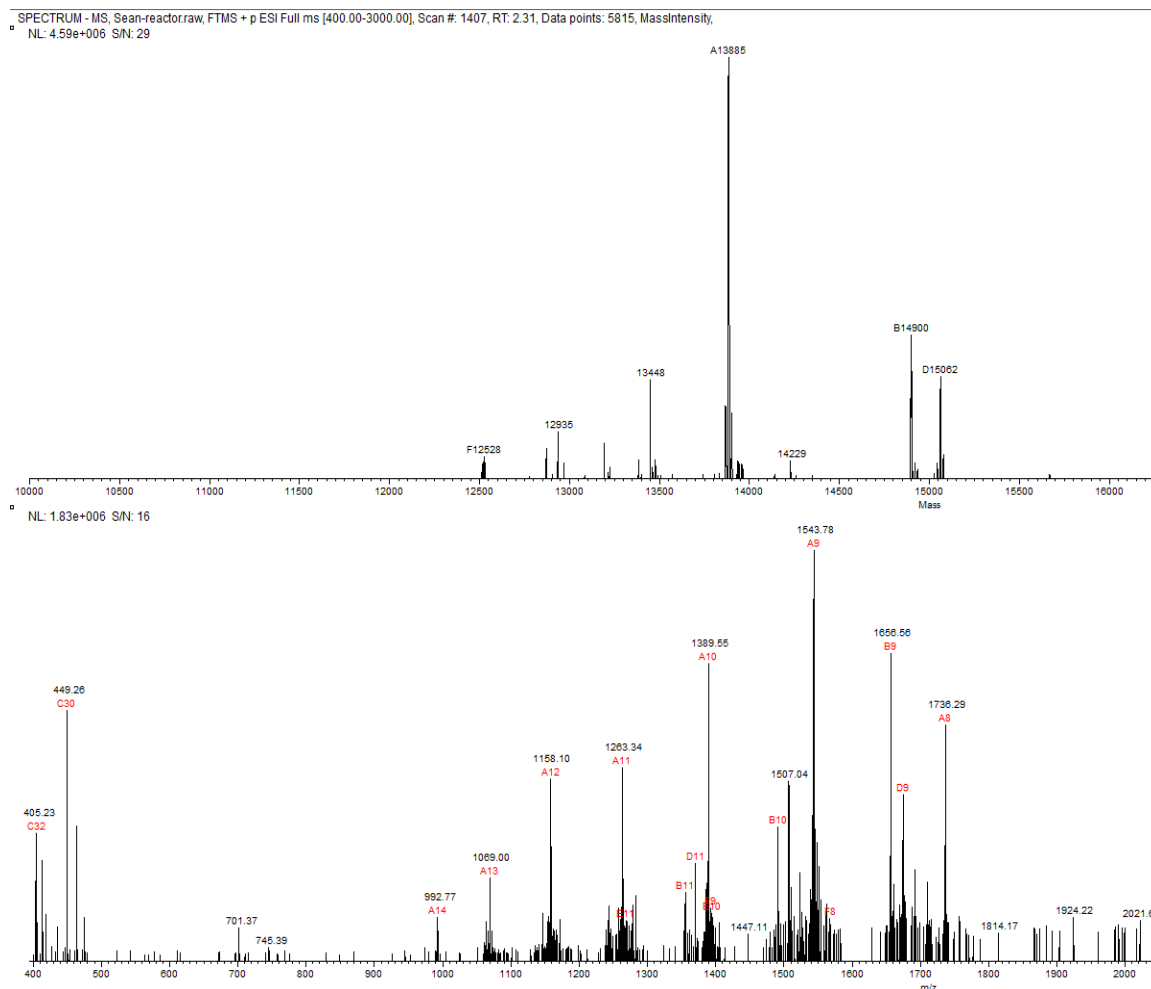


Figure 37: DMS for RNaseB Glyco-Reactor at 14 hour digest.

Even though the gel was not able to detect any leftover RNaseB in the evaporated Glyco-Reactor digest, the Mass Spec analysis was able to get signal, albeit at low signal intensity (Figure 36), nonetheless the data shows that the chip was indeed performing deglycosylation prior to drying out. On the chromatographic conditions used RNaseB was found to elute at ~2.2min. In the EIC of Figures 36 and 37, the B9 fragment ion (m/z 1656.56) corresponds to Man5 glycoform, with the A8 fragment ion (m/z 1736.29) corresponds to Man9 glycoform, the A9 fragment ion (m/z 1543.78) corresponds to deglycosylated form of RNaseB. In the top of Figure of 37, the masses of 13885-, 14900- and 15062-Da correspond to deglycosylated, Man5 and Man6 glycoforms of

RNaseB respectively. It can be noted that the presence of both intact and deglycosylated species in the evaporated glyco-reactor sample, indicates that the reaction probably stopped upon being dried out, as the Man5 and Man6 glycoforms were still present prior to evaporation.

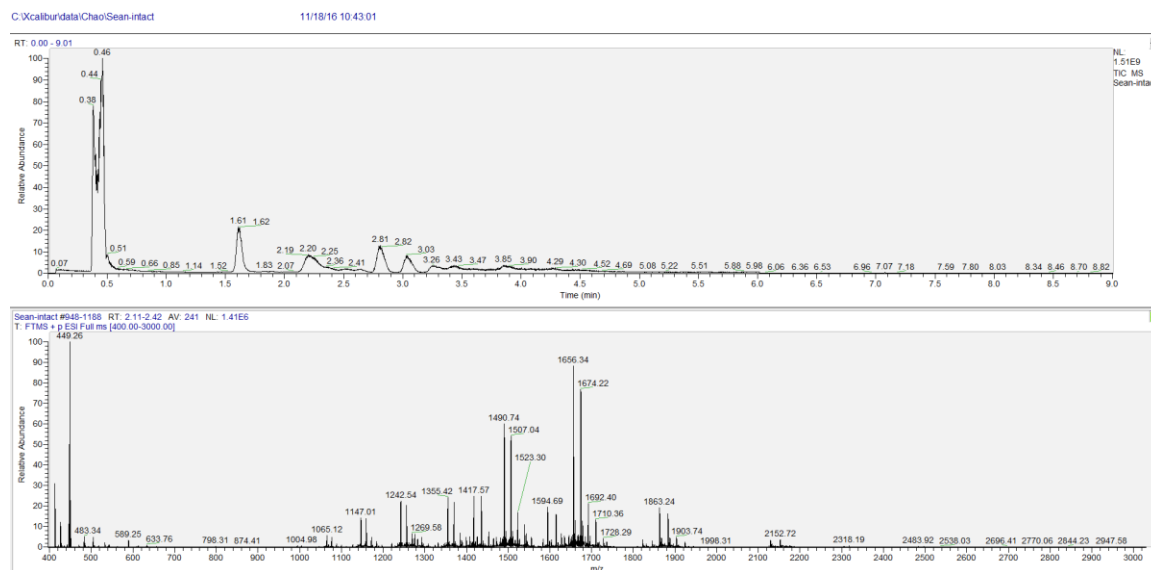


Figure 38: TIC and EIC for Intact RNaseB.

In the top of Figure of 39, the masses of 14898-, 15222-, 15385- and 15062-Da correspond to Man5, Man6, Man7 and Man8 glycoforms of intact RNaseB respectively.



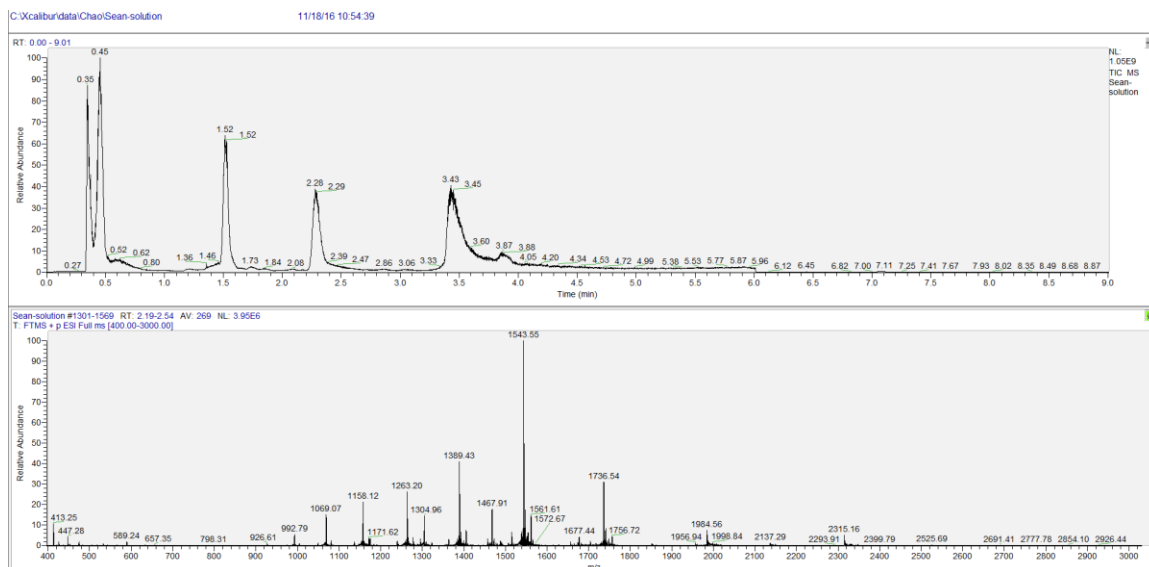


Figure 40: TIC and EIC for Endo-H digested RNaseB in solution.

As shown in Figure 40, the RNaseB molecule elutes at ~2.3 minutes and the Endo-H enzyme at ~3.4 minutes.

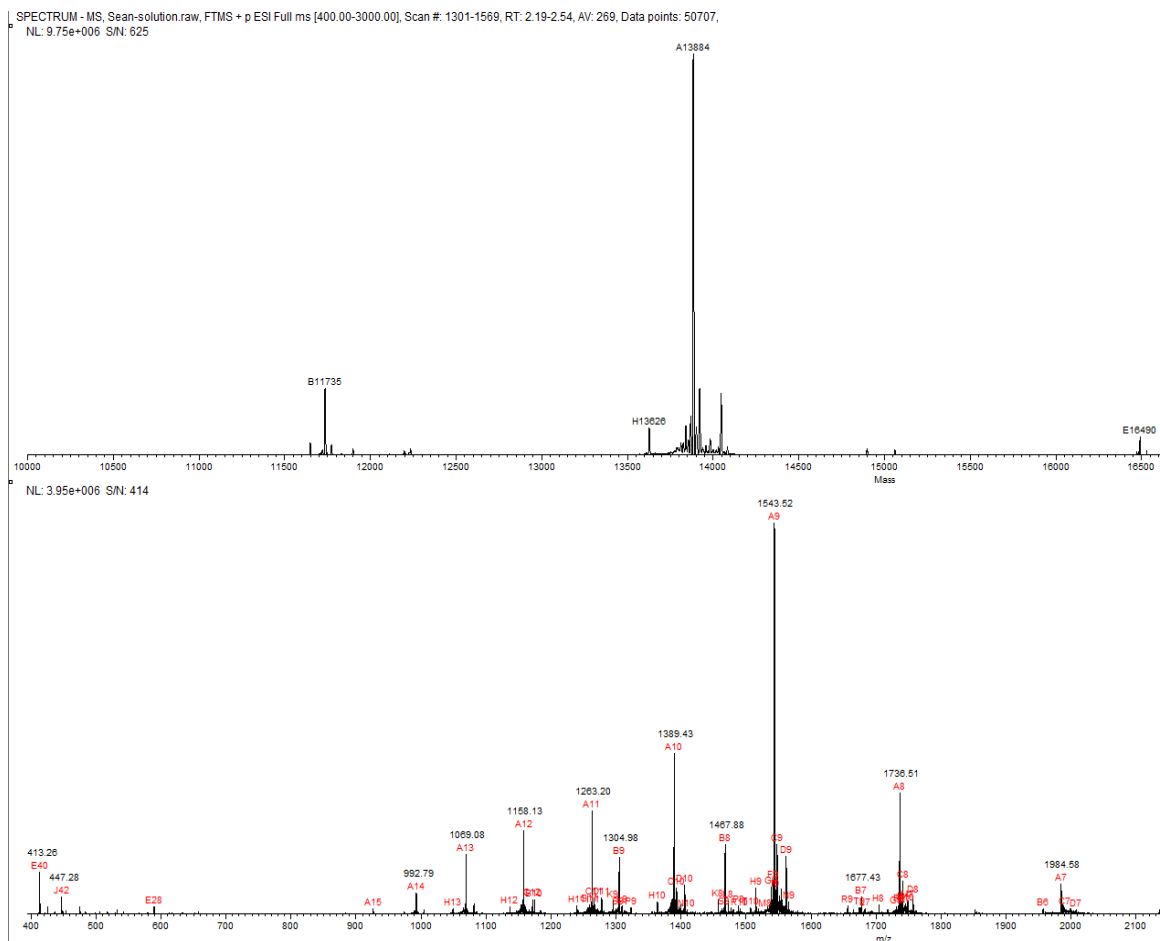
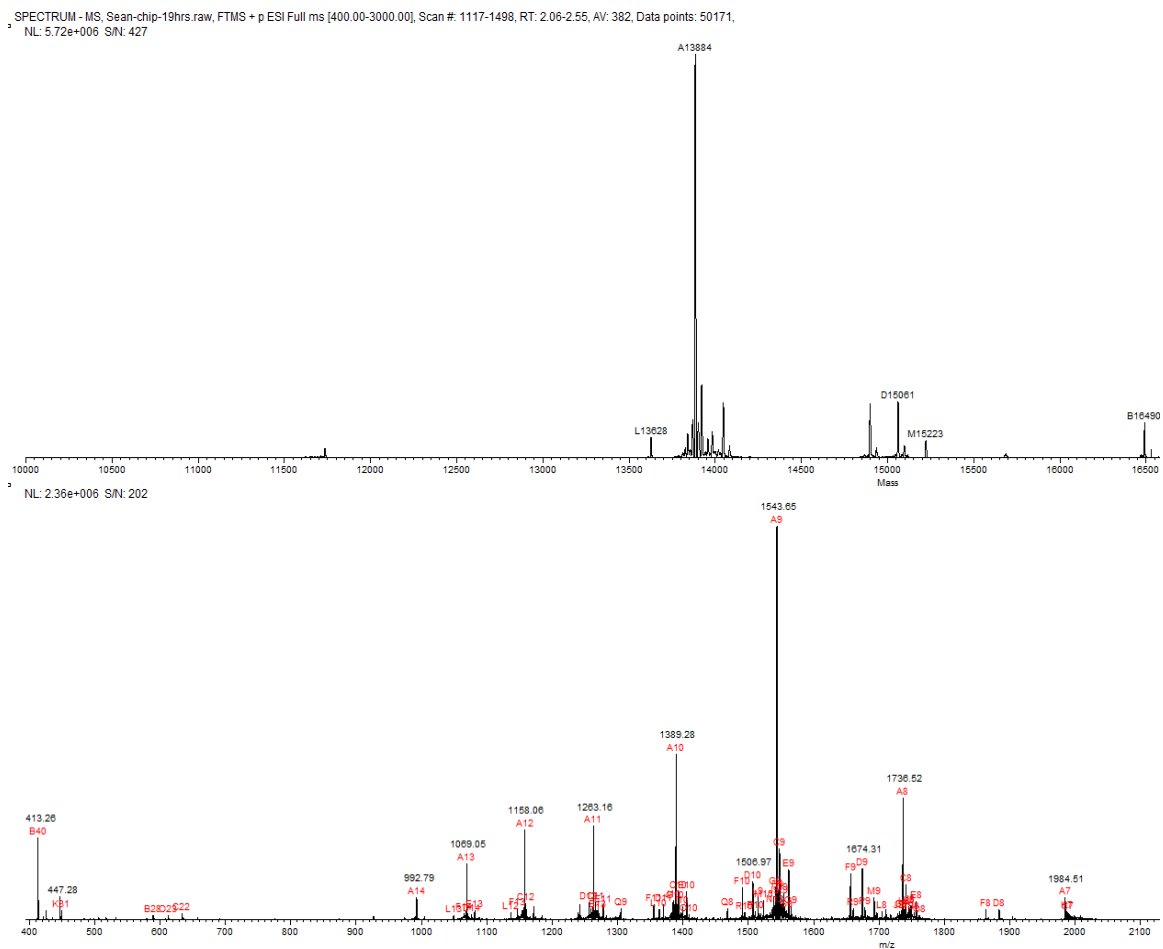
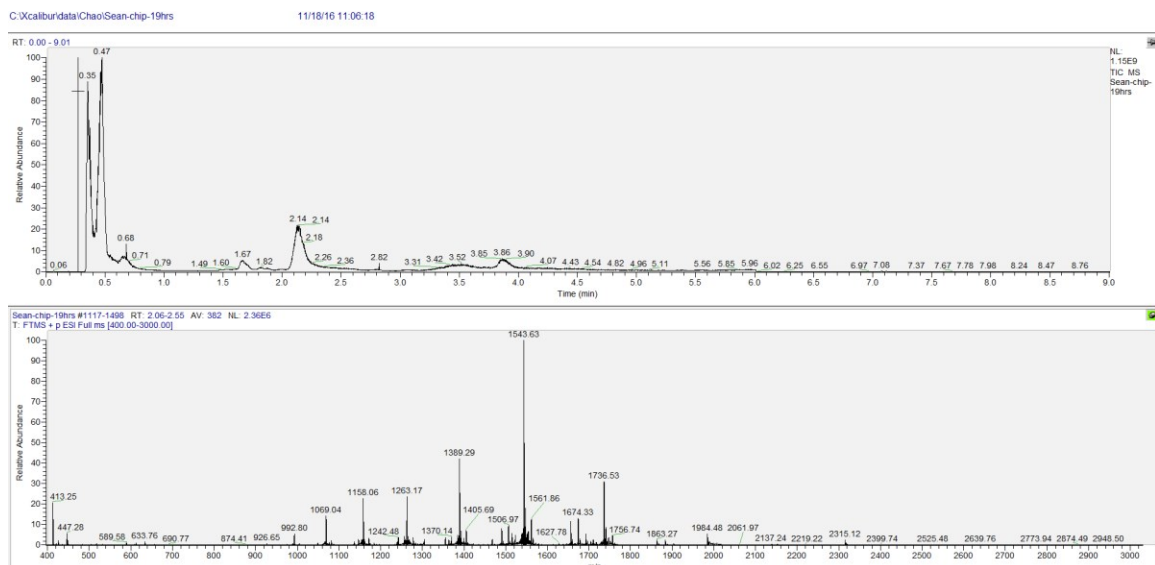


Figure 41: DMS for Endo-H digested RNaseB in solution.

As shown in Figure 41, the reaction of RNaseB digested in solution with Endo-H achieved complete deglycosylation to the mass of 13884 Da corresponding to the RNaseB containing GlcNAc stump.



As seen in Figure 43, can be seen that both the glycosylated (molecular weights at 15061 and 15223 Da corresponding to Man5 and Man6) and deglycosylated (molecular weight at 13884 Da) glycoforms of RNaseB exist in the Endo-H SiNW chip digest at 19 hours.

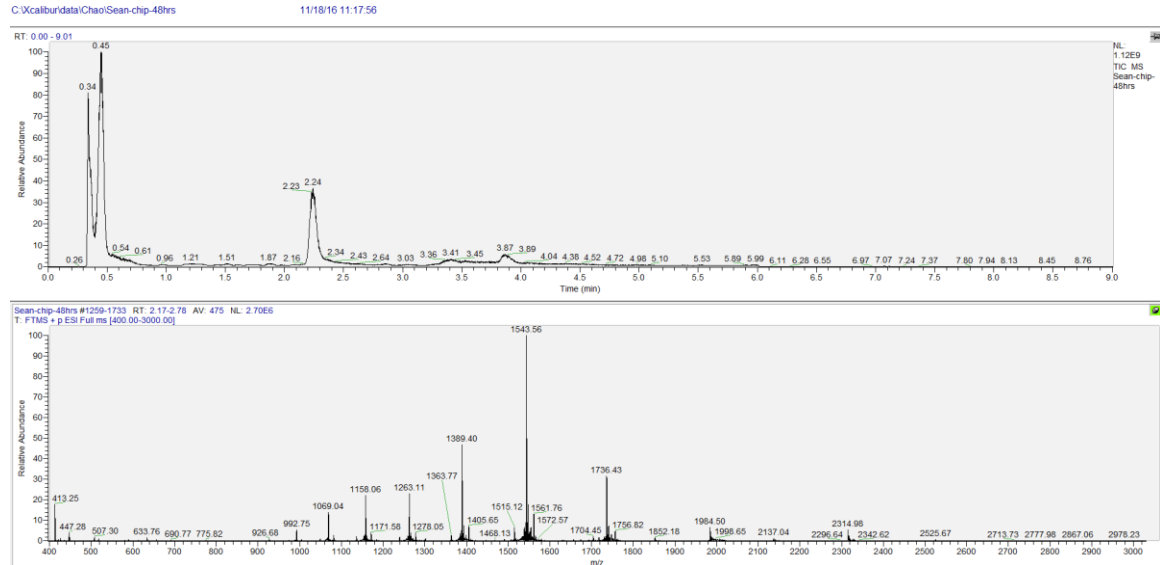


Figure 44: TIC and EIC for glyco-chip digestion at 48 hours.

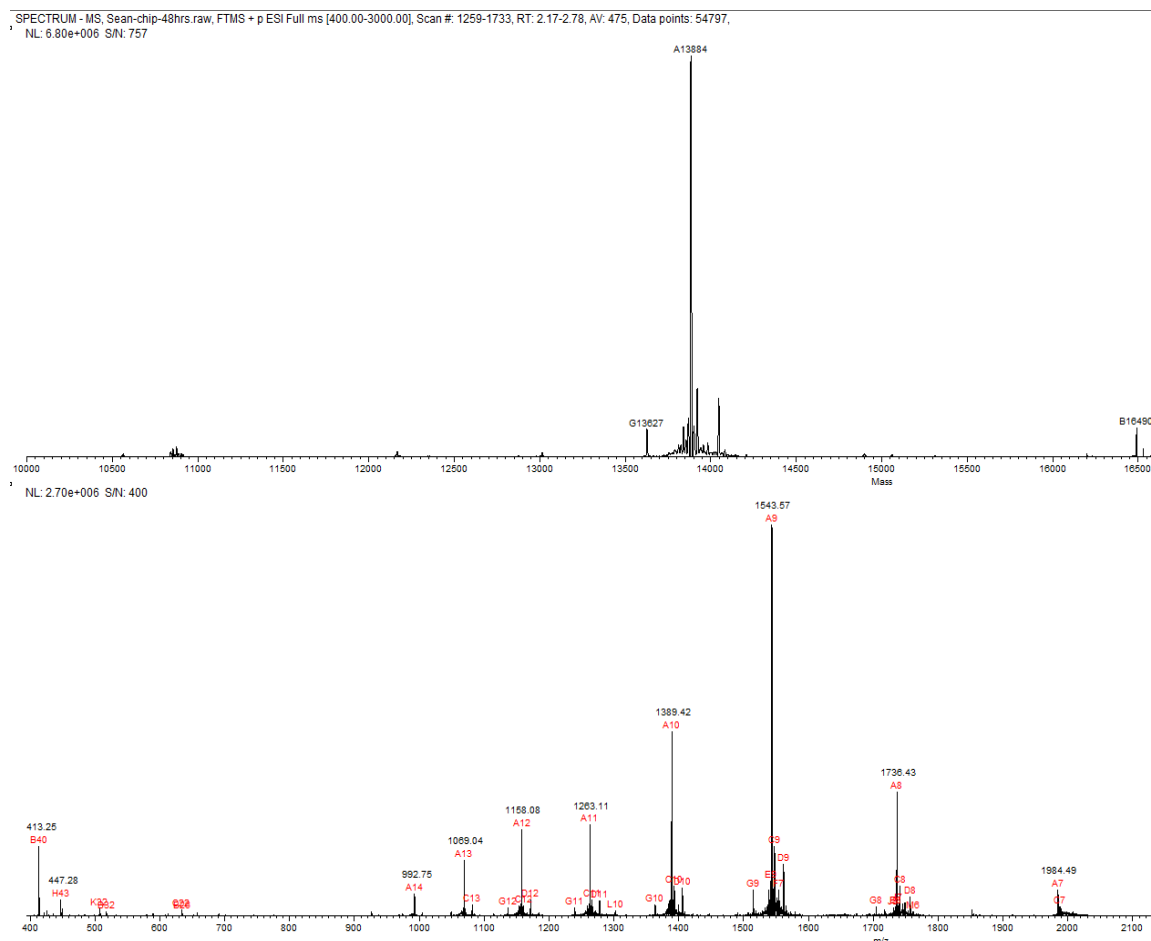


Figure 45: DMS for glyco-chip digestion at 48 hours.

In Figure 45, the Endo-H SiNW chip digest of RNaseB at 48 hours shows complete deglycosylation to the mass of 13884 Da corresponding to the RNaseB containing GlcNAc stump, this weight correlates with the gel image of Figure 34.

Next IgG was subjected to glyco-chip digestion. 400 $\mu$ L of 0.1 mg/mL IgG were incubated with the Endo-H SiNW chip for 48 hours in 37°C incubator. A separate digest by PNGaseF was done to prove that the complex glycans attached to the IgG could be removed, 10 micro-grams of IgG were mixed with 1 $\mu$ L of PNGaseF and allowed to incubate for 24 hours at 37°C. As can be seen in Figure 46 SDS-PAGE gel, the molecular weight of IgG heavy chain is ~50 kDa, and that of IgG light chain is ~25 kDa. The IgG light chains show no variation in molecular weight in all cases because IgG do

not typically contain Fab linked glycosylation. The heavy chain mass stays constant in the the intact IgG standard under both reduced and non-reduced conditions, lanes 2-3, and in the glyco-chip with the Endo-H enzyme showing no reaction towards complex glycans (which is the expected result as Endo-H cannot cleave complex glycans found on IgG), lane 5, while in lane 4 the PNGaseF digested IgG resulted in a lower molecular weight heavy chain corresponding to the removal of complex glycans of ~1500 Da.

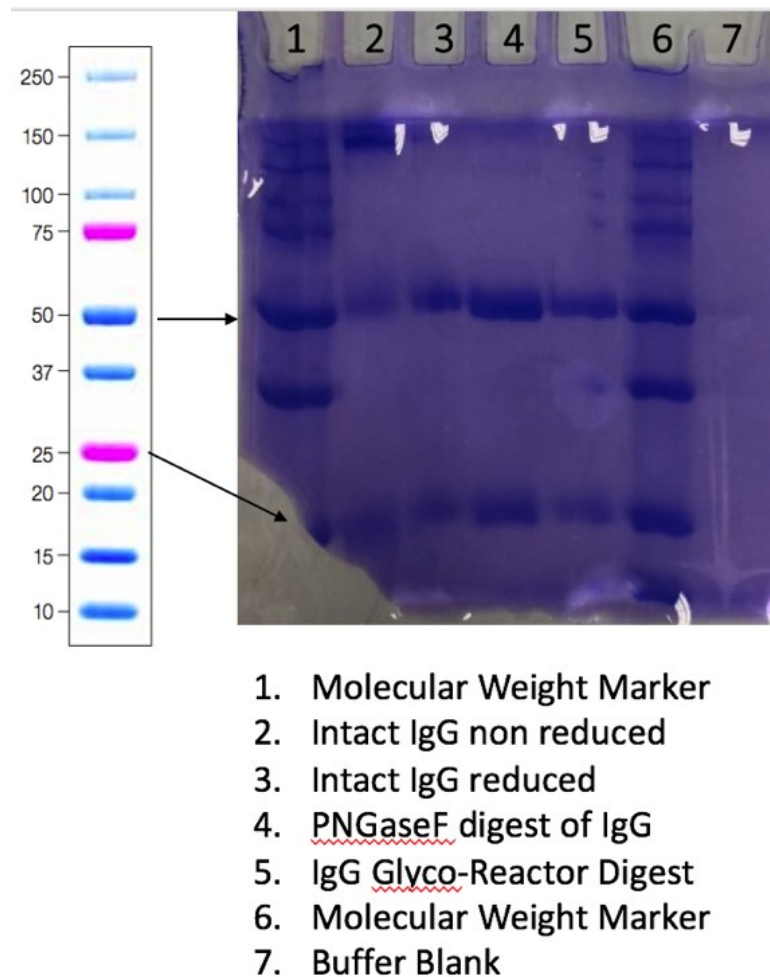


Figure 46: SDS-PAGE gel of IgG digest using Endo-H SiNW chip. 1.8 $\mu$ g load of protein.

## 5.4 Discussion

Achieving uniform, consistent and specified protein glycosylation in cell expression systems remains a case-by-case basis requiring a certain set of gene/protein/enzyme expression and activity levels, as well as the spatial availability of the nucleotide sugar substrates in the ER and Golgi, involved in glycosylation product formation. To overcome the tedious and inherently expensive cell culture based approach towards controlling glycosylation, aim two of this thesis has demonstrated an in vitro approach that uncouples glycosylation products from cell, media and process conditions. This approach utilized a cell-free bioreactor to remove glycans from proteins generating uniform, structurally defined glycoforms.

The microfluidic system presented herein was designed to reduce sample volume, analysis time and cost. In this process herein, the enzyme Endoglycosidase-H was conjugated to a forest of vertical silicon nano-wires to carry out the deglycosylation under physiological buffer conditions leaving the terminal GlcNAc of the chitobiose core attached to the asparagine. However, a major drawback of this enzyme is it's limited and/or no reactivity toward certain hybrid and complex glycoforms, preventing the glyco re-modelling of mAb's (predominantly complex glycoforms G0-,G1-, and G2-F). Future studies should conjugate Endoglycosidase-M or Endoglycosidase-S to be amenable to a wider variety of protein substrates.

The yield of modified glycoproteins is strongly dependent of the surface concentration of viable Endo-H enzymes, the rate of the enzymatic reaction, and by controlling the extent of the reverse reaction. Future efforts should determine the concentration of conjugated Endo-H enzyme to the silicon nanowires. Due to bound

enzyme on a very small surface area, long reaction times are required to compensate. Currently operated in batch mode but larger surface area could allow for continuous mode operation.

The device is “short-circuited” meaning it is currently grounded on itself. Resistance is measured across an object; need to measure voltage between two electrode plates, not on the same one.

The surface area on the enzyme chip available is too small for any high-throughput application. However, it is envisioned that upon scale-up of this reactor configuration, continuous mode operation could be achieved where-in it would become an additional unit operation within bio-process laboratories. The glycosidase “Endo-H” is not reactive towards complex glycans and shows limited toward hybrid glycan structures. This was demonstrated not to work with IgG whose predominant glycoform is complex. Though more expensive; Endo-S, Endo-A or Endo-M glycosidase enzymes may be better enzymes to conjugate going forward to allow wider access for different protein glycoforms. It is critical that these glycosidase leave the terminal GlcNAc stump attached to the asparagine or it will not be compatible with LX Wang’s trans-glycosylation machinery.

Future steps for this process would be to acquire the transglycosidases and oxazoline substrates (Wang, 2014) then used for en bloc transfer of desired glycoforms back onto the deglycosylated protein. In this way, in principle, any specific and desired glycoform can then be incorporated onto a protein. The improved efficiency and flexibility in making various glycans would facilitate glycoform specific use in research, clinical and industrial applications.



## Conclusions and Future Work

A new paradigm in the manufacturing process issued by the main regulatory bodies such as the United States Food and Drug Administration (USFDA) and European Medicines Agency (EMA), encourage the implementation of Quality by Design (QbD) into the manufacturing process. The tenets of QbD are the development and manufacture of pharmaceutical products through well-understood processes to ensure consistent, predefined quality at the end of the manufacturing process, therefore facilitating reduced approval times and increased flexibility towards changes in manufacturing process conditions. This is accomplished by defining the desired product performance, identifying critical product attributes and the parameters that affect those product attributes, and timely measurements of those attributes to achieve the defined product performance. This requires definition of acceptance limits, and the eventual testing of the product's quality throughout production for validation of such specified process parameter ranges. Glycosylation is a main source of product heterogeneity in biotherapeutics (Del Val, 2010) serving essential functions of the biotherapeutic (Spahn, 2014), and thus is a critical protein quality attribute to consider its biogenesis during the biopharmaceutical manufacturing process. Once the biotherapeutic (protein) and its desired glycosylation pattern with associated efficacy are set, the QbD methodology synergizes how the manufacturing conditions give rise to the desired product profile with built-in analytical tests to ensure a self-correcting mechanism of action towards those specified product attributes. Thus by applying a DoE approach (e.g., factorial design) streamlines the investigation of the impact of multi-factors, multi-variables, and their interactions on N-glycosylation. Towards this goal, Thesis Objective One entailed

developing a toolset to provide inputs to defining such acceptable criteria during the manufacturing campaign, through HPLC-based methods to determine the amino acid composition, glycosylation patterns, nucleotide sugar distributions and titer. As amino acids are substrates for nucleotides, which are components of nucleotide sugars, which are the substrates for glycosylation on the synthesized protein, which determines the glycosylation pattern, these assays synergize how the glycosylation profile is inextricably linked to substrate availability, enzyme activities and cellular metabolism. Thus providing a systematic framework to facilitate the exploration and screening of process conditions, media compositions, and cell lines that command desired glycosylation of the biotherapeutic. Furthermore, this framework can be used to track the cellular status during production steps for monitoring conditions as added quality control measures to prove the production run falls within set specifications. Such identification of “bad batches” would allow early termination of runs not in specification and thereby prevent prolonged and expensive continuation of doomed cultures. It is envisioned that this could become a novel analytical toolset in Chemistry Manufacturing and Control data sections to support increased knowledge of process conditions and ways to ensure that the product is controlled within specified quality criteria throughout production. Principally this method could be used to identify bottle necks in cellular metabolism and glycosylation, and consequently engineering strategies to overcome them. In medical application, the metabolic phenotypes of healthy and diseased cells are not homogeneous, but instead depend strongly on the molecular alterations and environmental factors at play in each case. Thus the hope in applying such technology to different cell types (or in principle, any cell type) will be to identify cell type specific metabolic signature’s that are

characteristic of each type. Especially intriguing is the elucidation of key metabolic regulatory check points based on changes in the intracellular processing events and enzyme activities, thereby increasing our understanding of the cellular mechanisms that have gone awry in healthy and diseased states. As an example, in many diseased states, including cancer, the distributions of glycan structures often differs from that of healthy cells, leading to the possibility that such disease-specific glycan phenotypes exist and that these differences can be exploited for thera-nostic purposes in the identification of disease-associated biomarkers and design of bioengineered glycan modifications. Additionally, measurement of these key glycosylation parameters can then serve as inputs to computational model-based investigations. A current challenge is to interrelate the different levels of available information, from the genome to the transcriptome to the proteome to the metabolome to the glycome, and how this experimental data can be modeled to recreate a given phenotype and ultimately make predictions about network topology and cellular behavior. Such predictions would facilitate more cost effective and faster alternatives to costly screening strategies, thereby reducing the experimental design space required to direct the glycosylation pattern. These systems-level analyses of glycosylation encompassing both experimental and computational data will elucidate deeper insights into the mechanisms underlying and controlling glycosylation.

Achieving uniform, consistent and specified protein glycosylation in cell expression systems remains a case-by-case basis requiring a certain set of gene/protein/enzyme expression and activity levels, as well as the spatial availability of the nucleotide sugar substrates in the ER and Golgi, involved in glycosylation product formation. To overcome the tedious and inherently expensive cell culture based

approach towards controlling glycosylation, aim two of this thesis has demonstrated an in vitro approach that uncouples glycosylation products from cell, media and process conditions. This approach utilized a cell-free bioreactor to remove glycans from proteins generating homogeneous glycoforms. In this process, the enzyme Endoglycosidase-H was conjugated to a forest of vertical silicon nano-wires to carry out the deglycosylation under physiological buffer conditions, leaving the terminal GlcNAc of the chitobiose core attached to the asparagine. However, a major drawback of this enzyme is it's limited and/or no reactivity toward certain hybrid and complex glycoforms, preventing the glyco re-modelling of mAb's (predominantly complex glycoforms G0-,G1-, and G2-F). Future studies should conjugate Endoglycosidase-H or Endoglycosidase-S to be amenable to a wider variety of protein substrates. Future steps for this process would be to acquire the transglycosidases and oxazoline substrates then used for en bloc transfer of desired glycoforms back onto the deglycosylated protein. In this way, in principle, any specific and desired glycoform can then be incorporated onto a protein, thereby facilitating glycoform specific use in research, clinical and industrial applications.

## Supplementary Materials

### Cell Counts

Cell counts were performed using a hemocytometer and a light microscope. After removing cells from the plate, a small aliquot was taken for cell counts. 50 uL cell/PBS mix was mixed with 750L trypan blue (Cellgro, Manassa, VO). 10 uL of this mixture was added to each side of the hemocytometer and stained cells were counted. Each count was repeated at least two times.

### Treatment of Cultures With 1,3,4- O-Bu<sub>3</sub>ManNAc and ManNAc

CHO-K1 cells were seeded at  $1 \times 10^6$  cells in 10 cm dishes in 10 ml Ham's F-12K media untreated or treated with 20 mM ManNAc (Sigma–Aldrich) or various concentrations of 1,3,4-O-Bu<sub>3</sub>ManNAc (50, 100, 150, 200, 250, 300, 350  $\mu$ M). Cells were collected at confluency at over 90% after 3 days. Supernatants were collected after 48 h incubation with or without treatment and then subjected to IgG purification.

### Protein-A IgG Affinity Chromatography to Assess mAb Titer

HPLC: Shimadzu LC-10Ai

Column: TSKgel Protein A-5PW, 20  $\mu$ m, 4.6 mm ID  $\times$  3.5 cm

MPA: 20mM NaPO<sub>4</sub> pH 7.20

MPB: 100mM NaPO<sub>4</sub> pH 3.00

Detector: U.V. Abs. 254 and 280nm

Flow Rate: 1 mL/min

Step-Gradient: T0 = 0%B, T3.20 = 100%B, T6 = %100B, T6.01 = 0%B, T10 = 0%B.

Injection Volume: 10  $\mu$ L

Sample Preparation: Cell media containing IgG filtered through 0.22  $\mu$ m syringe-filter.

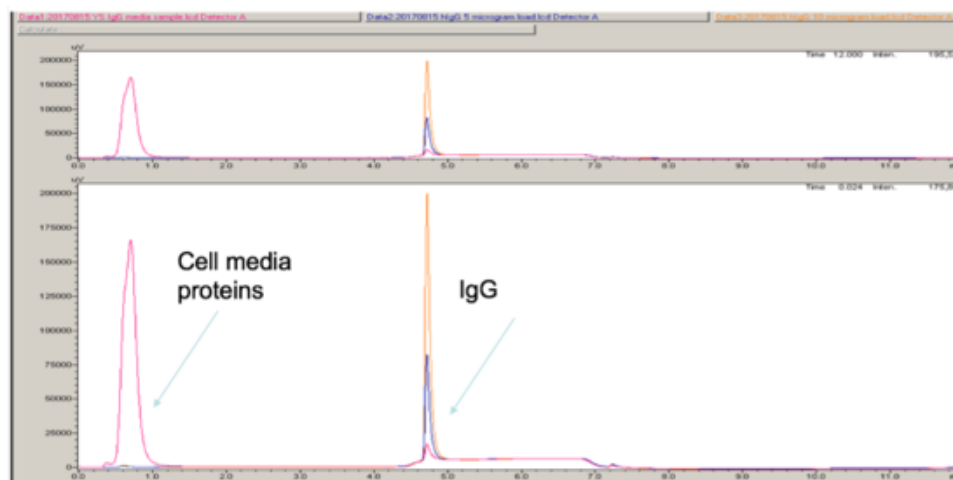


Figure 47: Protein-A HPLC Chromatogram.  
Human-IgG Std: Orange 1mg/mL, Blue .5mg/mL. Media Sample at day 4: pink.

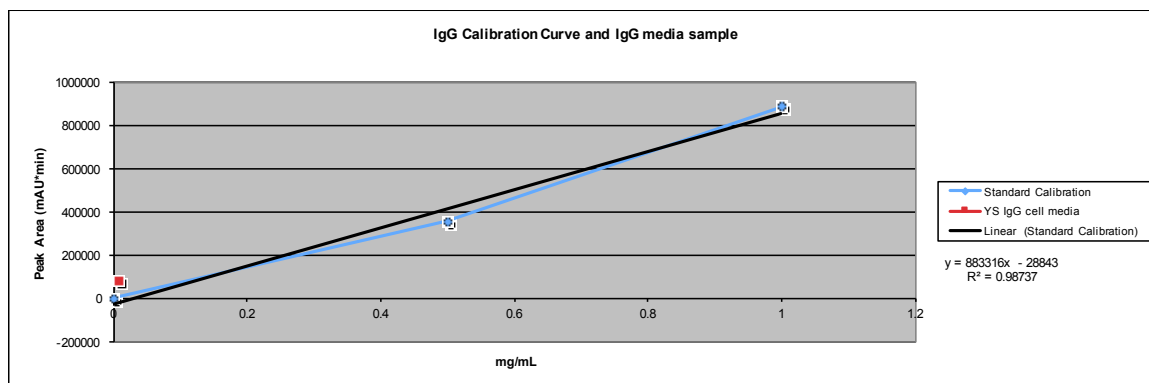


Figure 48: Protein-A Chromatography IgG Calibration Curve. The cell media sample was determined to be 0.011mg/mL at day 4 of cell growth.

## Bibliography

### A

Allinquant, B., Musenger, C., & Schuller, E. (1985). Reversed-phase high-performance liquid chromatography of nucleotides and oligonucleotides. *Journal of Chromatography A*, 326, 281-291. doi:10.1016/s0021-9673(01)87453-7

Anghileri, A., Lantto, R., Kruus, K., Arosio, C., Freddi, G. (2007). Tyrosinase-catalyzed grafting of sericin peptides onto chitosan and production of protein-polysaccharide bioconjugates. *Journal of biotechnology*. 127(3):508-19. doi:10.1016/j.jbiotec.2006.07.021

Antoniewicz, M. R., Kelleher, J. K., & Stephanopoulos, G. (2007). Accurate assessment of amino acid mass isotopomer distributions for metabolic flux analysis. *Analytical chemistry*, 79(19), 7554-7559. doi:10.1021/ac0708893

### B

Barnes, J., Tian, L., Loftis, J., Hiznay, J., Comhair, S., Lauer, M., & Dweik, R. (2016). Isolation and analysis of sugar nucleotides using solid phase extraction and fluorophore assisted carbohydrate electrophoresis. *MethodsX*, 3, 251-260. doi:10.1016/j.mex.2016.03.010

Bar-Peled, M., & O'Neill, M. A. (2011). Plant nucleotide sugar formation, interconversion, and salvage by sugar recycling. *Annual review of plant biology*, 62, 127-155. doi:10.1146/annurev-arplant-042110-103918

Bhushan, R., & Brückner, H. (2011). Use of Marfey's reagent and analogs for chiral amino acid analysis: Assessment and applications to natural products and biological systems. *Journal of Chromatography B*, 879(29), 3148-3161. doi:10.1016/j.jchromb.2011.05.058

Bonfiglio, R., King, R. C., Olah, T. V., & Merkle, K. (1999). The effects of sample preparation methods on the variability of the electrospray ionization response for model drug compounds. *Rapid Communications in Mass Spectrometry*, 13(12), 1175-1185. doi:10.1002/(SICI)1097-0231(19990630)13:12<1175::AID-RCM639>3.0.CO;2-0

Braasch, K., Villacrés, C., & Butler, M. (2015). Evaluation of Quenching and Extraction Methods for Nucleotide/Nucleotide Sugar Analysis. *Glyco-Engineering: Methods and Protocols*, 1321, 361-372. doi:10.1007/978-1-4939-2760-9\_24

Burleigh, S. C., van de Laar, T., Stroop, C. J., van Grunsven, W. M., O'Donoghue, N., Rudd, P. M., & Davey, G. P. (2011). Synergizing metabolic flux analysis and nucleotide sugar metabolism to understand the control of glycosylation of recombinant protein in CHO cells. *BMC biotechnology*, 11(1), 95. doi:10.1186/1472-6750-11-95

Butler, M. (2006). Optimisation of the cellular metabolism of glycosylation for recombinant proteins produced by mammalian cell systems. *Cytotechnology*, 50(1-3), 57. doi:10.1007/s10616-005-4537-x

## C

Chung, C., Wang, Q., Yang, S., Yin, B., Zhang, H., & Betenbaugh, M. (2017). Integrated Genome and Protein Editing Swaps  $\alpha$ -2,6 Sialylation for  $\alpha$ -2,3 Sialic Acid on Recombinant Antibodies from CHO. *Biotechnology Journal*, 12(2), 1600502. doi:10.1002/biot.201600502

Cohen, S. A., & Michaud, D. P. (1993). Synthesis of a fluorescent derivatizing reagent, 6-aminoquinolyl-N-hydroxysuccinimidyl carbamate, and its application for the analysis of hydrolysate amino acids via high-performance liquid chromatography. *Analytical biochemistry*, 211(2), 279-287. doi:10.1006/abio.1993.1270

Cohen, S. A. (2003). Amino Acid Analysis Using Pre-Column Derivatization with 6-Aminoquinolyl N-Hydroxysuccinimidyl Carbamate: Analysis of Hydrolyzed Proteins and Electroblotted Samples. *Protein Sequencing Protocols*, 211, 143-154.

Cook, M.C., Kaldas, S.J., Muradia, G., Rosu-Myles, M., Kunkel, J.P. (2015). Comparison of orthogonal chromatographic and lectin-affinity microarray methods for glycan profiling of a therapeutic monoclonal antibody. *J Chromatogr B Analyt Technol Biomed Life Sci*. 997:162-78. doi:10.1016/j.jchromb.2015.05.035.

Cui, Y., Wei, Q., Park, H., Lieber, C.M. (2001). Nanowire nanosensors for highly sensitive and selective detection of biological and chemical species. *Science*. 293(5533):1289-92. doi:10.1126/science.1062711

## D

Davies, J., Jiang, L., Pan, L. Z., LaBarre, M. J., Anderson, D., & Reff, M. (2001). Expression of GnTIII in a recombinant anti-CD20 CHO production cell line: expression of antibodies with altered glycoforms leads to an increase in ADCC through higher affinity for FC $\gamma$ RIII. *Biotechnology and bioengineering*, 74(4), 288-294. doi:10.1002/bit.1119

Del Val, I. J., Kyriakopoulos, S., Polizzi, K. M., & Kontoravdi, C. (2013). An optimized method for extraction and quantification of nucleotides and nucleotide sugars from mammalian cells. *Analytical biochemistry*, 443(2), 172-180. doi:10.1016/j.ab.2013.09.005

Dell A., Sastre F. (2014) Glycosylation: A Phenomenon Shared by All Domains of Life. In: Delitala M., Ajmone Marsan G. (eds) Managing Complexity, Reducing Perplexity. Springer Proceedings in Mathematics & Statistics, vol 67. Springer, Cham doi:10.1007/978-3-319-03759-2\_7



Dietmair, S., Timmins, N. E., Gray, P. P., Nielsen, L. K., & Krömer, J. O. (2010). Towards quantitative metabolomics of mammalian cells: development of a metabolite extraction protocol. *Analytical biochemistry*, 404(2), 155-164. doi:10.1016/j.ab.2010.04.031

## E

Ecker, D. M., Jones, S. D., & Levine, H. L. (2015). The therapeutic monoclonal antibody market. *MAbs*, 7(1), 9-14. doi:10.4161/19420862.2015.989042

Egrie, J. C., Dwyer, E., Browne, J. K., Hitz, A., & Lykos, M. A. (2003). Darbepoetin alfa has a longer circulating half-life and greater in vivo potency than recombinant human erythropoietin. *Experimental hematology*, 31(4), 290-299. doi:10.1016/S0301-472X(03)00006-7

## F

Fan, Y., Jimenez Del Val, I., Müller, C., Wagtberg Sen, J., Rasmussen, S. K., Kontoravdi, C., ... & Andersen, M. R. (2015). Amino acid and glucose metabolism in fed-batch CHO cell culture affects antibody production and glycosylation. *Biotechnology and bioengineering*, 112(3), 521-535. doi:10.1002/bit.25450

Fan, Y., Kildegard, H. F., & Andersen, M. R. (2017). Engineer Medium and Feed for Modulating N-Glycosylation of Recombinant Protein Production in CHO Cell Culture. *Heterologous Protein Production in CHO Cells: Methods and Protocols*, 209-226. doi:10.1007/978-1-4939-6972-2\_14

FDA, Guidance for Industry, PAT--A Framework for Innovative Pharmaceutical Development, Manufacturing, and Quality Assurance (Rockville, MD, Sept. 2004).

Federn, H., & Ristow, H. (1986). Isolation of standard-, deoxy-and highly phosphorylated nucleotides from *Bacillus brevis* and their separation by ion-pair high-performance liquid chromatography. *Chromatographia*, 22(7), 287-291.

Folch, J., Lees, M., & Sloane Stanley, G. H. (1957). A simple method for the isolation and purification of total lipids from animal tissues. *J biol Chem*, 226(1), 497-509.

Fukuda, M. N., Sasaki, H., Lopez, L., & Fukuda, M. (1989). Survival of recombinant erythropoietin in the circulation: the role of carbohydrates. *Blood*, 73(1), 84-89.

## G

Giddens, J. P., & Wang, L. X. (2015). Chemoenzymatic glyco-engineering of monoclonal antibodies. *Methods Mol Biol*. 1321: 375–387. doi:10.1007/978-1-4939-2760-9\_25

Gillmeister, M. P., Tomiya, N., Jacobia, S. J., Lee, Y. C., Gorfien, S. F., & Betenbaugh, M. J. (2009). An HPLC-MALDI MS method for N-glycan analyses using smaller size

samples: application to monitor glycan modulation by medium conditions. *Glycoconjugate journal*, 26(9), 1135-1149. doi:10.1007/s10719-009-9235-z

Glacken, M. W., Adema, E., & Sinskey, A. J. (1988). Mathematical descriptions of hybridoma culture kinetics: I. Initial metabolic rates. *Biotechnology and bioengineering*, 32(4), 491-506. doi:10.1002/bit.260320412

Goldwasser, E., Kung, C. K. H., & Eliason, J. (1974). On the mechanism of erythropoietin-induced differentiation XIII. The role of sialic acid in erythropoietin action. *Journal of Biological Chemistry*, 249(13), 4202-4206.

Grigorian, A., Mkhikian, H., Li, C. F., Newton, B. L., Zhou, R. W., & Demetriou, M. (2012). Pathogenesis of multiple sclerosis via environmental and genetic dysregulation of N-glycosylation. *Seminars in Immunopathology*, 34(3), 415-424. doi:10.1007/s00281-012-0307-y

## H

Hansen, H. A., & Emborg, C. (1994). Influence of ammonium on growth, metabolism, and productivity of a continuous suspension Chinese hamster ovary cell culture. *Biotechnology progress*, 10(1), 121-124. doi:10.1021/bp00025a014

Hanson, S. R., Culyba, E. K., Hsu, T. L., Wong, C. H., Kelly, J. W., & Powers, E. T. (2009). The core trisaccharide of an N-linked glycoprotein intrinsically accelerates folding and enhances stability. *Proceedings of the National Academy of Sciences*, 106(9), 3131-3136. doi:10.1073/pnas.0810318105

Harada, Y., Nakajima, K., Masahara-Negishi, Y., Freeze, H. H., Angata, T., Taniguchi, N., & Suzuki, T. (2013). Metabolically programmed quality control system for dolichol-linked oligosaccharides. *Proceedings of the National Academy of Sciences*, 110(48), 19366-19371. doi:10.1073/pnas.1312187110

Higuchi, M., Oh-eda, M., Kuboniwa, H., Tomonoh, K., Shimonaka, Y., & Ochi, N. (1992). Role of sugar chains in the expression of the biological activity of human erythropoietin. *Journal of Biological Chemistry*, 267(11), 7703-7709.

Hills, A. E., Patel, A., Boyd, P., & James, D. C. (2001). Metabolic control of recombinant monoclonal antibody N-glycosylation in GS-NS0 cells. *Biotechnology and Bioengineering*, 75(2), 239-251. doi:10.1002/bit.10022

Hossler, P., Khattak, S. F., & Li, Z. J. (2009). Optimal and consistent protein glycosylation in mammalian cell culture. *Glycobiology*, 19(9), 936-949. doi:10.1093/glycob/cwp079

Hossler, P., Mulukutla, B. C., & Hu, W. S. (2007). Systems analysis of N-glycan processing in mammalian cells. *PloS one*, 2(8), e713. doi:10.1371/journal.pone.0000713

Hossler, P., Chumsae, C., Racicot, C., Ouellette, D., Ibraghimov, A., Serna, D., ... & Carrillo, R. (2017). Arabinosylation of recombinant human immunoglobulin-based protein therapeutics. *MAbs*, 9(4), 715-734. doi:10.1080/19420862.2017.1294295

Hou, W., Qiu, Y., Hashimoto, N., Ching, W. K., & Aoki-Kinoshita, K. F. (2016). A systematic framework to derive N-glycan biosynthesis process and the automated construction of glycosylation networks. *BMC bioinformatics*, 17(S7), 465-472. doi:10.1186/s12859-016-1094-6

Hsieh, Y., Chintala, M., Mei, H., Agans, J., Brisson, J. M., Ng, K., & Korfmacher, W. A. (2001). Quantitative screening and matrix effect studies of drug discovery compounds in monkey plasma using fast-gradient liquid chromatography/tandem mass spectrometry. *Rapid communications in mass spectrometry*, 15(24), 2481-2487. doi:10.1002/rcm.479

## I

ICH, Q5E Specifications: Test Procedures and Acceptance Criteria for Biotechnological/Biological Products, EMA Document CPMP/ICH/5721/03 (Geneva, 2003).

ICH Q6B Specifications: Test Procedures and Acceptance Criteria for Biotechnological/Biological Products, EMA Document CPMP/ICH/365/96 (Geneva, 1999).

Imai-Nishiya, H., Mori, K., Inoue, M., Wakitani, M., Iida, S., Shitara, K., & Satoh, M. (2007). Double knockdown of  $\alpha$ 1, 6-fucosyltransferase (FUT8) and GDP-mannose 4, 6-dehydratase (GMD) in antibody-producing cells: a new strategy for generating fully non-fucosylated therapeutic antibodies with enhanced ADCC. *BMC biotechnology*, 7(1), 84. doi:10.1186/1472-6750-7-84

Ivarsson, M., Villiger, T. K., Morbidelli, M., & Soos, M. (2014). Evaluating the impact of cell culture process parameters on monoclonal antibody N-glycosylation. *Journal of biotechnology*, 188, 88-96. doi:10.1016/j.jbiotec.2014.08.026

## J

Jacobs, P. P., & Callewaert, N. (2009). N-glycosylation engineering of biopharmaceutical expression systems. *Current molecular medicine*, 9(7), 774-800.

Jadhav, V., Hackl, M., Druz, A., Shridhar, S., Chung, C. Y., Heffner, K. M., ... & Grillari, J. (2013). CHO microRNA engineering is growing up: Recent successes and future challenges. *Biotechnology advances*, 31(8), 1501-1513. doi:10.1016/j.biotechadv.2013.07.007

Jaeken, J. (2013). Congenital disorders of glycosylation. *Handbook of clinical neurology*, 113, 1737-1743. doi:10.1016/b978-0-444-59565-2.00044-7

Jassal, R., Jenkins, N., Charlwood, J., Camilleri, P., Jefferis, R., & Lund, J. (2001). Sialylation of human IgG-Fc carbohydrate by transfected rat  $\alpha$ 2, 6-sialyltransferase. *Biochemical and biophysical research communications*, 286(2), 243-249. doi:10.1006/bbrc.2001.5382

Jedrzejewski, P. M., del Val, I. J., Constantinou, A., Dell, A., Haslam, S. M., Polizzi, K. M., & Kontoravdi, C. (2014). Towards controlling the glycoform: a model framework linking extracellular metabolites to antibody glycosylation. *International journal of molecular sciences*, 15(3), 4492-4522. doi:10.3390/ijms15034492

Jefferis, R. (2009). Glycosylation as a strategy to improve antibody-based therapeutics. *Nat Rev Drug Discov*. 8(3):226-34. doi: 10.1038/nrd2804.

## K

Khmelnitsky, Y. L. (2004). Current strategies for in vitro protein glycosylation. *Journal of Molecular Catalysis B: Enzymatic*, 31(4), 73-81. doi:10.1016/j.molcatb.2004.07.002

Kochanowski, N., Blanchard, F., Cacan, R., Chirat, F., Guedon, E., Marc, A., & Goergen, J. L. (2006). Intracellular nucleotide and nucleotide sugar contents of cultured CHO cells determined by a fast, sensitive, and high-resolution ion-pair RP-HPLC. *Analytical biochemistry*, 348(2), 243-251.

Koek, M. M., Muilwijk, B., van der Werf, M. J., & Hankemeier, T. (2006). Microbial metabolomics with gas chromatography/mass spectrometry. *Analytical chemistry*, 78(4), 1272-1281. doi:10.1021/ac051683+

Krambeck, F. J., Bennun, S. V., Narang, S., Choi, S., Yarema, K. J., & Betenbaugh, M. J. (2009). A mathematical model to derive N-glycan structures and cellular enzyme activities from mass spectrometric data. *Glycobiology*, 19(11), 1163-1175. doi:10.1093/glycob/cwp081

## L

Lane, A. N., & Fan, T. W. M. (2015). Regulation of mammalian nucleotide metabolism and biosynthesis. *Nucleic acids research*, 43(4), 2466-2485. doi:10.1093/nar/gkv047

López, S. L., Moal, J., & Serrano, F. S. (2000). Development of a method for the analysis of nucleotides from the mantle tissue of the mussel *Mytilus galloprovincialis*. *Journal of Chromatography A*, 891(1), 99-107. doi:10.1016/s0021-9673(00)00637-3

López-Gutiérrez, B., Dinglasan, R. R., & Izquierdo, L. (2017). Sugar nucleotide quantification by liquid chromatography tandem mass spectrometry reveals a distinct profile in *Plasmodium falciparum* sexual stage parasites. *Biochemical Journal*, 474(6), 897-905. doi:10.1042/BCJ20161030

## M

Millard, P., Cahoreau, E., Heuillet, M., Portais, J. C., & Lippens, G. (2017). <sup>15</sup>N-NMR-Based Approach for Amino Acids-Based <sup>13</sup>C-Metabolic Flux Analysis of Metabolism. *Analytical Chemistry*, 89(3), 2101-2106. doi:10.1021/acs.analchem.6b04767

Melmer, M., Stangler, T., Schiefermeier, M., Brunner, W., Toll, H., Rupprechter, A., Lindner, W., Premstaller, A. (2010). HILIC analysis of fluorescence-labeled N-glycans from recombinant biopharmaceuticals. *Anal Bioanal Chem*. 398(2):905-14. doi:10.1007/s00216-010-3988-x.

Morell, A.G., Irvine, R.A., Sternlieb, I., Scheinberg, I.H., & Ashwell, G. (1968). Physical and chemical studies on ceruloplasmin V. Metabolic studies on sialic acid-free ceruloplasmin in vivo. *Journal of Biological Chemistry*, 243(1), 155-159.

Murrell, M.P., Yarema, K.J., & Levchenko, A. (2004). The systems biology of glycosylation. *ChemBioChem*, 5(10), 1334-1347. doi:10.1002/cbic.200400143

Müller, C., Schäfer, P., Störtzel, M., Vogt, S., & Weinmann, W. (2002). Ion suppression effects in liquid chromatography–electrospray-ionisation transport-region collision induced dissociation mass spectrometry with different serum extraction methods for systematic toxicological analysis with mass spectra libraries. *Journal of Chromatography B*, 773(1), 47-52. doi:10.1016/s1570-0232(02)00142-3

## N

Nakajima, K., Kitazume, S., Angata, T., Fujinawa, R., Ohtsubo, K., Miyoshi, E., & Taniguchi, N. (2010). Simultaneous determination of nucleotide sugars with ion-pair reversed-phase HPLC. *Glycobiology*, 20(7), 865-871. doi:10.1093/glycob/cwq044

Nakajima, K., Ito, E., Ohtsubo, K., Shirato, K., Takamiya, R., Kitazume, S., ... & Taniguchi, N. (2013). Mass isotopomer analysis of metabolically labeled nucleotide sugars and N-and O-glycans for tracing nucleotide sugar metabolisms. *Molecular & Cellular Proteomics*, 12(9), 2468-2480. doi:10.1074/mcp.M112.027151

Nolan, R. P., & Lee, K. (2011). Dynamic model of CHO cell metabolism. *Metabolic engineering*, 13(1), 108-124. doi:10.1016/j.ymben.2010.09.003

## O

Ohtsubo, K., & Marth, J. D. (2006). Glycosylation in Cellular Mechanisms of Health and Disease. *Cell*, 126(5), 855-867. doi:10.1016/j.cell.2006.08.019

Orellana, A., Moraga, C., Araya, M., & Moreno, A. (2016). Overview of nucleotide sugar transporter gene family functions across multiple species. *Journal of molecular biology*, 428(16), 3150-3165. doi:10.1016/j.jmb.2016.05.021

## P

Pabst, M., Grass, J., Fischl, R., Léonard, R., Jin, C., Hinterkörner, G., ... & Altmann, F. (2010). Nucleotide and nucleotide sugar analysis by liquid chromatography-electrospray ionization-mass spectrometry on surface-conditioned porous graphitic carbon. *Analytical chemistry*, 82(23), 9782-9788. doi:10.1021/ac101975k

Palm, A.K., Novotny, M.V. (2005). A monolithic PNGase F enzyme microreactor enabling glycan mass mapping of glycoproteins by mass spectrometry. *Rapid Commun Mass Spectrom.* 19(12):1730-8. doi:10.1002/rcm.1979

Peace, R. W., & Gilani, G. S. (2005). Chromatographic determination of amino acids in foods. *Journal of AOAC International*, 88(3), 877-887.

## Q

## R

Rahman, A. M. A., Pawling, J., Ryczko, M., Caudy, A. A., & Dennis, J. W. (2014). Targeted metabolomics in cultured cells and tissues by mass spectrometry: Method development and validation. *Analytica chimica acta*, 845, 53-61. doi:10.1016/j.aca.2014.06.012

Ramm, M., Wolfender, J. L., Queiroz, E. F., Hostettmann, K., & Hamburger, M. (2004). Rapid analysis of nucleotide-activated sugars by high-performance liquid chromatography coupled with diode-array detection, electrospray ionization mass spectrometry and nuclear magnetic resonance. *Journal of Chromatography A*, 1034(1), 139-148. doi:10.1016/j.chroma.2004.02.023

Reiter, W. (2008). Biochemical genetics of nucleotide sugar interconversion reactions. *Current Opinion in Plant Biology*, 11(3), 236-243. doi:10.1016/j.pbi.2008.03.009

## S

Sauer, U. (2006). Metabolic networks in motion: 13 C-based flux analysis. *Molecular systems biology*, 2(1), 62. doi:10.1038/msb4100109

Schwarz, F., Huang, W., Li, C., Schulz, B. L., Lizak, C., Palumbo, A., ... & Wang, L. X. (2010). A combined method for producing homogeneous glycoproteins with eukaryotic N-glycosylation. *Nature chemical biology*, 6(4), 264-266. doi:10.1038/nchembio.314

Sellick, C. A., Hansen, R., Maqsood, A. R., Dunn, W. B., Stephens, G. M., Goodacre, R., & Dickson, A. J. (2008). Effective quenching processes for physiologically valid metabolite profiling of suspension cultured mammalian cells. *Analytical chemistry*, 81(1), 174-183. doi:10.1021/ac8016899

Sha, S., Agarabi, C., Brorson, K., Lee, D., & Yoon, S. (2016). N-Glycosylation Design and Control of Therapeutic Monoclonal Antibodies. *Trends in Biotechnology*, 34(10), 835-846. doi:10.1016/j.tibtech.2016.02.013

Shade, K., & Anthony, R. (2013). Antibody Glycosylation and Inflammation. *Antibodies*, 2(3), 392-414. doi:10.3390/antib2030392

Spahn, P. N., & Lewis, N. E. (2014). Systems glycobiology for glycoengineering. *Current opinion in biotechnology*, 30, 218-224. doi:10.1016/j.copbio.2014.08.004

Stenerson, K. K. (2011). The derivatization and analysis of amino acids by GC-MS. Sigma-Aldrich. Reporter US, 25.

Stewart, B. J., Navid, A., Turteltaub, K. W., & Bench, G. (2010). Yeast dynamic metabolic flux measurement in nutrient-rich media by HPLC and accelerator mass spectrometry. *Analytical chemistry*, 82(23), 9812-9817. doi:10.1021/ac102065f

## T

Thomann, M., Schlothauer, T., Dashivets, T., Malik, S., Avenal, C., Bulau, P., ... & Reusch, D. (2015). In vitro glycoengineering of IgG1 and its effect on Fc receptor binding and ADCC activity. *PLoS One*, 10(8), e0134949. doi:10.1371/journal.pone.0134949

## U

Uesugi, T., Sano, K., Uesawa, Y., Ikegami, Y., & Mohri, K. (1997). Ion-pair reversed-phase high-performance liquid chromatography of adenine nucleotides and nucleoside using triethylamine as a counterion. *Journal of Chromatography B: Biomedical Sciences and Applications*, 703(1-2), 63-74. doi:10.1016/s0378-4347(97)00430-1

## V

Villiger, T. K., Steinhoff, R. F., Ivarsson, M., Solacroup, T., Stettler, M., Broly, H., ... & Soos, M. (2016). High-throughput profiling of nucleotides and nucleotide sugars to evaluate their impact on antibody N-glycosylation. *Journal of biotechnology*, 229, 3-12. doi:10.1016/j.jbiotec.2016.04.039

## W

Wang, L-X. & Amin, M.N. (2014). Chemical and Chemoenzymatic Synthesis of Glycoproteins for Deciphering Functions. *Chemistry & biology*. 21(1):51-66. doi:10.1016/j.chembiol.2014.01.001

Wang L-X, Lomino JV. (2012). Emerging Technologies for Making Glycan-Defined Glycoproteins. *ACS Chemical Biology*. 7(1):110-22. doi:10.1021/cb200429n

Wang, Q., Yin, B., Chung, C. Y., & Betenbaugh, M. J. (2017). Glycoengineering of CHO Cells to Improve Product Quality. *Heterologous Protein Production in CHO Cells: Methods and Protocols*, 25-44. doi:10.1007/978-1-4939-6972-2\_2

Walsh, G., & Jefferis, R. (2006). Post-translational modifications in the context of therapeutic proteins. *Nature Biotechnology*, 24(10), 1241-1252. doi:10.1038/nbt1252

Weikert, S., Papac, D., Briggs, J., Cowfer, D., Tom, S., Gawlitzek, M., ... & Eppler, S. (1999). Engineering Chinese hamster ovary cells to maximize sialic acid content of recombinant glycoproteins. *Nature biotechnology*, 17(11). 1116-1121.

White, J. A., Hart, R. J., & Fry, J. C. (1986). An evaluation of the Waters Pico-Tag system for the amino-acid analysis of food materials. *Journal of Analytical Methods in Chemistry*, 8(4), 170-177. doi:10.1155/S1463924686000330

Wiebe, M. E., Becker, F., Lazar, R., May, L., Casto, B., Semense, M., & Fautz, C. (1989). A multifaceted approach to assure that recombinant tPA is free of adventitious virus.

Wong, N. S., Wati, L., Nissom, P. M., Feng, H. T., Lee, M. M., & Yap, M. G. (2010). An investigation of intracellular glycosylation activities in CHO cells: effects of nucleotide sugar precursor feeding. *Biotechnology and bioengineering*, 107(2), 321-336. doi:10.1002/bit.22812

X

Y

Yamane-Ohnuki, N., Kinoshita, S., Inoue-Urakubo, M., Kusunoki, M., Iida, S., Nakano, R., ... & Shitara, K. (2004). Establishment of FUT8 knockout Chinese hamster ovary cells: An ideal host cell line for producing completely defucosylated antibodies with enhanced antibody-dependent cellular cytotoxicity. *Biotechnology and bioengineering*, 87(5), 614-622. doi:10.1002/bit.20151

Yarema, K. J., & Bertozzi, C. R. (2001). Characterizing glycosylation pathways. *Genome Biology*, 2(5), reviews0004.1–reviews0004.10

Yin, B., Wang, Q., Chung, C., Bhattacharya, R., Ren, X., Tang, J., ... & Betenbaugh, M. J. (2017). A novel sugar analog enhances sialic acid production and biotherapeutic sialylation in CHO cells. *Biotechnology and Bioengineering*, 114(8), 1899-1902. doi:10.1002/bit.26291

Yoo, H., Antoniewicz, M. R., Stephanopoulos, G., & Kelleher, J. K. (2008). Quantifying reductive carboxylation flux of glutamine to lipid in a brown adipocyte cell line. *Journal of Biological Chemistry*, 283(30), 20621-20627. doi:10.1074/jbc.M706494200



Young, J. D. (2014). INCA: a computational platform for isotopically non-stationary metabolic flux analysis. *Bioinformatics*, 30(9), 1333-1335.  
doi:10.1093/bioinformatics/btu015

## Z

Zhang L, Luo S, Zhang B. (2016). Glycan analysis of therapeutic glycoproteins. *MAbs*. 8(2):205-15. doi: 10.1080/19420862.2015.1117719.

# Curriculum Vitae

## Sean Alexander Ponce

Born: May 6, 1985 in Los Angeles, California

### EDUCATION

**Johns Hopkins University**, Baltimore, MD, August 2015- August 2017

M.S.E. Chemical and Bio-Molecular Engineering

*Thesis: Experimental Approaches Towards Controlling the Glycoform*

*Advisors: Michael Betenbaugh and Kevin Yarema*

**University California Santa Barbara**, Santa Barbara, CA, September 2008 - June 2011

B.S. Biochemistry, emphasis in Protein Engineering

B.A. Physics, emphasis in Optics

**Moorpark College**, Moorpark, CA, 2006-2008

General Education

### PROFESSIONAL EXPERIENCE

**Michael J. Betenbaugh Lab, JHU, Department of Chemical Engineering,  
Graduate Student Researcher**

November 2015 – Present

- Fostered a collaboration with Anne Le, MD/PhD, Johns Hopkins Pathology; Metabolomic studies of human cell lines (PANC,P493) using stable isotopically labelled cell media feeds incorporating <sup>13</sup>C-Glucose or <sup>13</sup>C,<sup>15</sup>N-Glutamine for correlating metabolite differences with biochemical relationships in metabolic pathways, developed LC-MS/MS methodologies using Agilent 1290 LC with 6550 Q-ToF MS and 6490 QQQ MS for identifying and quantifying various bio-molecules using Agilent's MassHunter and Qualitative and Quantitative analysis software
- Transported, re-built, maintained and operated a Shimadzu LC-10Ai HPLC system for a variety of analytical assays, Trained and supervised instruction of other students in the theory and practice of LC utilizing Agilent Infinity 1260 LC
- HPLC analytical assays; furans, IgG using Protein-A, Amino Acids (Water's AccQ), metabolites, and Nucleotides/Nucleosides/Nucleotide Sugars
- Glycan analysis techniques: HPLC N-Glycans using HILIC with FLD 2-AB and 2-AA derivatization, Fluorescence Assisted Carbohydrate Electrophoresis (FACE) of monosaccharides
- Metabolic Flux Analysis of CHO cells to create flux maps of biochemical pathways using INCA/ETA software through numerical solution of stoichiometric balances coupled with isotopologue distributions of TBDMS derivatized metabolites on Shimadzu GC17A-QP5050A GC/MS
- Molecular Biology skills: Aseptic and sterile cell culture techniques, passaging of

cells, cell counting (Beckman Coulter cell counter and hemocytometer), cell lysis and metabolite extraction, performed on cell lines: CHOZN GS, CHO K1, PANC, and P493

- Microfluidic device: Construction of a micro-reactor using PDMS housing for in-vitro glycosylation using solid phase enzyme catalysis (Endo-H) on etched silicon nanowires to produce homogenous glycoforms of proteins: Alpha-Amylase, RNaseB, and IgG

***Paragon Bioservices, Baltimore, MD, Bio-Process Development Department, Student Intern***

July 2015 - January 2016

- Temporary job to serve for stipend assistance in paying for school, resigned for graduate research
- Performed molecular biology techniques: SDS-PAGE, Western Blot, DNA quantitation by RT-qPCR and ELISA analysis of proteins produced from baculovirus transfected insect cell lines

***Coherus Biosciences, Camarillo, CA, Department of Analytical Research & Development, Research Associate***

April 2012 - June 2015

- Employee #13 in company, first hired research associate in both company & department under two Research Scientists and Chief Scientific Officer, company now employing ~100 people, entering Stage 3 clinical trials and initial public offering closed November 2014
- Extensive hands-on research experience in antibody, fusion protein and heavily-glycosylated protein chemistry
- Provide data for submission of multiple Investigational New Drug Applications to FDA, North American and European healthcare regulatory agencies
- Understanding of how up-stream (cell media and culture) and downstream (purification) bio-process engineering changes affect protein product outcome
- Pioneered, developed, and refined nearly all in-house methods of analytical protein characterization
- Wrote standard operating procedures (SOPs), method development reports, method validation reports and inter-departmental memos
- Troubleshoot method and technology transfers across consultants and partners
- Train all incoming research associates and research scientists on use of scientific equipment and methodologies whilst developing their proper user techniques for best practice
- Expert level of chromatographic techniques (Dionex HPLC and Chromeleon Software): RPC, HIC, CEC, AEC, HILIC, IC and HPAEC-PAD (ICS-5000+), Affinity, and SEC
- Intermediate level of mass spectrometry analysis (Waters Xevo QToF, Thermo LTQ Orbitrap XL): Intact mass analysis, bottom-up and top-down proteomics, peptide mapping, glycopeptide mapping, and disulfide mapping
- Sub-Visible Particle Analytical Techniques: Nanoparticle Tracking Analysis (Nanosight NS500) for nanometer range and MFI (Protein Simple 5200) for micrometer range

- Light Scattering Techniques: SEC or Flow Field Fractionation (FFF) (Wyatt Eclipse Dualtec) in conjunction with Static Multi Angle Light Scattering (MALS) (Wyatt Optilab T-rEX and miniDAWN TREOS) and Dynamic MALS (Wyatt DynaPro Plate Reader II) for measuring protein aggregation, oligomeric state, hydrodynamic radii and protein conjugate analysis (PEGylation and glycosylation)

- Carry out long-term protein stability studies by forced thermal, mechanical (shear stress), pH (acidic and basic), oxidative, formulation selection, and freeze/thaw cycling
- Post-translational protein modification studies: iso-aspartate isomerism and free thiol assessment (Ellman's reagent and fluorescent derivatization)
- Determination, quantitation, and identification of process-related impurities
- Determination of solution protein concentration (A280) using Nanodrop, Jasco, and Tecan plate reader spectrophotometers
- Automated liquid handling and pipetting robot device (Eppendorf epMotion)
- Electrophoretic techniques: SDS-PAGE, Native PAGE, Isoelectric Focusing (IEF gels and cIEF (Protein Simple iCE3), Western Blot
- Developed and performed kit-based ELISA assays
- Glycobiology: N-linked glycan analysis, O-linked glycan analysis, sialic acid content and total monosaccharide analysis
- Tracking, processing, maintaining and ordering chemical and sample inventory
- Responsible for shipping and receiving of incoming and outgoing materials
- Unofficially named the department IT support; excellent computer and programming skills for troubleshooting PC-related problems
- Report findings to superiors in a timely and efficient manner
- Resigned to attend graduate school

***Baxter Bioscience, Glendale, CA, Technical Services Department, Process Development Group, Research Associate***

September 2011- April 2012

Reported to Vladamir Shlimak, D.Sci. and Irene Ch'en, Ph.D.

- Hired to work as a process engineer for the FDA submission of process changes to the Baxter AHF-M process to demonstrate process comparability
- Glendale Baxter plant is World's largest and most advanced human blood plasma-fractionation protein production facility
- Responsible for process steps from thawing of frozen blood plasma to viral reduction/inactivation to plasma component separation to affinity chromatography to nanofiltration
- Wrote the programs and operations for automating all process steps onto GE AKTA series FLPC
- Sole author of departments SOP on instrument description, calibration, operation and maintenance
- Conducted laboratory bench and pilot plant scale protein purification and separation studies, including sample collection, sample preparation, and sample submission
- Used sophisticated laboratory instrumentation and computer systems to collect and record data
- Hands-on operation, set-up, cleaning, and sanitization of bioreactors and lab equipment
- Performed and developed advanced biochemical assays requiring precise analytical

skills and understanding of biology and chemical principles: ELISA, Western Blot & UV-Vis

- Completed all testing and analyses of experimental materials in a timely and appropriate manner
- Prepared study protocols/final reports, maintained data integrity, and ensured compliance with company SOPs, GLP and cGMP regulations
- Participated in cross-functional team discussions motivating, driving and directing pilot scale studies and production
- Prepared buffers and solutions, performed equipment maintenance and calibrations as required: pipettes, pH, Conductivity & pressure monitors
- Worked as a 'runner' of documents requiring authorization by all departments of quality assurance, biochemistry, quality control, engineering, validation, regulatory, and technical services helping to expedite document change revisions for inter-departmental agreement leading to endorsement of activities relating to plan and set objectives and goals

***Daniel E. Morse Lab, Materials Science & Bio-Molecular Engineering Group, Marine Biotechnology, UCSB, Research Intern***

September 2010 – June 2011

Reported to Daniel DeMartini, Ph.D.

- Elucidation of Physico-Biochemical Mechanism of Adaptive Squid Bio-Luminescence in Cephalopod Iridophore tissue via a Bragg Reflector Optical Construction Mechanism -Preparing solutions and buffers, carrying out assigned experiments, analyzing data, implementing subsequent research objectives, recording all duties performed & data obtained in lab and presenting findings in weekly interdisciplinary group discussions
- PCR, Protein expression in E. Coli, Extensive protein purification using HPLC/FPLC (Fisher Bioscience): IEX & HIC, spin columns, SDS-PAGE and Western Blot, ELISA, lyophilization, TEM & SEM (cell imaging), Zeta-Potential (hydrodynamic radius), MALDI-ToF Mass Spectrometry (the kind you drive with a joystick), determination of protein refractive indices (custom construction of a micro-volume interferometer Snell's Law), Circular Dichroism (secondary structure), sterile filtration techniques, filling syringes and vials, fume hood work, studying protein cross-linkage and post-translational modifications, mapping neural molecular pathways through enzyme inhibition and activation using neurotransmitters and small molecules, dissection skills: tweezers and scalpel under microscope for tissue excision and isolation

***M. Scott Shell Lab, Bio-Physics & Condensed Matter Group, Department of Chemical Engineering, UCSB, Research Intern***

March 2009 - Jun 2010

- Computer simulations to probe protein folding pathway energy landscapes and conformational spaces using Molecular Mechanics
- Helped to develop protein docking simulations using free energy minimization calculations -Developed algorithms to probe molecular interaction theories using AMBER force field parameters
- Utilized analytical software such as Mathematica, Matlab, MS Excel to identify data correlations

-Record all duties performed & data obtained in lab notebook, analyzed data and presented findings in weekly group discussions

***In-N-Out Burger Inc., Part-Time Manager***

February 2004 - August 2008

-Responsible for general overall supervision of store; maintaining inventory, employee schedules and ensuring company guidelines and policies were followed

-Balanced cash sheets and daily monetary reports

**PUBLICATIONS**

***Combinatorial genome and protein engineering yields monoclonal antibodies with hypergalactosylation from CHO cells***

Biotechnology and Bioengineering, 2017 doi:10.1002/bit.26375

Andrew Chung, Qiong Wang, Shuang Yang, Sean Ponce, Brian Kirsch, Hui Zhang, Michael Betenbaugh

***Isoform separation of proteins by mixed-mode chromatography.***

Protein Expr Purif. 2015 Dec;116:144-51. doi:10.1016/j.pep.2015.08.013

Arakawa T, Ponce S, Young G.

**FELLOWSHIPS & AWARDS**

**JHU Chemistry NMR Certification, 2016**

**UCSB Materials Research Laboratory, *CAMP Intern*, 2010-2011**

Selected candidates conduct work in a UCSB laboratory focusing on materials science and engineering research, participate in weekly group meetings, attend special seminars and present their results at an end-of-quarter poster sessions

**UCSB *Dean's List* 2009**

**INTERESTS**

Cycling, cooking, design: art & architecture, cars (motorsport) and surfing